



I³N *Innovative
Integrated
Instrumentation
for Nanoscience*



**POLITECNICO
MILANO 1863**

Seminar within the “Quantum Circuits and Devices” course

Measuring quantum devices below 4K

Cryogenic electronics

Giorgio Ferrari

Milano, December 2023

Who I am

Innovative Integrated Instruments for the Nanoscience Lab

M. Sampietro G. Ferrari
D. Natali F. Zanetto
+ E. Prati (UniMI)

Photonic Integrated Circuits

Control electronics for large-scale programmable photonic circuits (telecom, sensing, optical computing...)

Quantum computing

Cryogenic electronics for the readout and characterization of spin-based qubits

Biosensors and bio-inspired electronics

*Electronic sensors for virus, antibodies, DNA
CMOS neuromorphic circuits for ultra-low power data acquisition and processing*

POLIFAB – Clean room facility



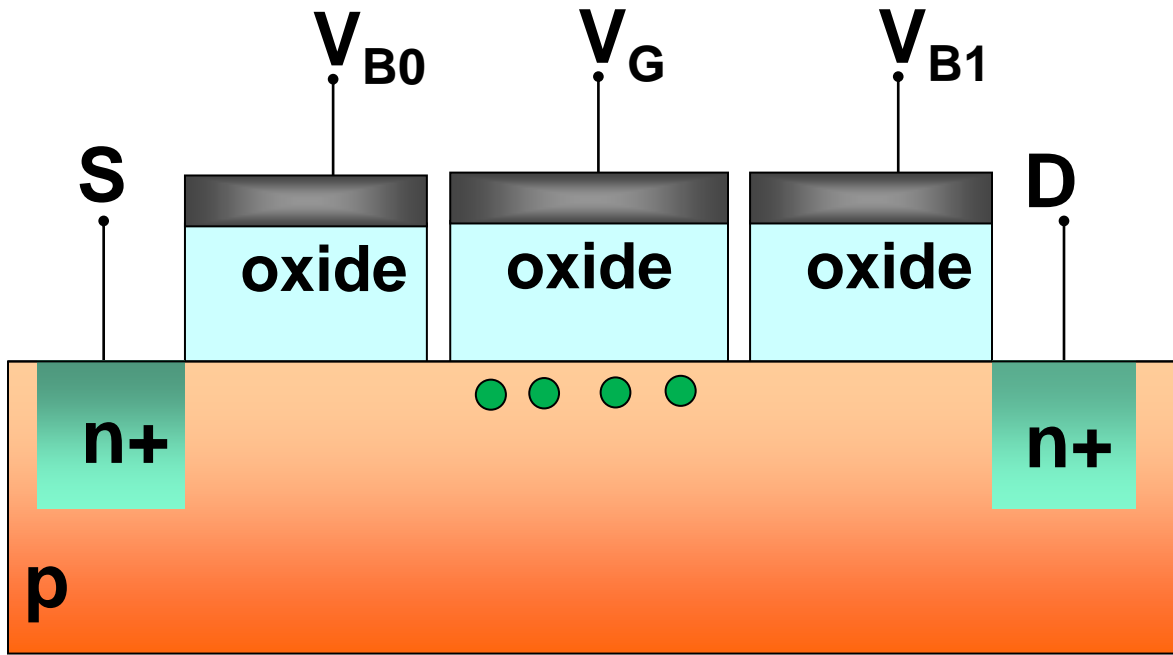
Cleanroom surrounded by a cluster of labs of micro- and nanoelectronics, photonics, photovoltaics, biotechnologies, spintronics, organic semiconductors

I3N lab is part of **polifab**, the micro and nano technology center of the Politecnico di Milano (750 m² of clean room)

Outline

- Spin detection using room temperature instrumentation
- Cryogenic electronics
 - Challenges
 - Design rules
- Examples & state of the art

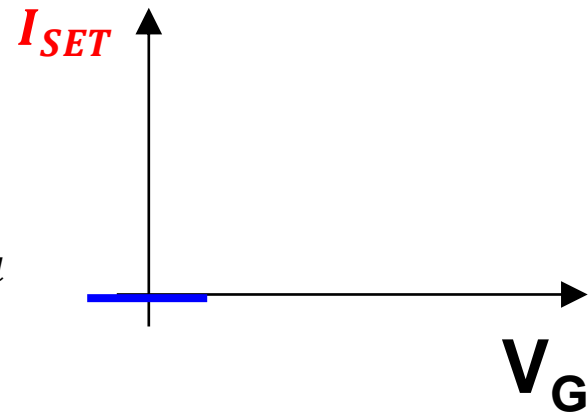
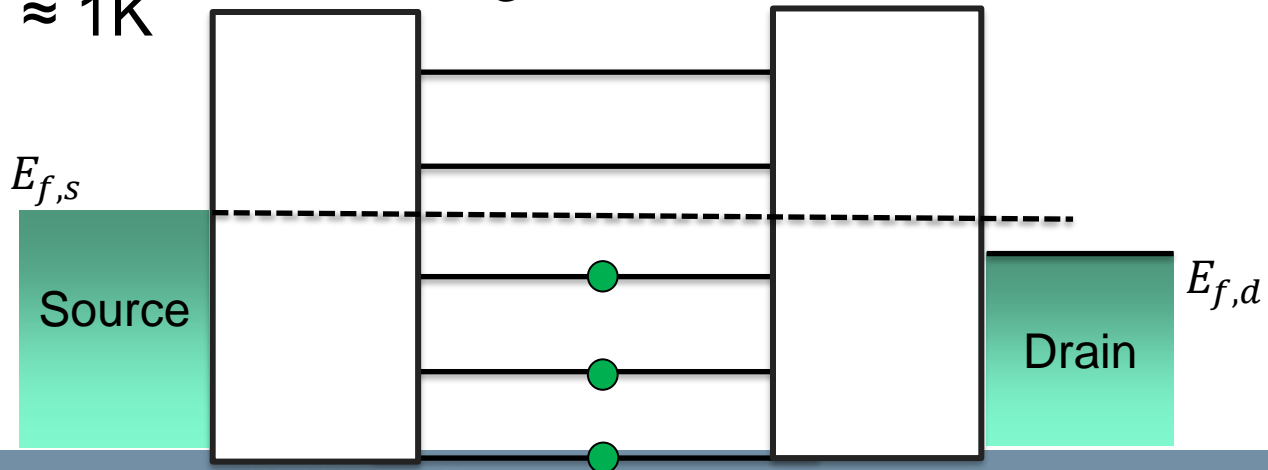
Single-Electron Transistor (SET)



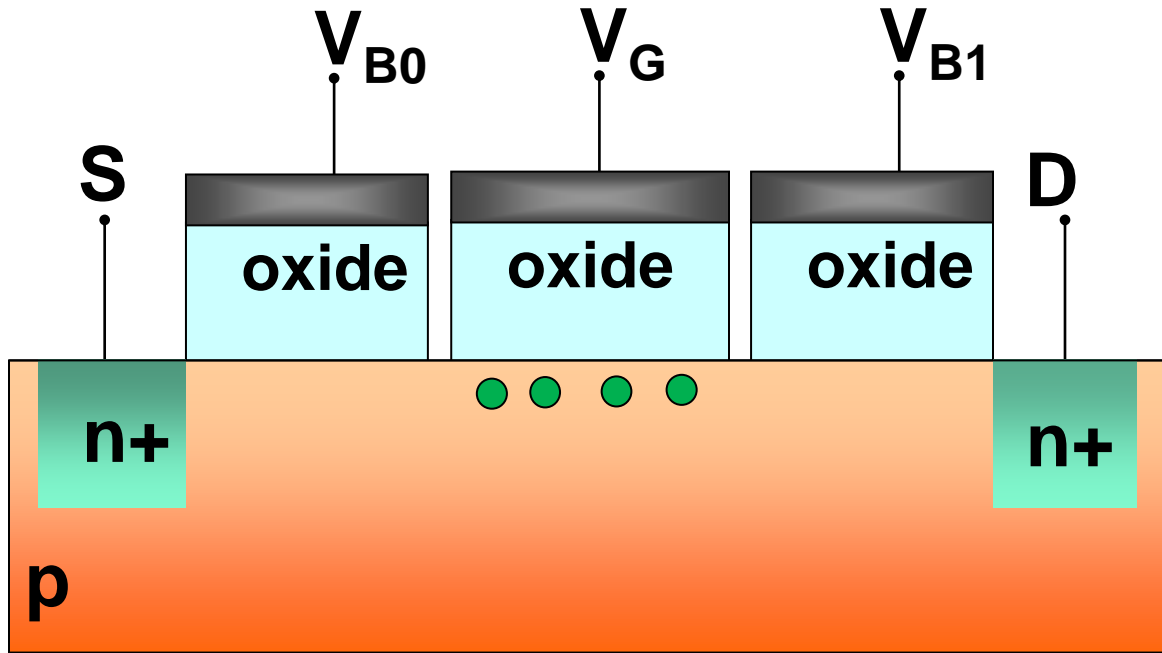
V_{B0} , V_{B1} biased to have an energy barrier for the electrons
The energy barrier is thin enough to allow tunneling

V_G controls the energy levels of the island

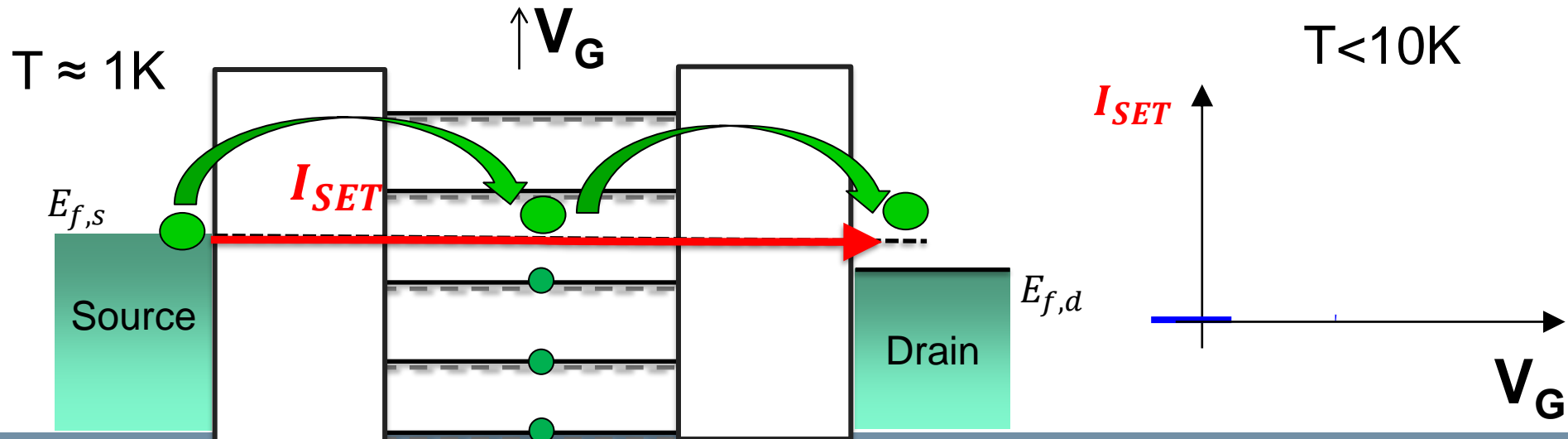
$T \approx 1K$



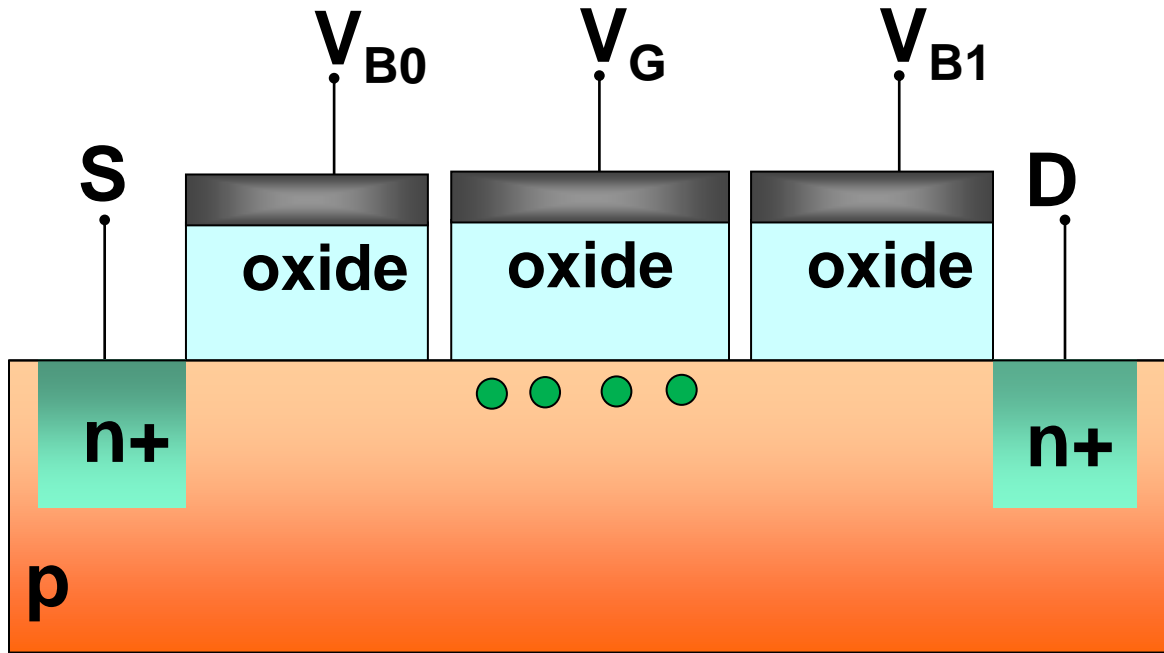
Single-Electron Transistor (SET)



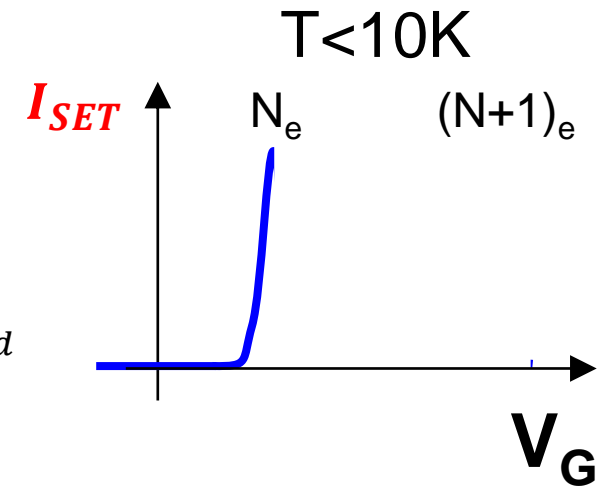
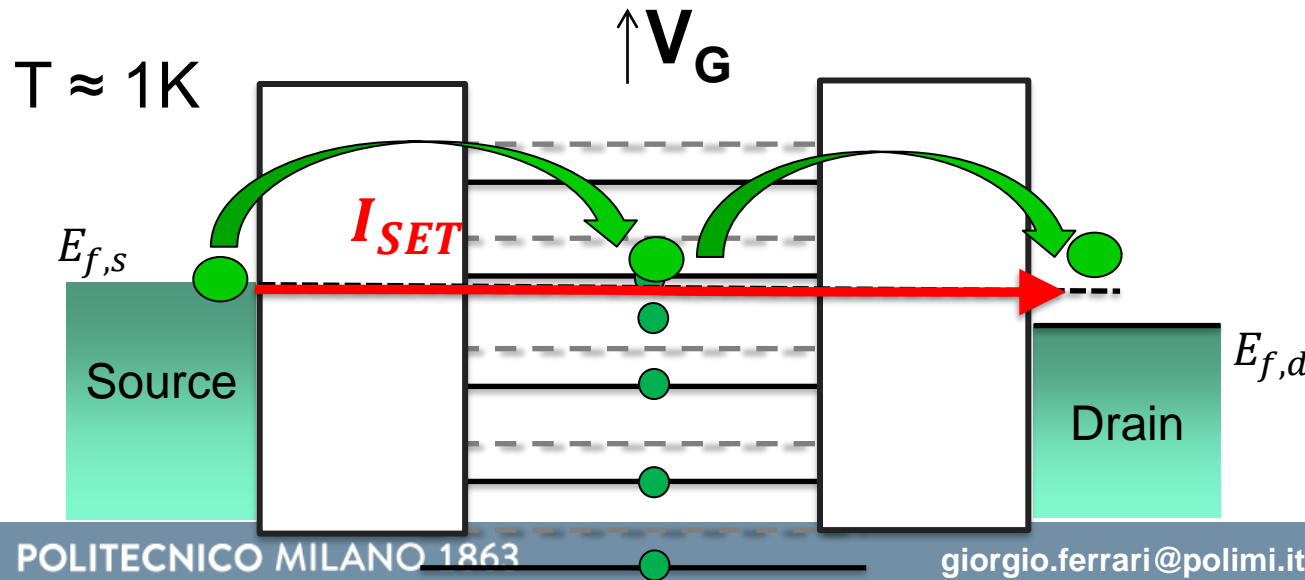
V_{B0} , V_{B1} biased to have an energy barrier for the electrons
The energy barrier is thin enough to allow tunneling



Single-Electron Transistor (SET)

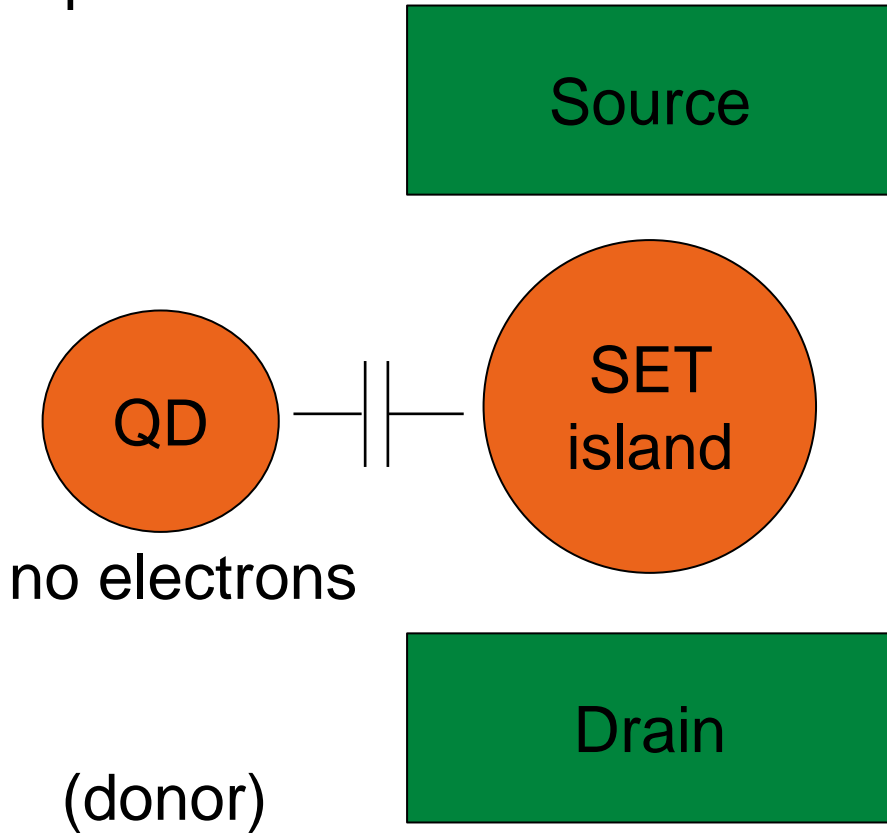


V_{B0} , V_{B1} biased to have an energy barrier for the electrons
 The energy barrier is thin enough to allow tunneling

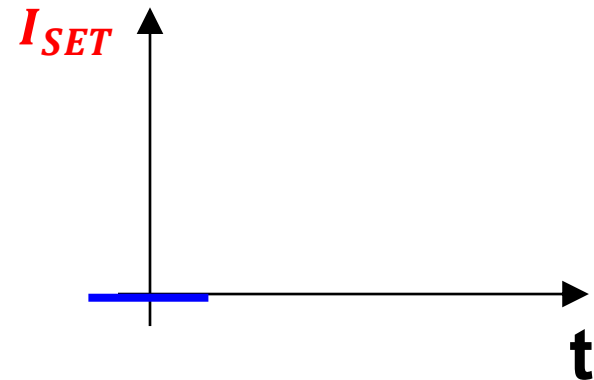
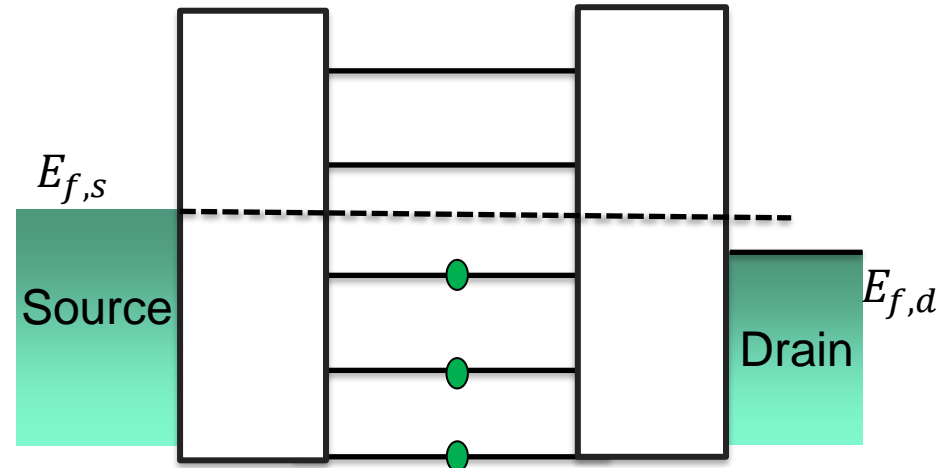


SET-based single-charge detector

Top view:

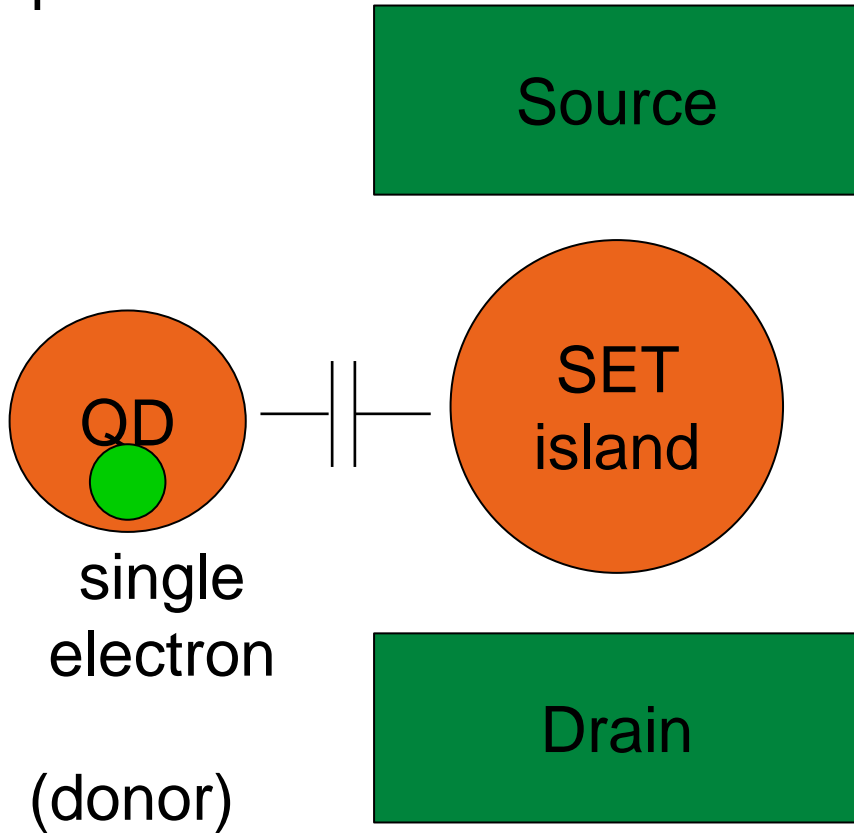


Energy levels:

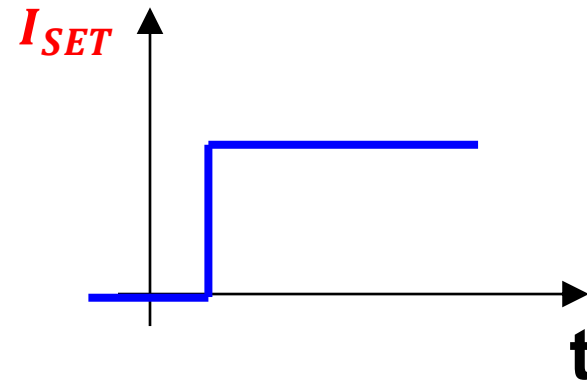
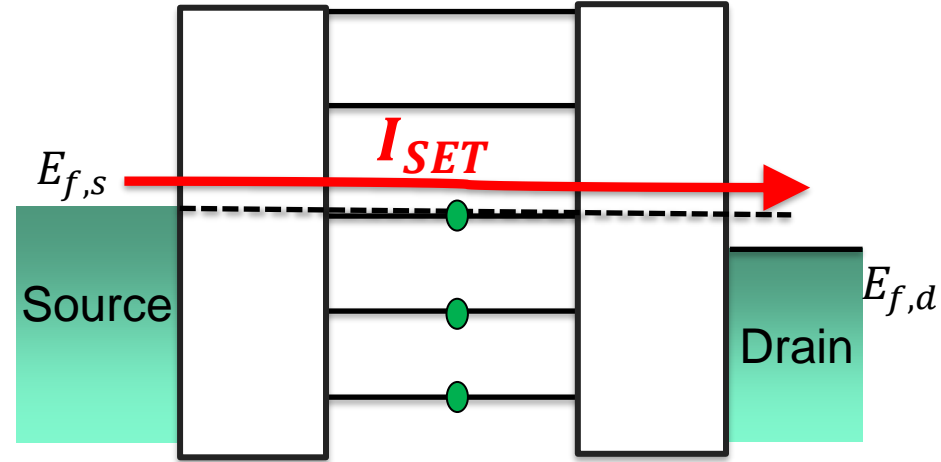


SET-based single-charge detector

Top view:

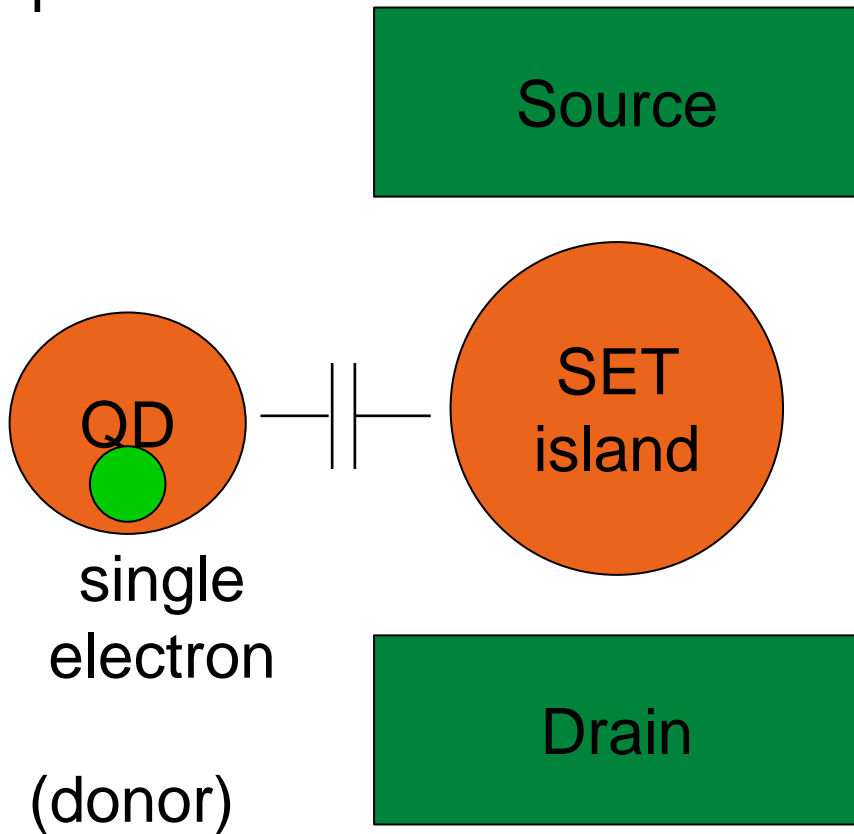


Energy levels:

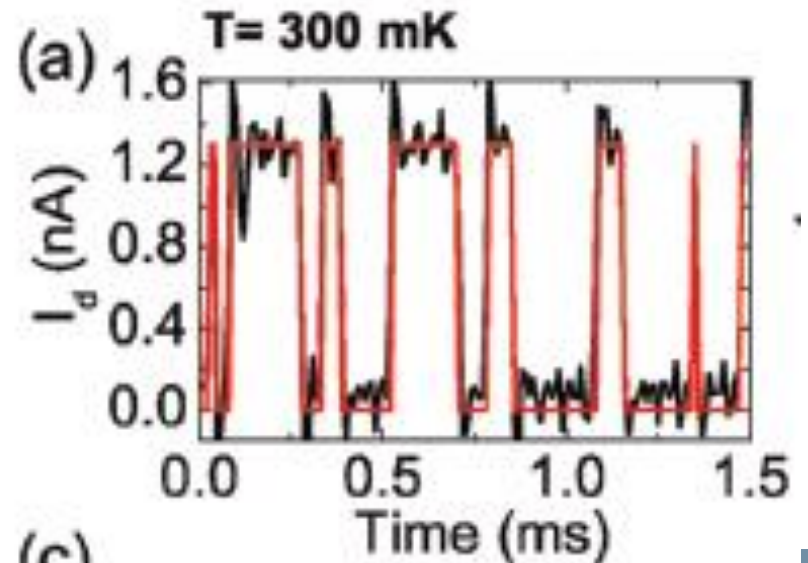
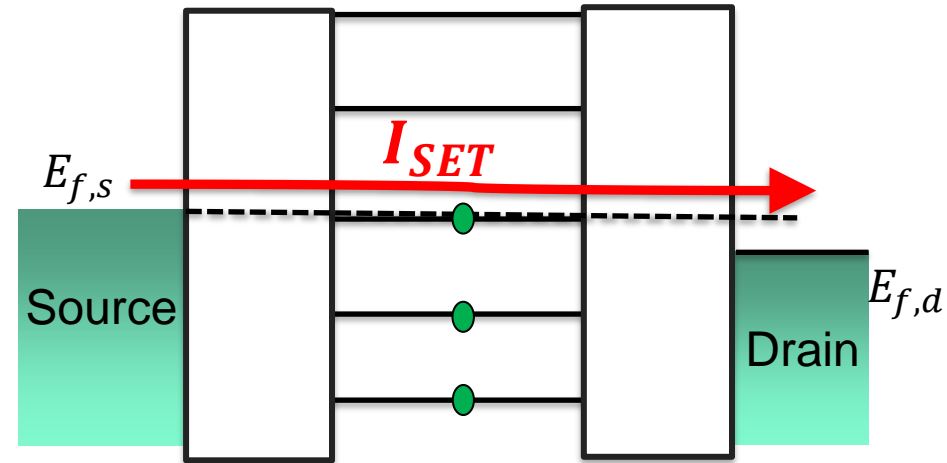


SET-based single-charge detector

Top view:

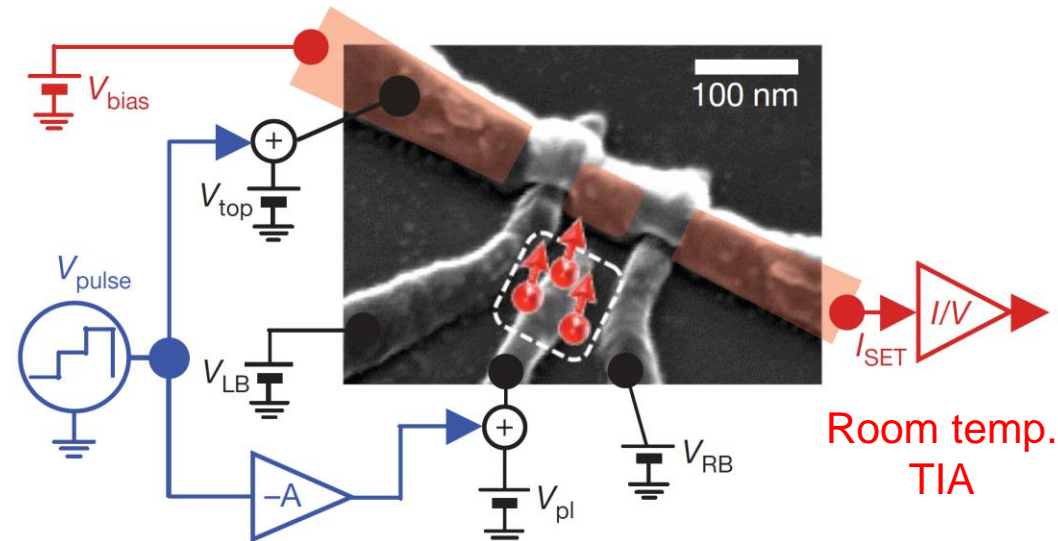
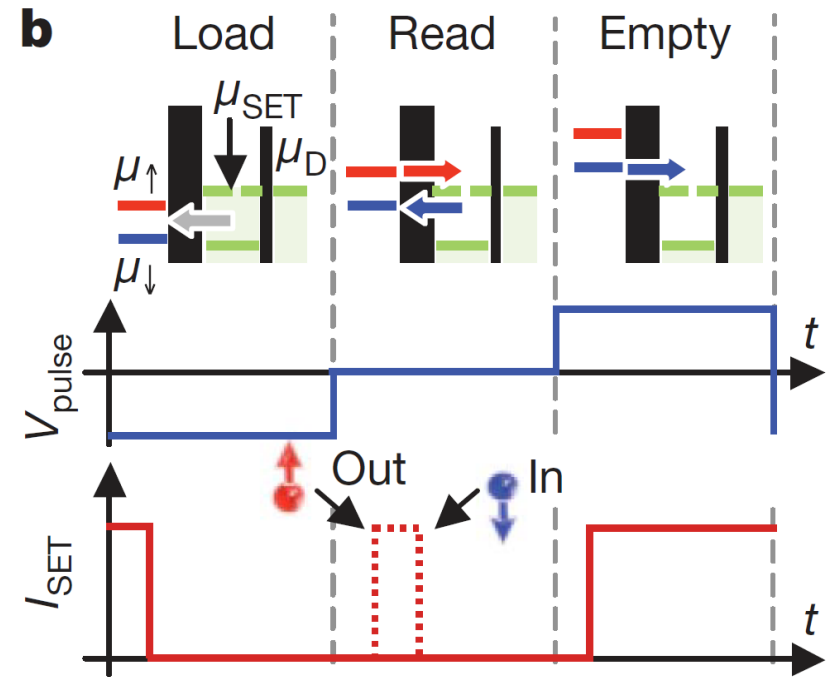
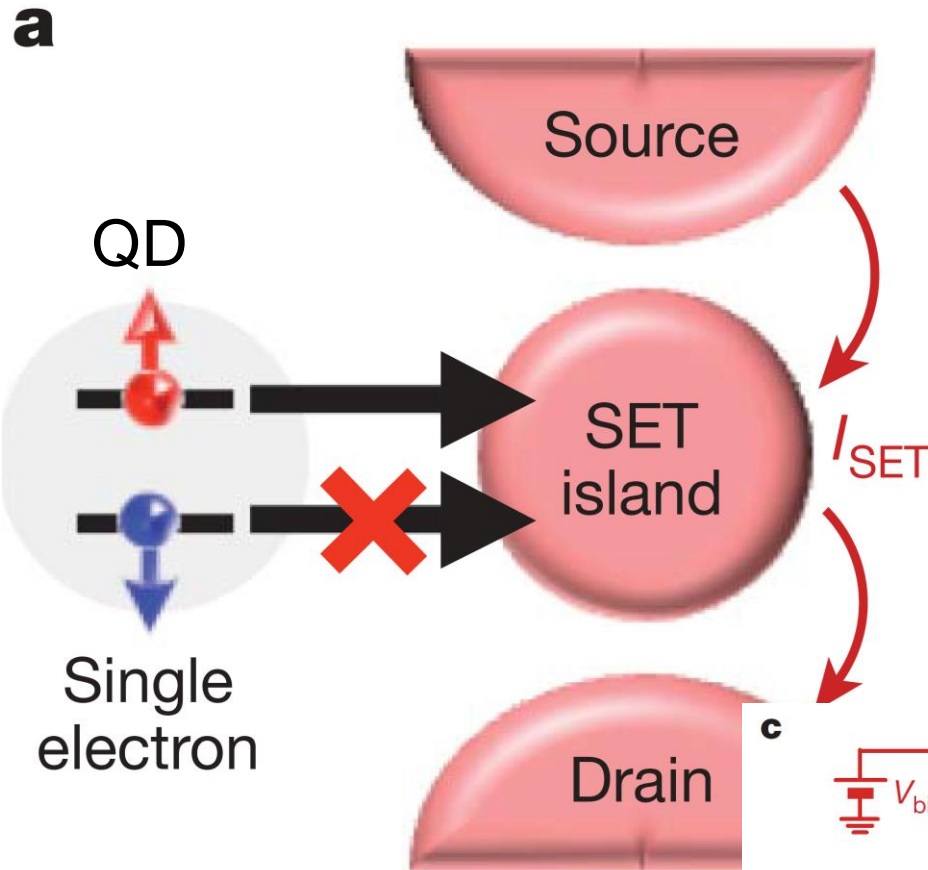


Energy levels:



Mazzeo, Prati, Ferrari et al APL 2012

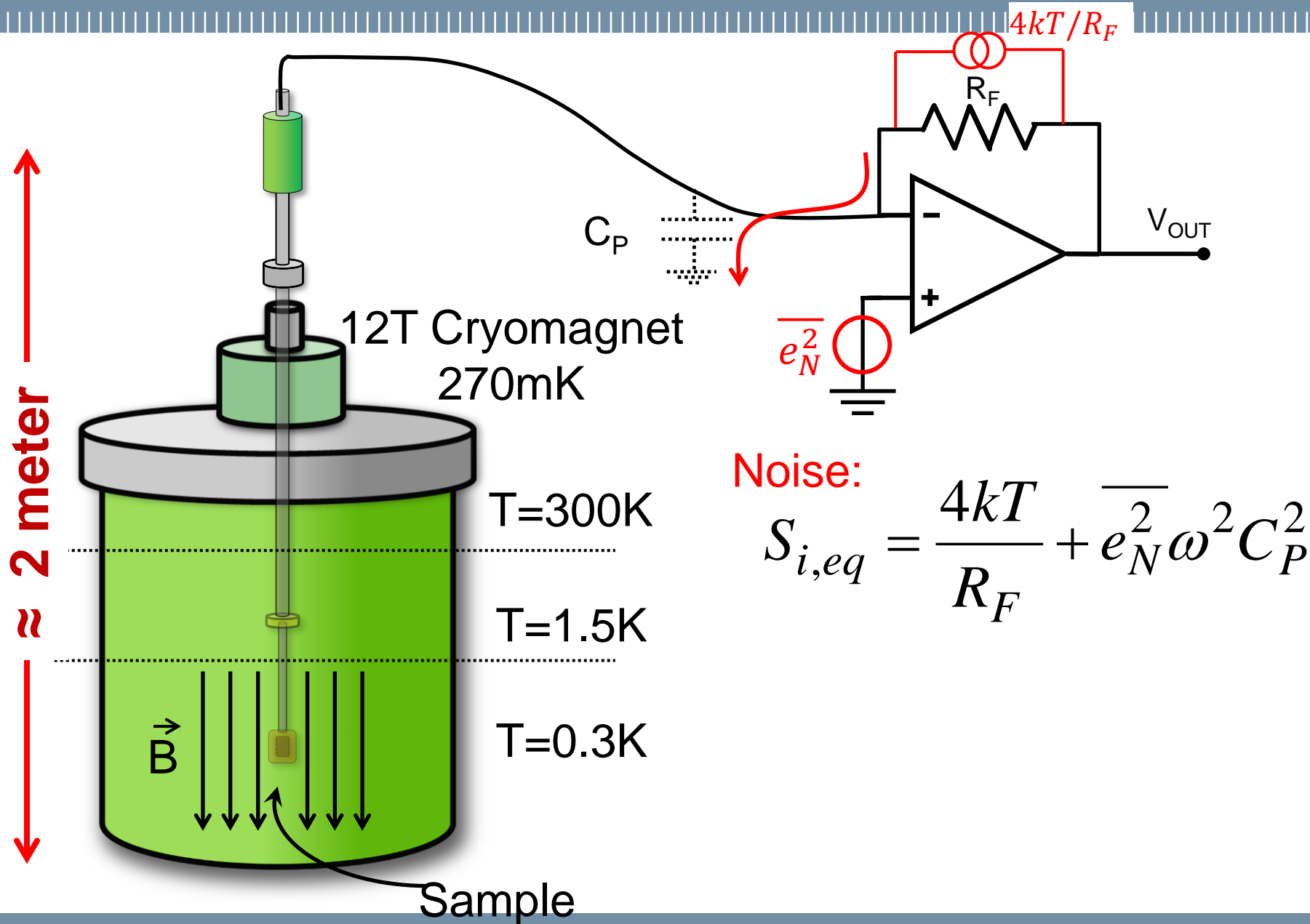
Spin state detection: spin-to-charge conversion



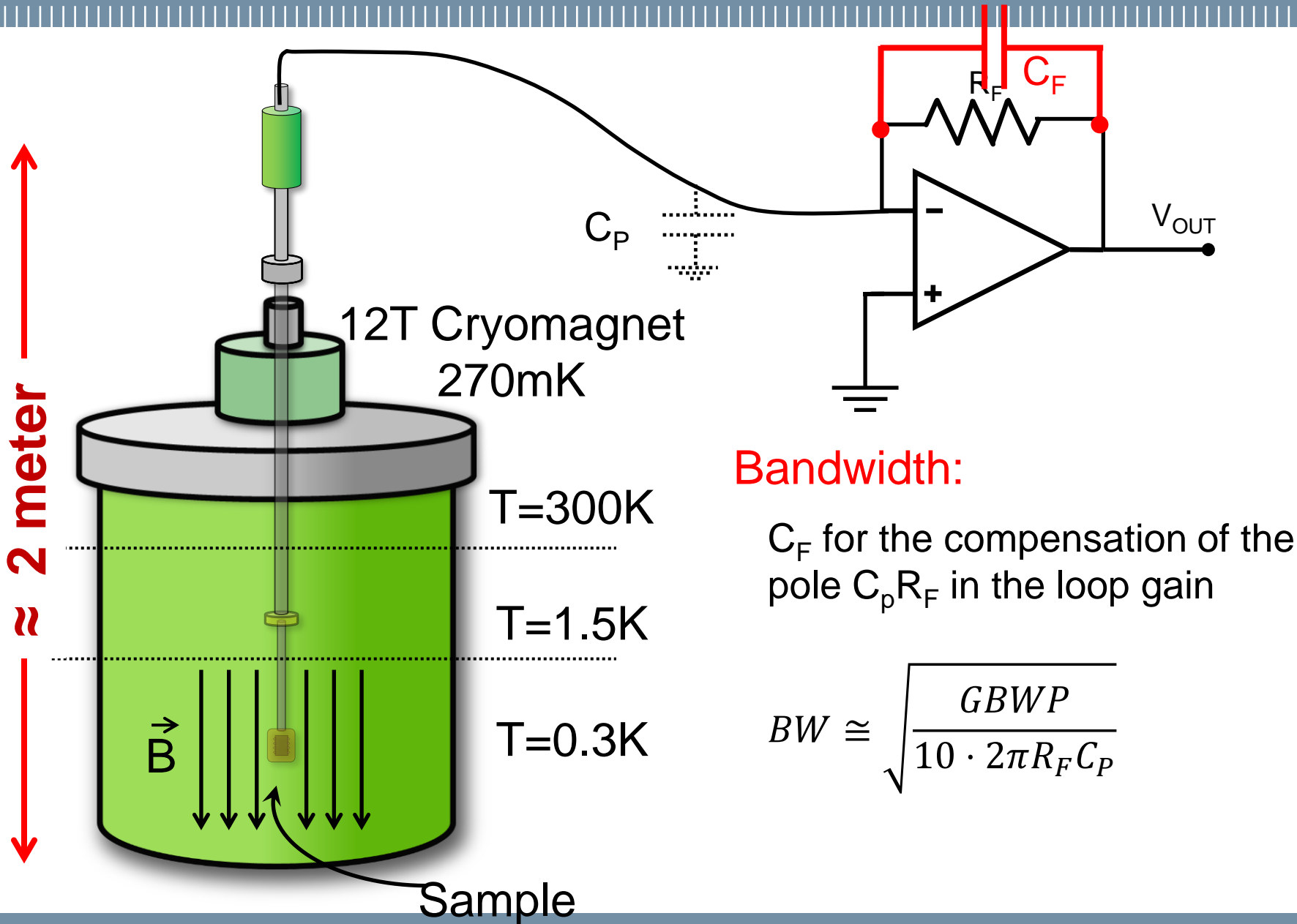
electron $\rightarrow I_{SET} \approx 0$
 void $\rightarrow I_{SET} > 0$

A. Morello, et al. *Nature*, no. 7316, pp. 687–91
 2010, doi: 10.1038/nature09392.

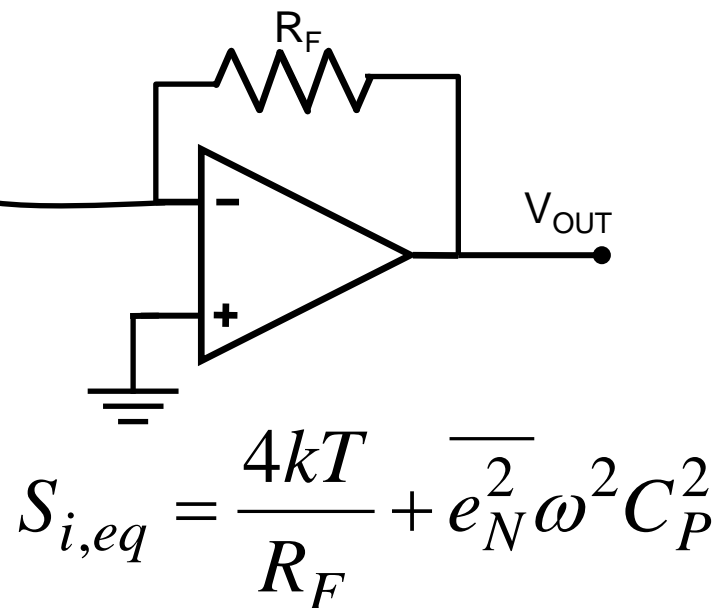
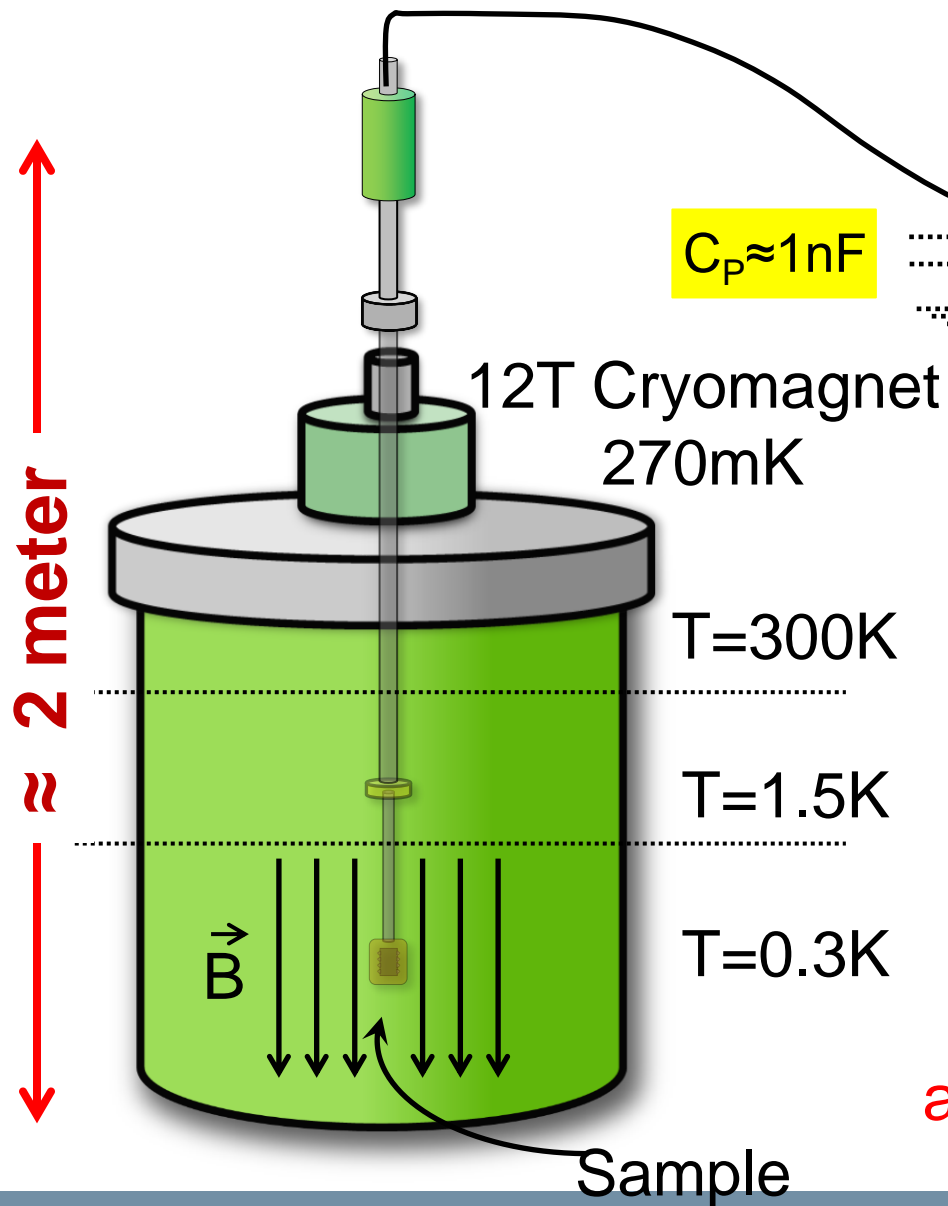
Experimental set-up to study quantum devices



Experimental set-up to study quantum devices



Experimental set-up to study quantum devices



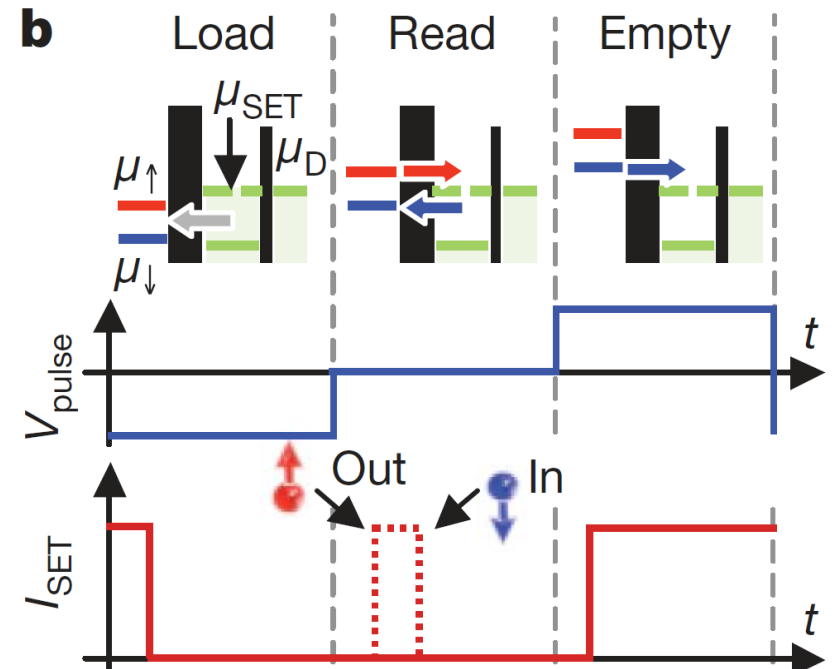
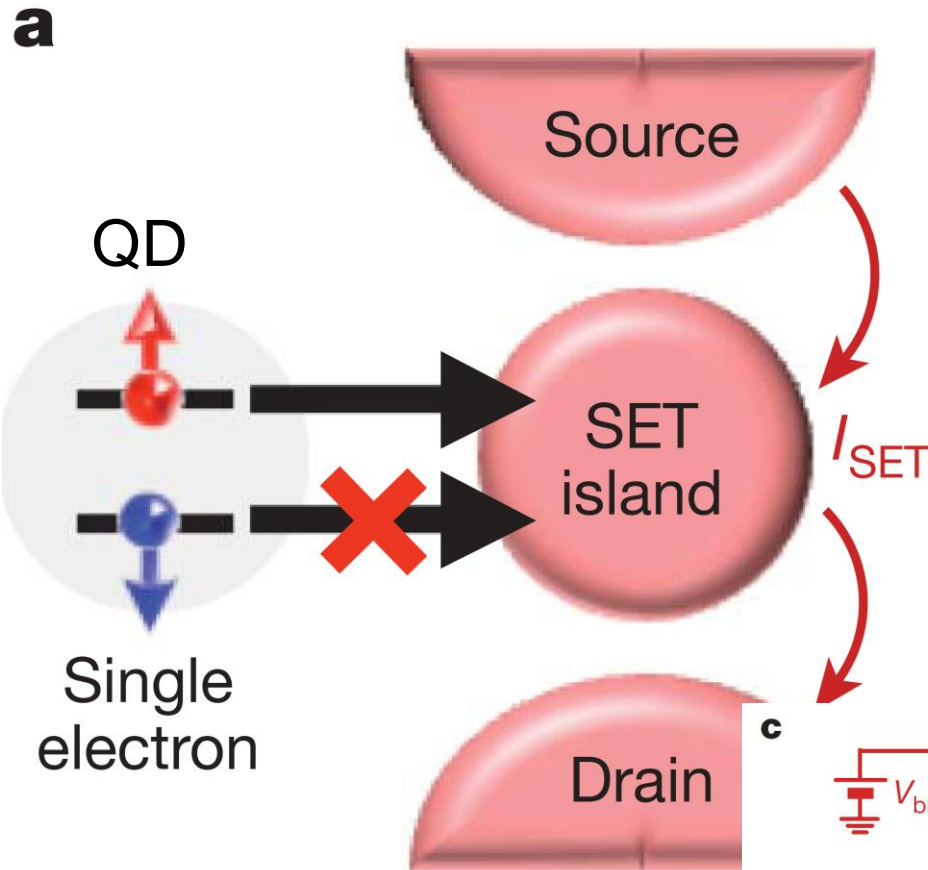
$$S_{i,eq} = \frac{4kT}{R_F} + \overline{e_N^2} \omega^2 C_P^2$$

$$I_{RMS} = \frac{2\pi e_N C_P BW^{3/2}}{\sqrt{3}}$$

$$BW = \sqrt{\frac{GBWP}{10 \cdot 2\pi R_F C_P}}$$

a large C_P reduces performances

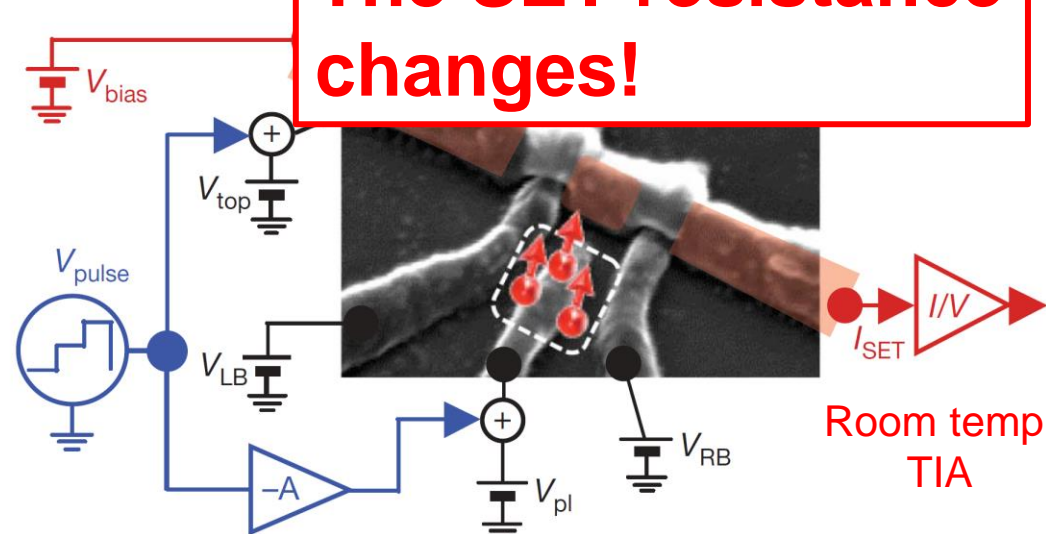
Spin state detection: spin-to-charge conversion



The SET resistance changes!

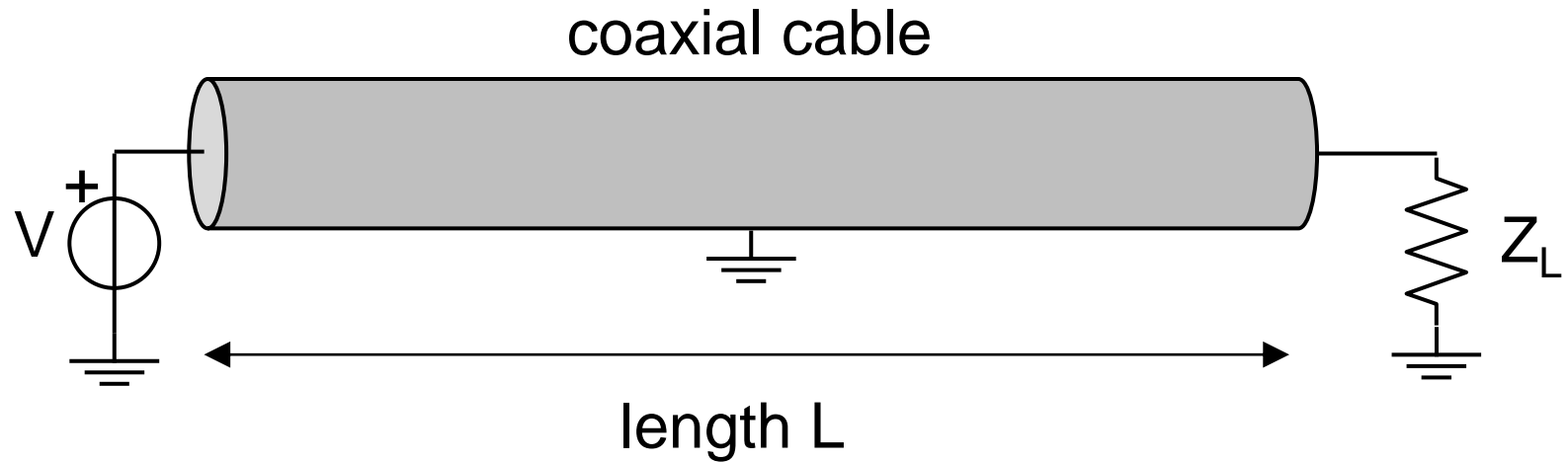
electron $\rightarrow I_{SET} \approx 0$
 void $\rightarrow I_{SET} > 0$

A. Morello, et al. *Nature*, no. 7316, pp. 687–91
 2010, doi: 10.1038/nature09392.

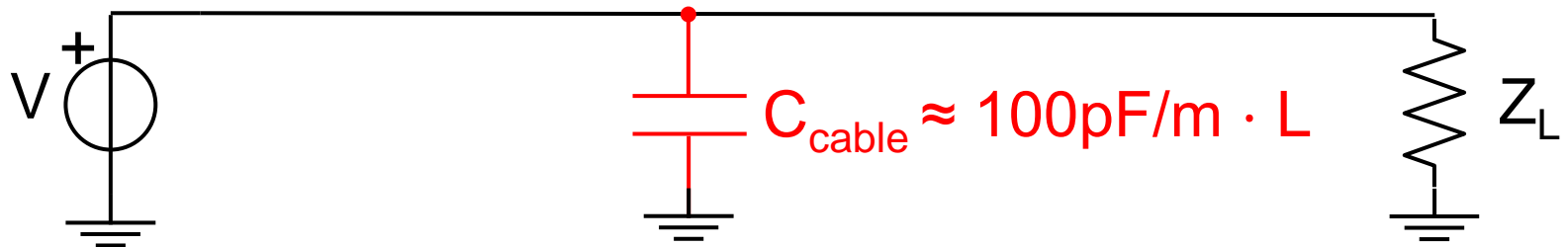


How to avoid being penalized by a long cable?

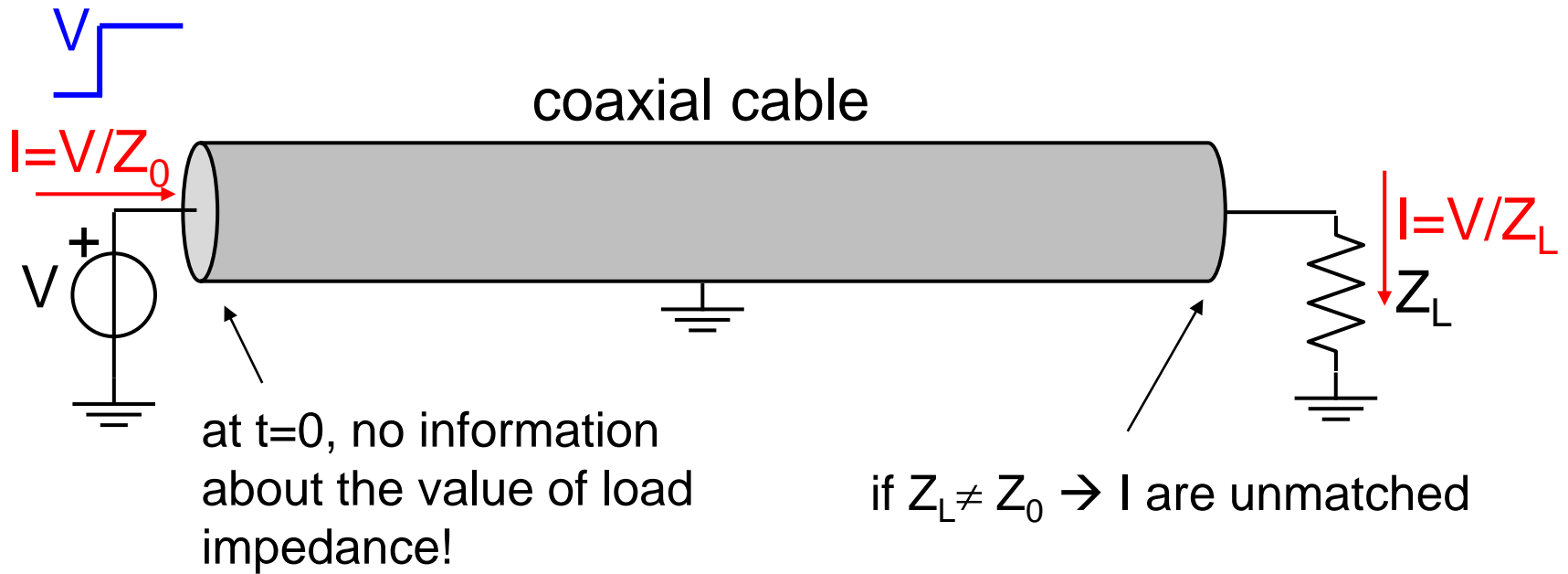
Measuring an impedance using the properties of the cable:



If V changes slowly compared to the transit time of the electromagnetic wave ($t_t = L/v_{\text{light}}$):

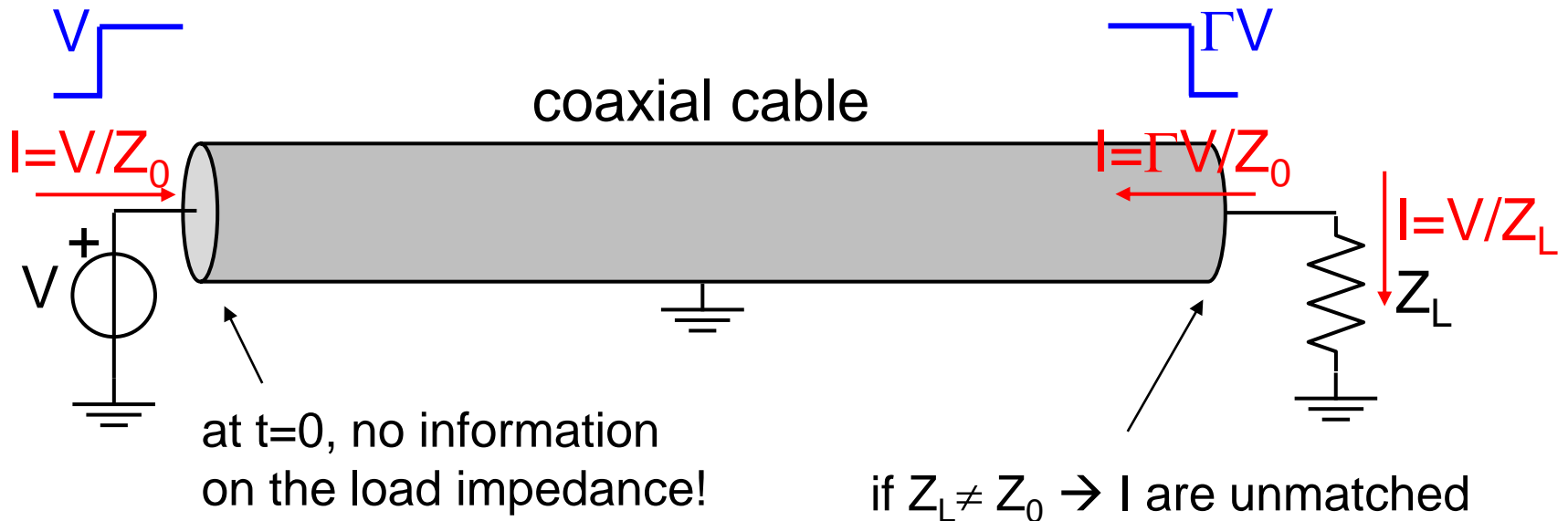


Transmission line



Z_0 = characteristic impedance of the cable, usually 50Ω

Transmission line



Z_0 = characteristic impedance of the cable, usually 50Ω

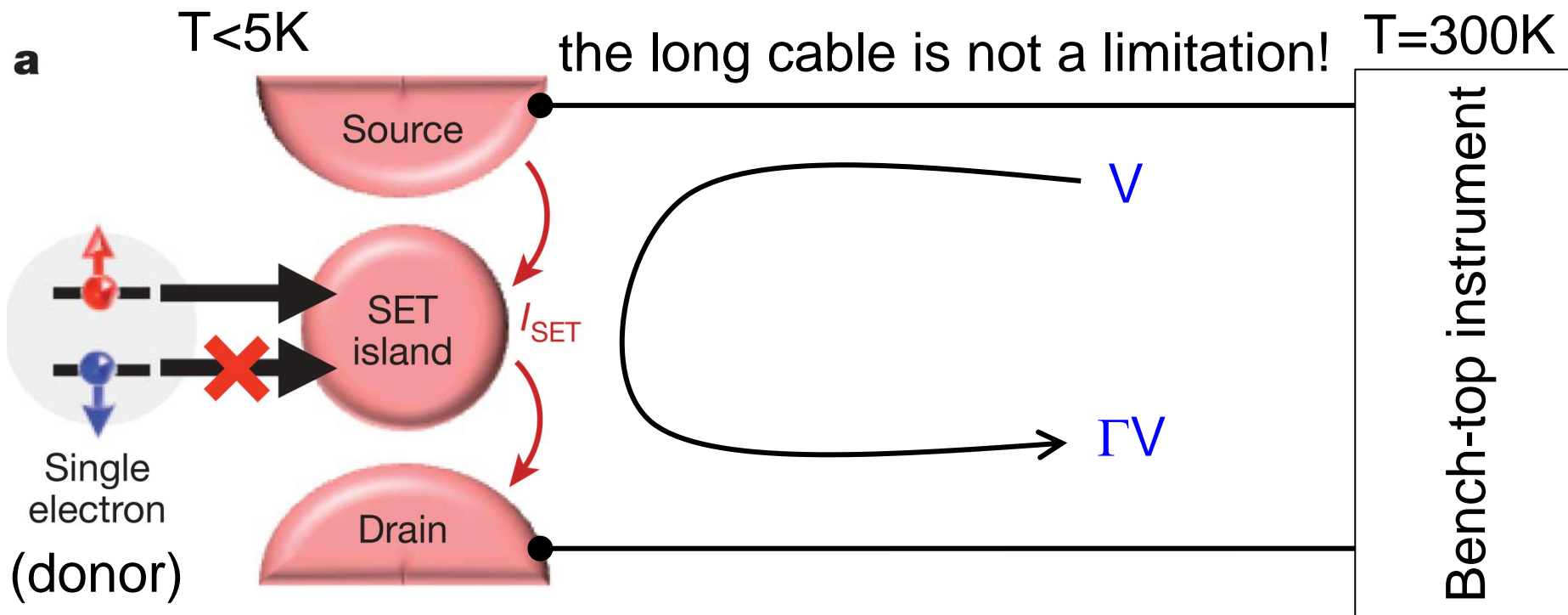
The reflected wave is related to the load impedance!

a reflected wave is created!

$$\Gamma = \frac{Z_L - Z_0}{Z_L + Z_0}$$

reflection coefficient

Radio-frequency spin readout

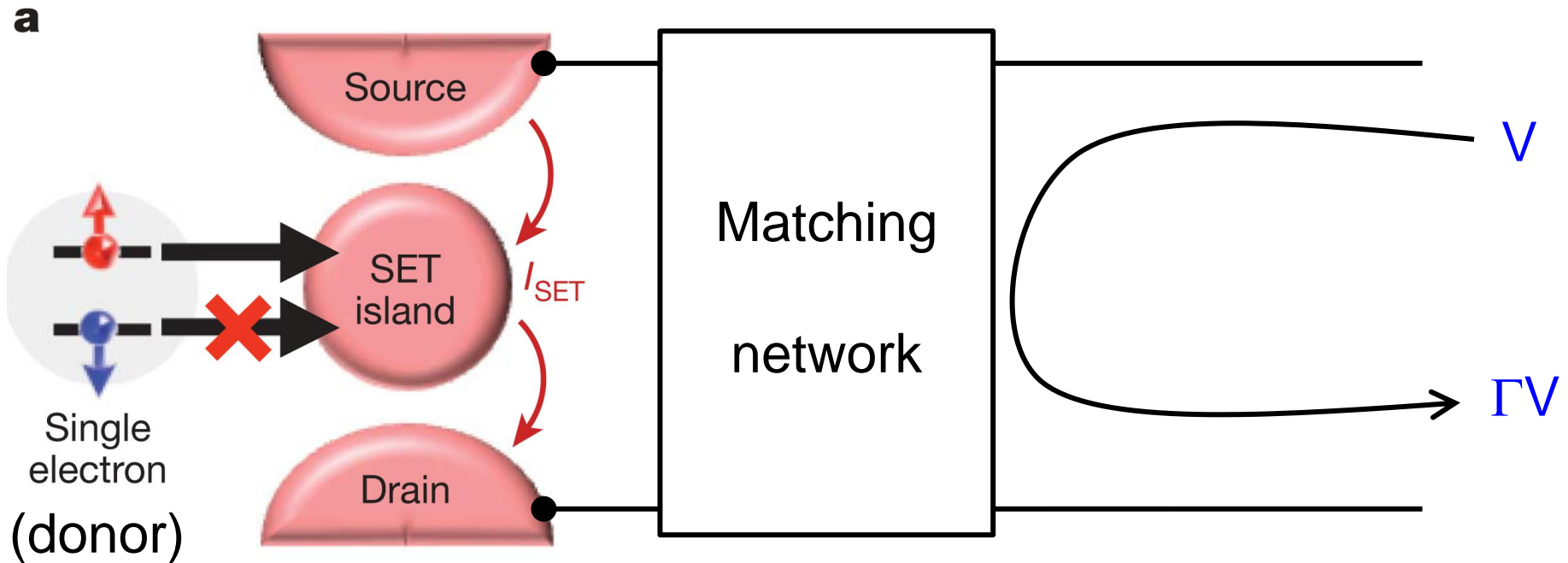


SET resistance depends on the donor charge that, in turn, depends on the spin

$$\Gamma = \frac{R_{SET} - Z_0}{R_{SET} + Z_0}$$

However, $R_{SET} > 25k\Omega$, $Z_0 \approx 50\Omega$ ➔ limited sensitivity

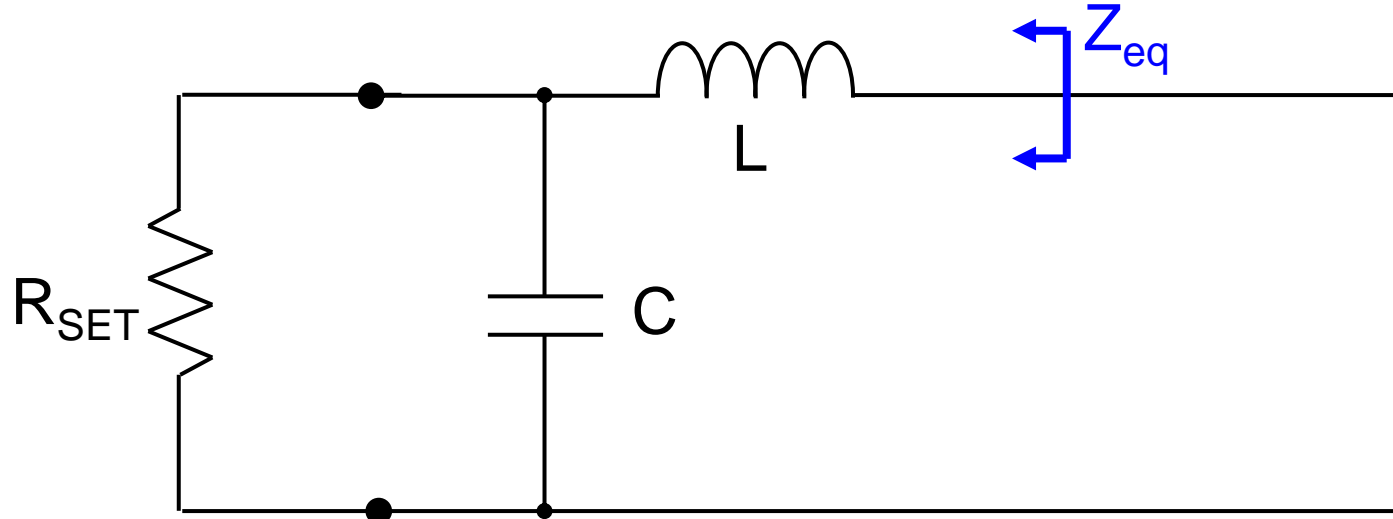
Matching network



SET resistance depends by the donor charge

Passive network to match the high resistance of the SET to the $Z_0=50\Omega$ of the line

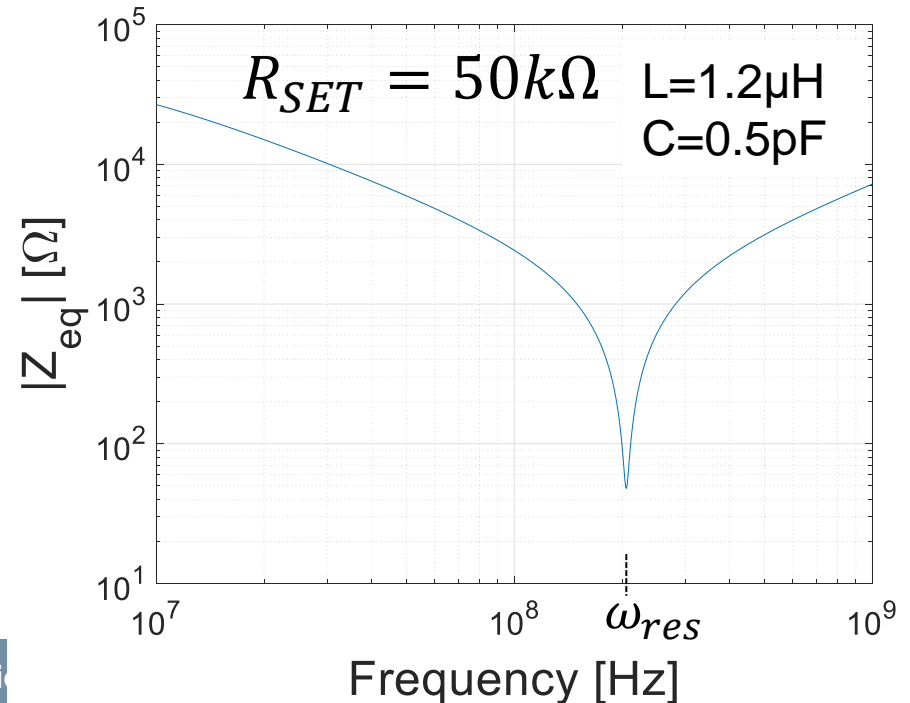
Matching network



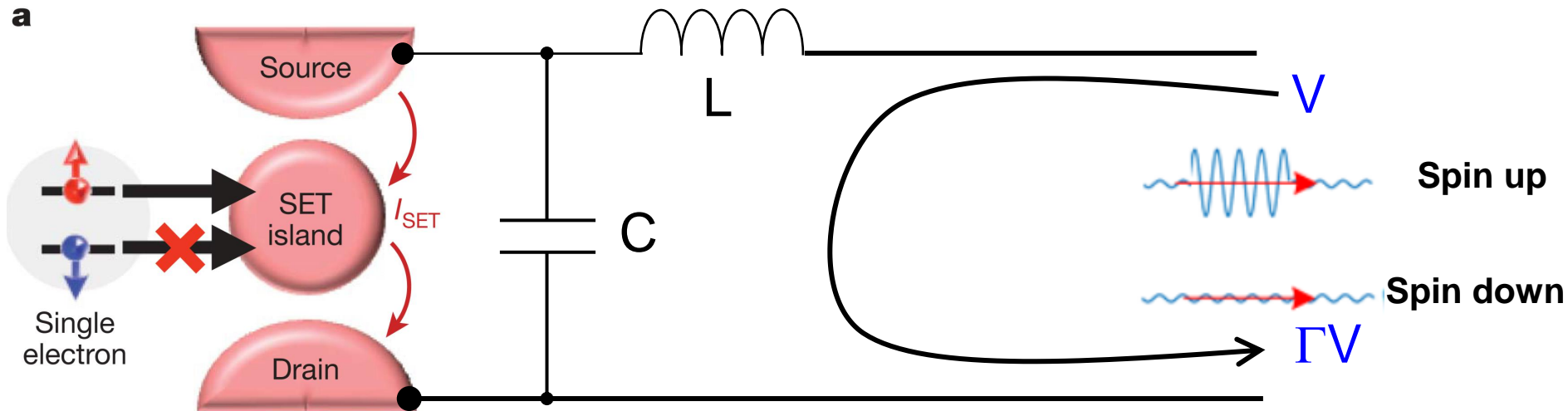
$$Z_{eq} = R_{SET} \frac{1 + \frac{sL}{R_{SET}} + s^2 LC}{1 + sCR_{SET}}$$

$$\omega_{res} = \frac{1}{\sqrt{LC}}$$

$$Z_{eq}(\omega_{res}) = \frac{L}{CR_{SET}}$$



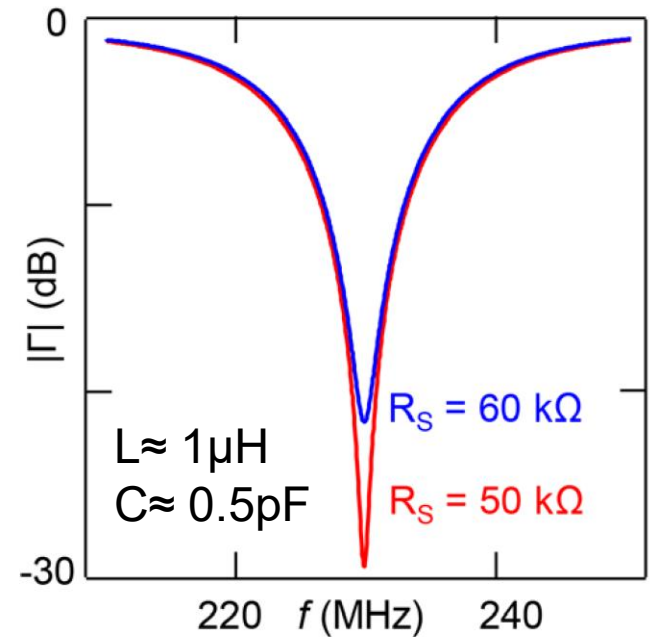
Matching network



$$\Gamma(\omega_{res}) = \frac{Z_{eq}(\omega_{res}) - Z_0}{Z_{eq}(\omega_{res}) + Z_0}$$

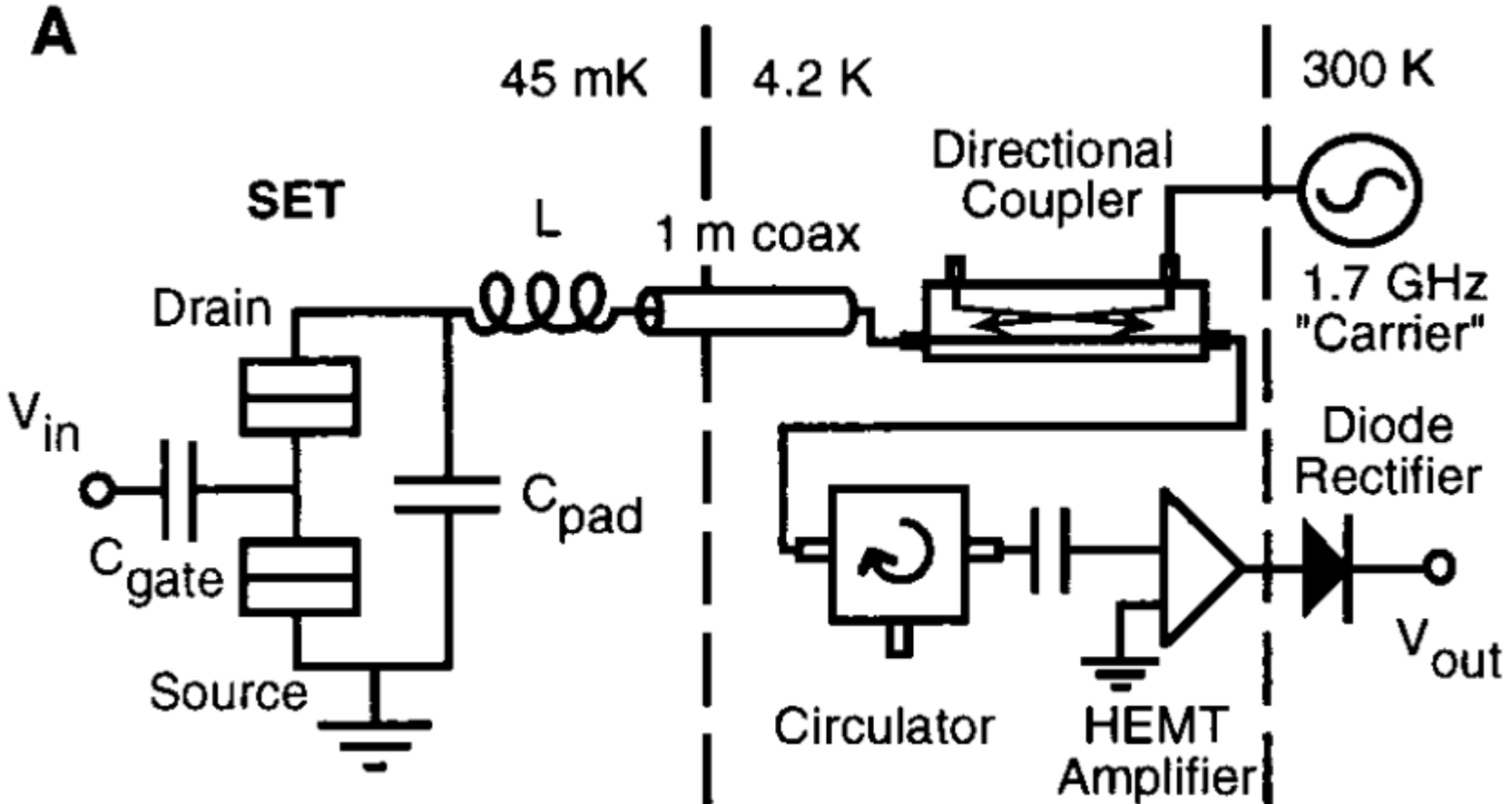
L, C selected to have $Z_L(\omega_{res}) \approx Z_0$

$$Z_{eq}(\omega_{res}) = \frac{L}{CR_{SET}}$$



Readout based on RF reflectometry

R. Schoelkopf, et al. "The radio-frequency single-electron transistor (RF-SET): A fast and ultrasensitive electrometer," *Science*, vol. 280, no. 5367, pp. 1238–42, May 1998



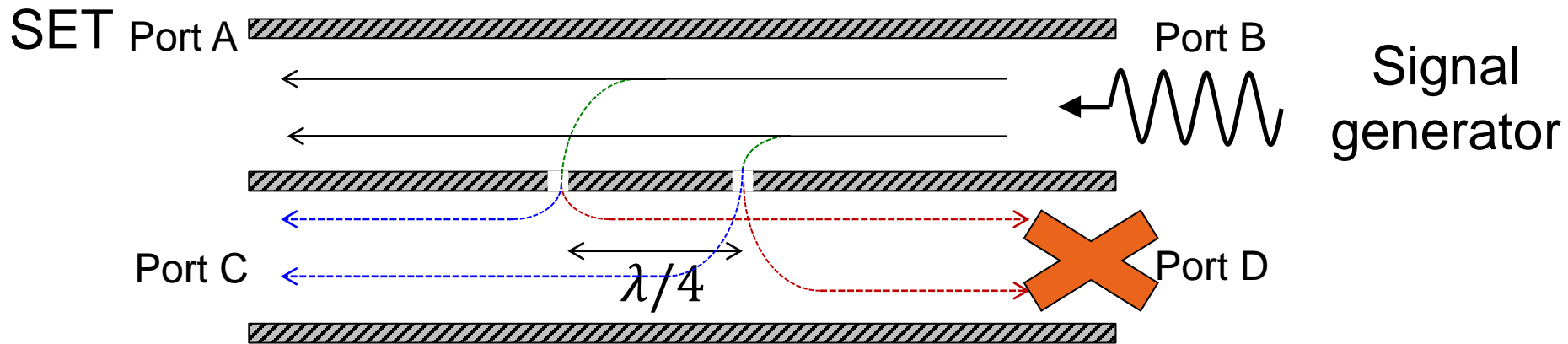
Reflectometry allows high-sensitivity impedance meas. despite long cables

(similar technique could be applied to the gate of the SET)

Recent review paper: F. Vigneau, et al. *Appl. Phys. Rev.* (2023), doi: 10.1063/5.0088229.

Directional coupler

Basic idea using waveguides:

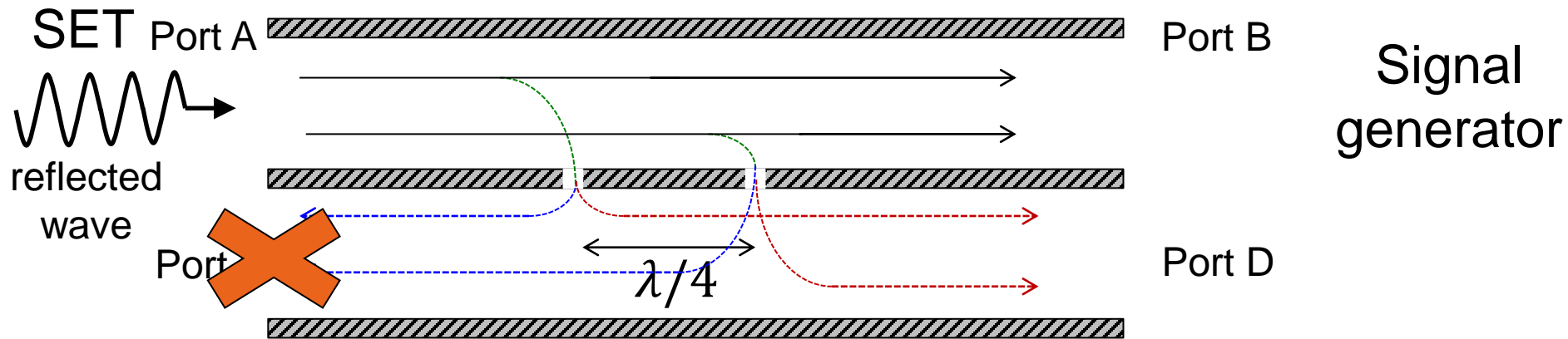


The contributions are added at port C.

However, since the paths differ in length by $\lambda/2$, they cancel at port D.

Directional coupler

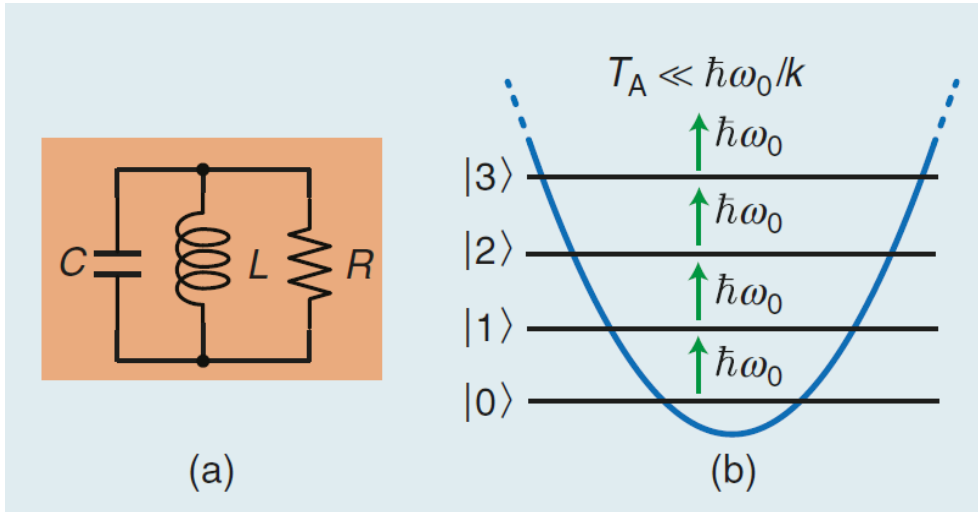
Basic idea using waveguides:



The only signal at port D is the reflected wave! (\ll voltage of the signal generator)

$$f=1\text{GHz} \rightarrow \lambda \approx 25\text{cm}$$

RF reflectometry for superconducting qubits

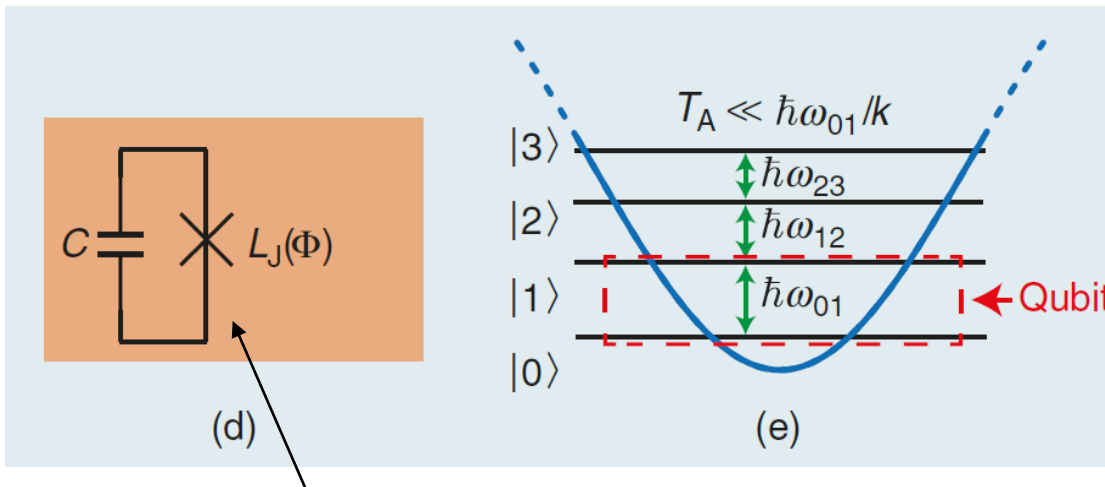


Standard linear resonator:

$$\hbar\omega_0 = 4\mu eV \text{ @ } 1\text{GHz}$$

$$\rightarrow T < 50\text{mK}$$

ω_0 excites all the transitions



non-linear resonator

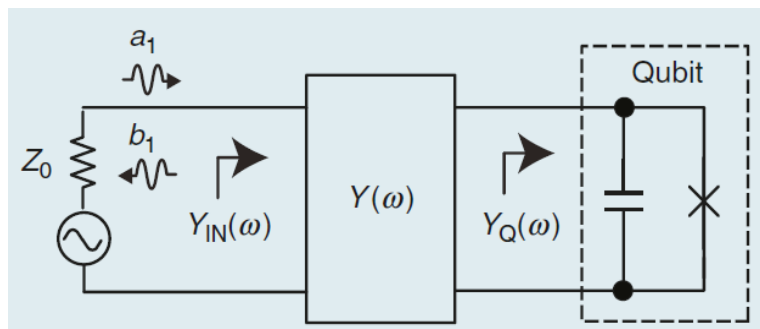
→ nonuniform energy level spacing

→ impedance depends on the oscillation amplitude, i.e. the qubit state!

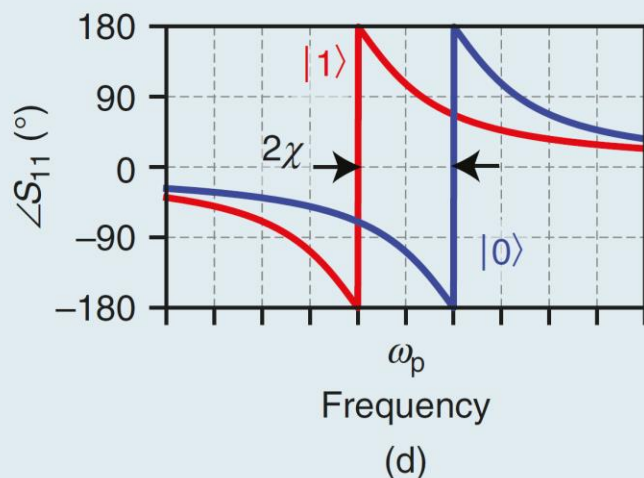
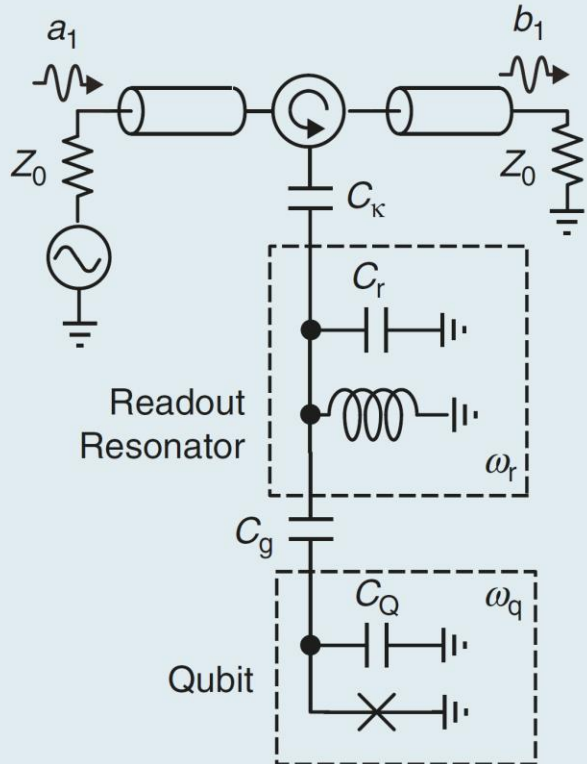
non-linear inductor
(Josephson junction)

[J. Bardin et al, IEEE Microwave Magazine, 2020]

Readout of superconducting qubits

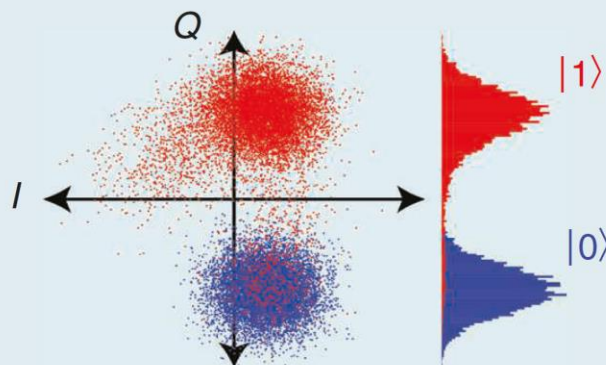


network $Y(\omega)$ for maximizing the signal and minimizing the perturbation on the qubit



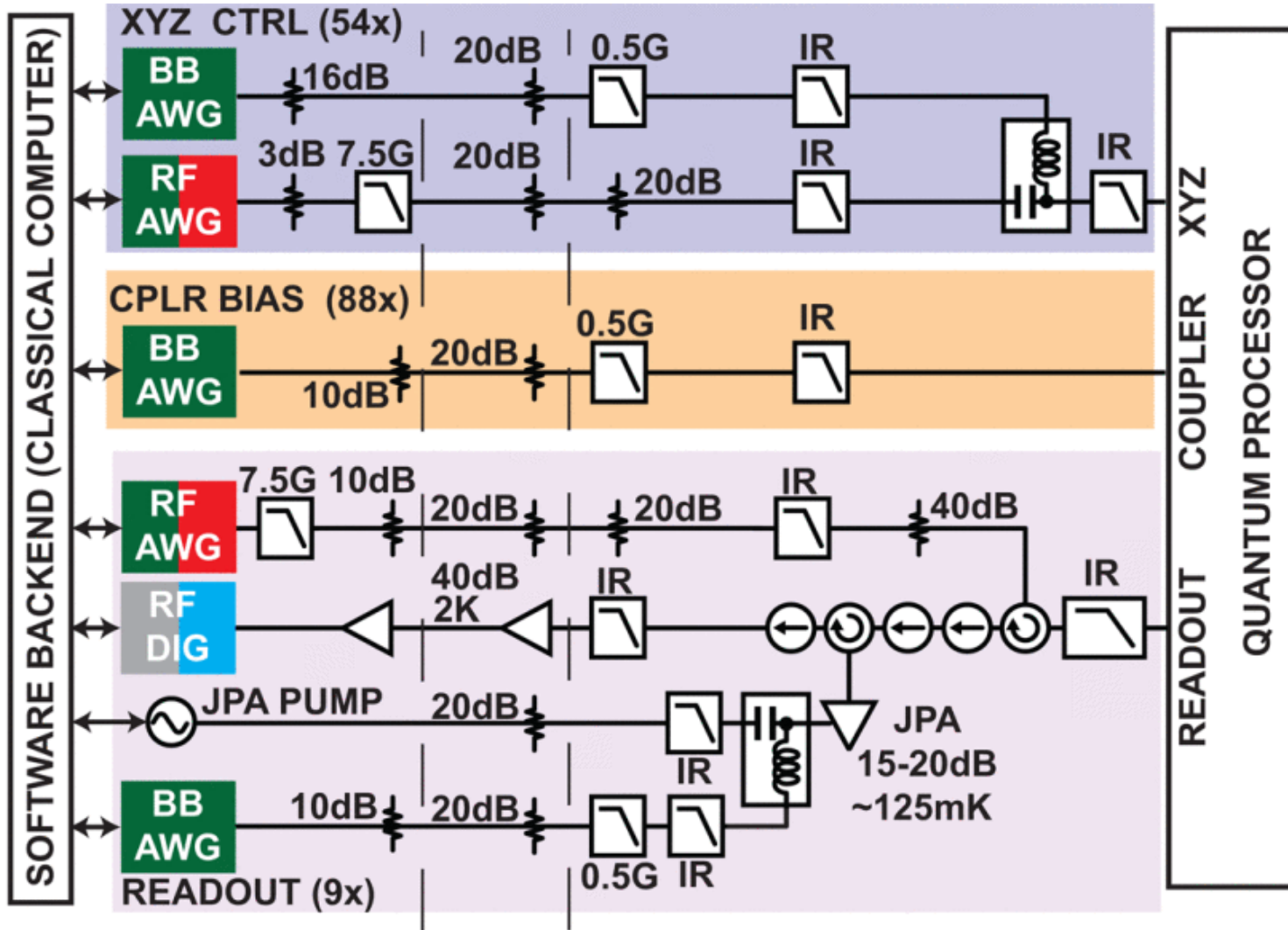
transmission line is not directly connected to the qubit

readout resonator freq. \neq qubit resonator freq.



[J. Bardin et al, IEEE Microwave Magazine, 2020]

Google quantum computer (sycamore)



54 qubits
(transmons)

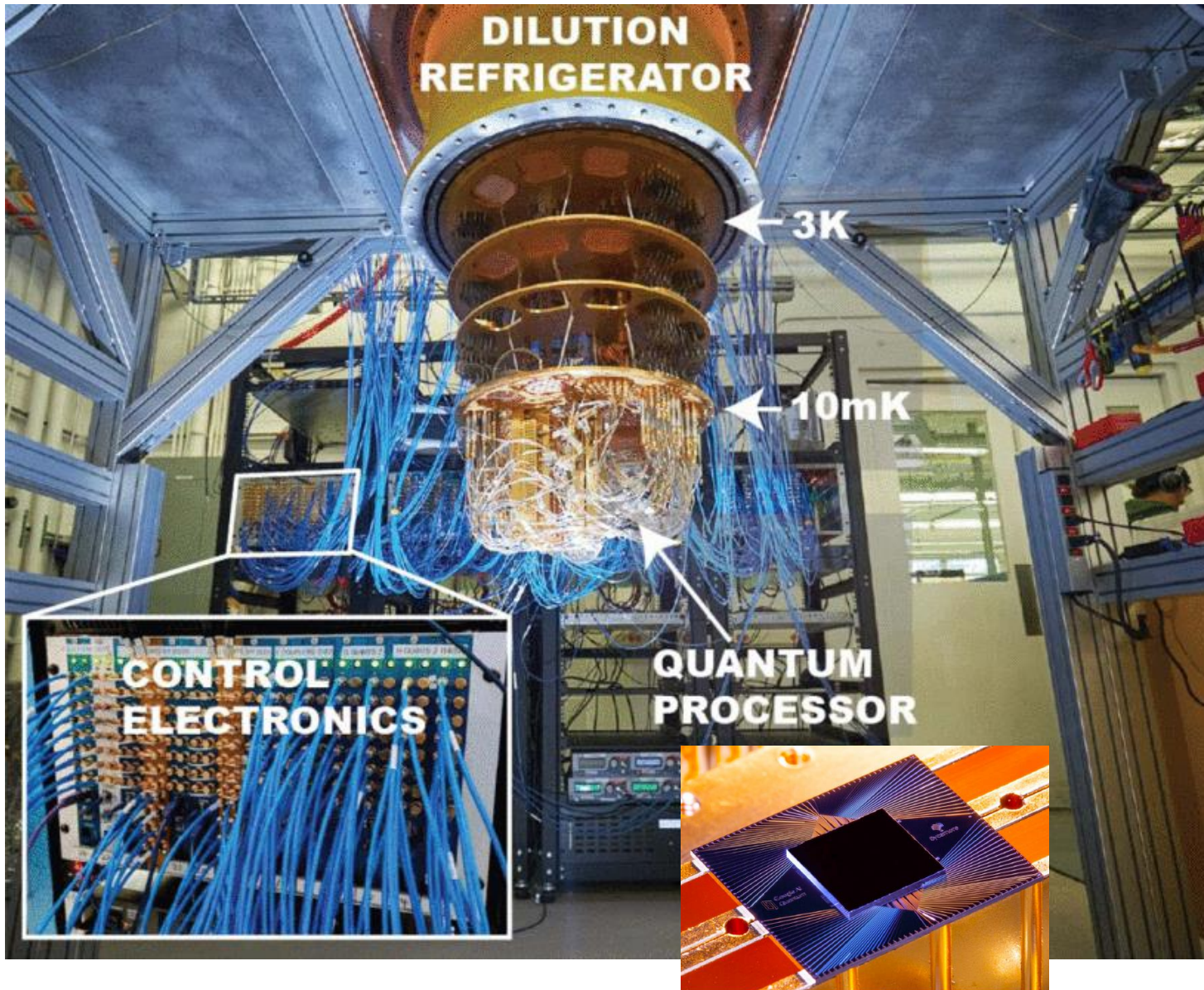
300 K

3 K

10 mK

[J. Bardin,
ISSSCC 2022]

Google quantum computer (sycamore)



[J. Bardin,
ISSCC 2022]

Quantum computer: wiring!

MIT
Technology
Review

Intelligent Machines

We'd have more
quantum computers if
it weren't so hard to
find the damn cables

by [Martin Giles](#), January 17, 2019

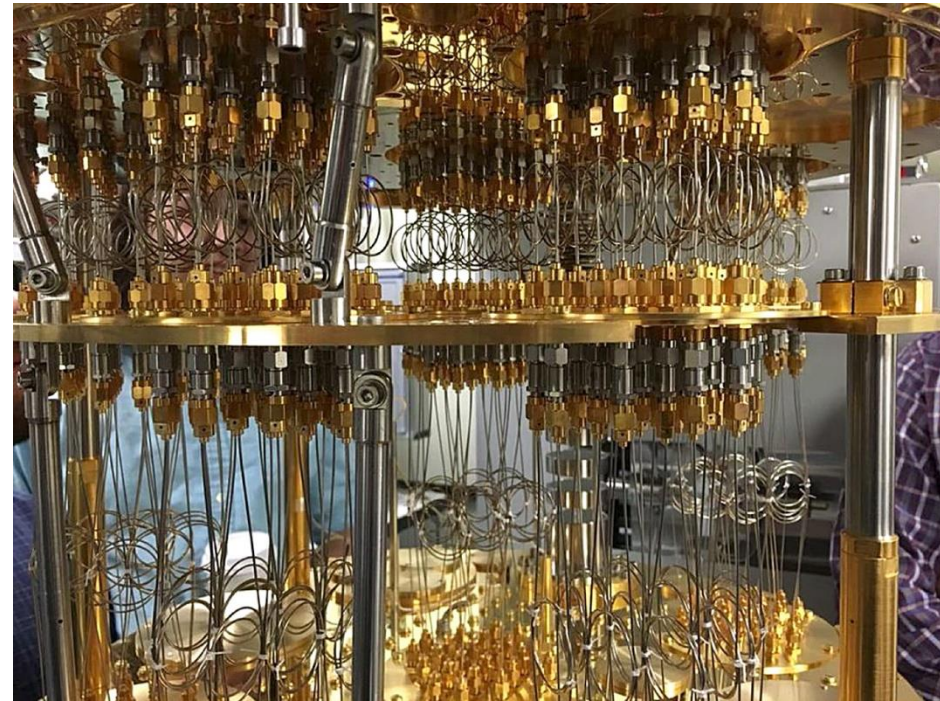
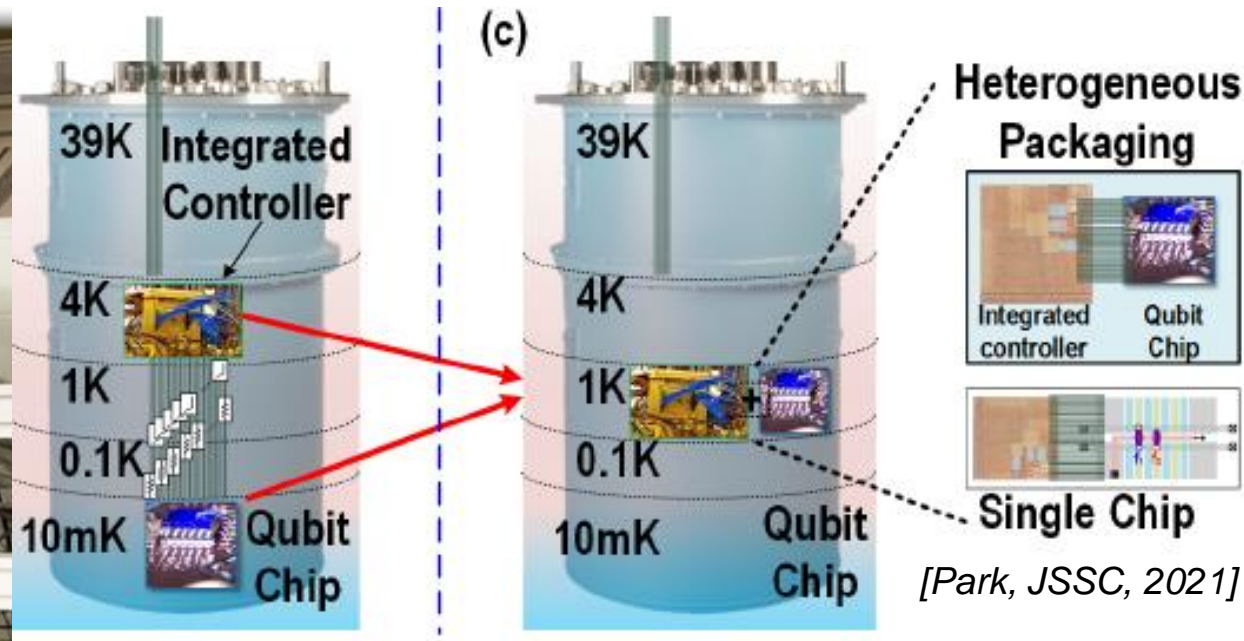
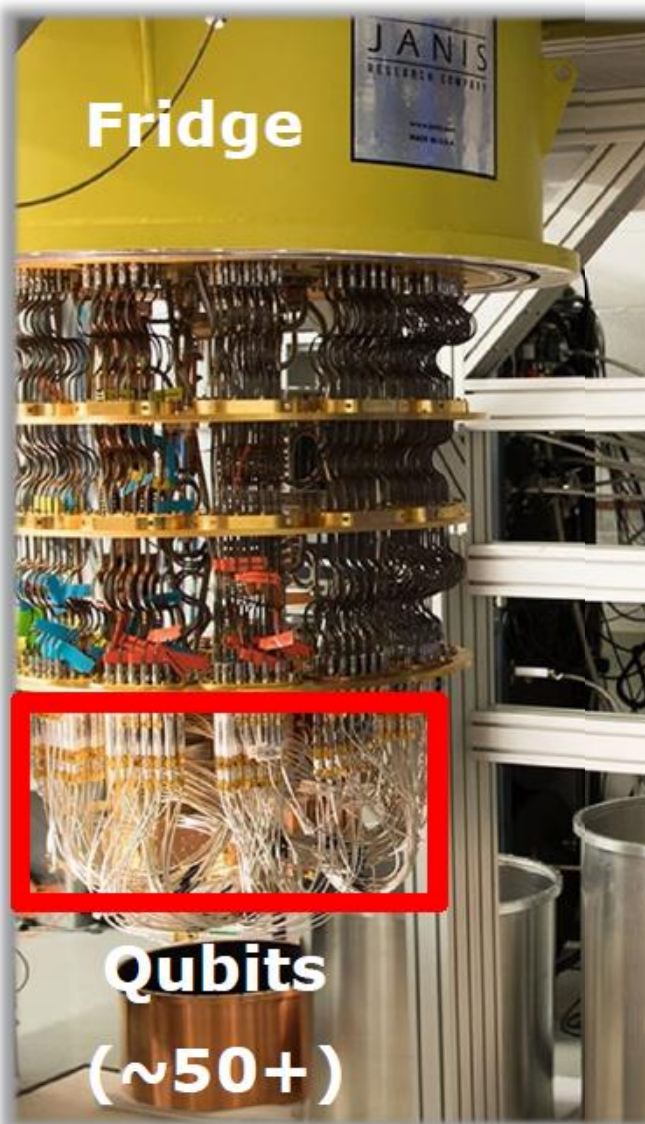


Image: IBM Research

Cables connecting qubits (<4K) to room temperature electronics are a limiting factor! (at least 2 coaxial cables / qubit)

- No space!
- No thermal budget! ($\approx 1\text{W}$ at 4K, $< 1\text{mW}$ at 10mK)

Quantum computer: cryogenic electronics!



Readout and control electronics should be operated at cryogenic temperature, ideally on the same chip of the qubits, to minimize the number of cables!

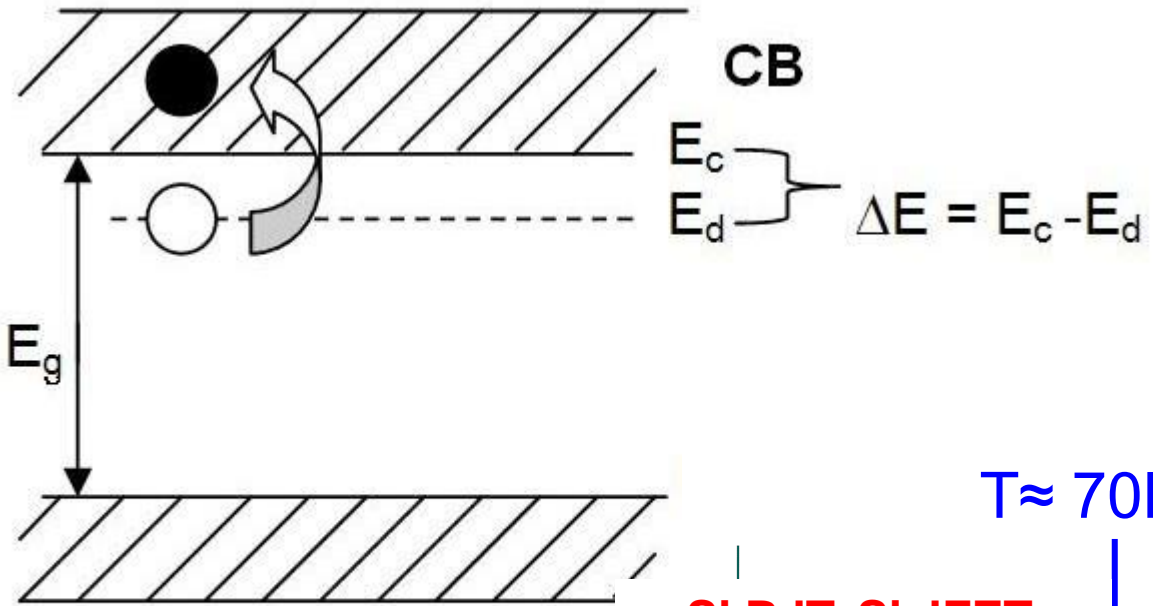
[Bardin, ISSCC 2019]

Outline

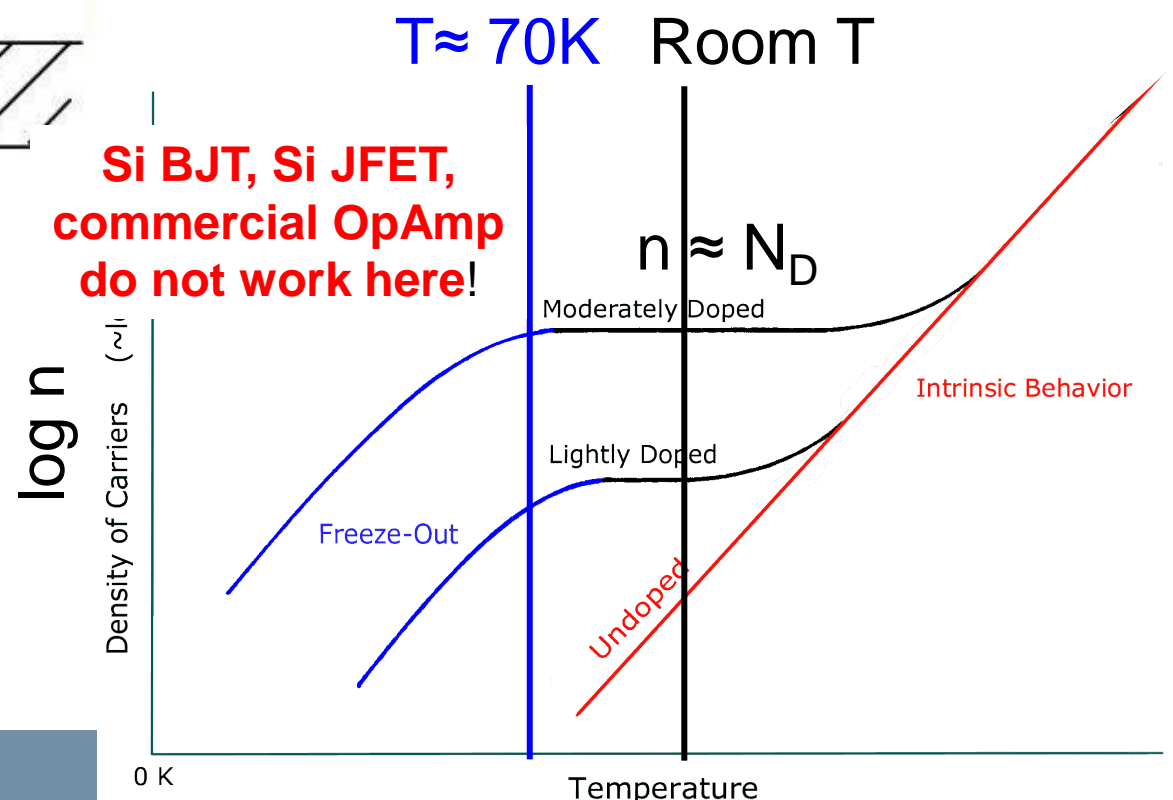
- Spin detection using room temperature instrumentation
- Cryogenic electronics
 - Challenges
 - Design rules
- Examples

Semiconductor freeze-out

<http://fog.ccsf.cc.ca.us/~wkaufmyn/>



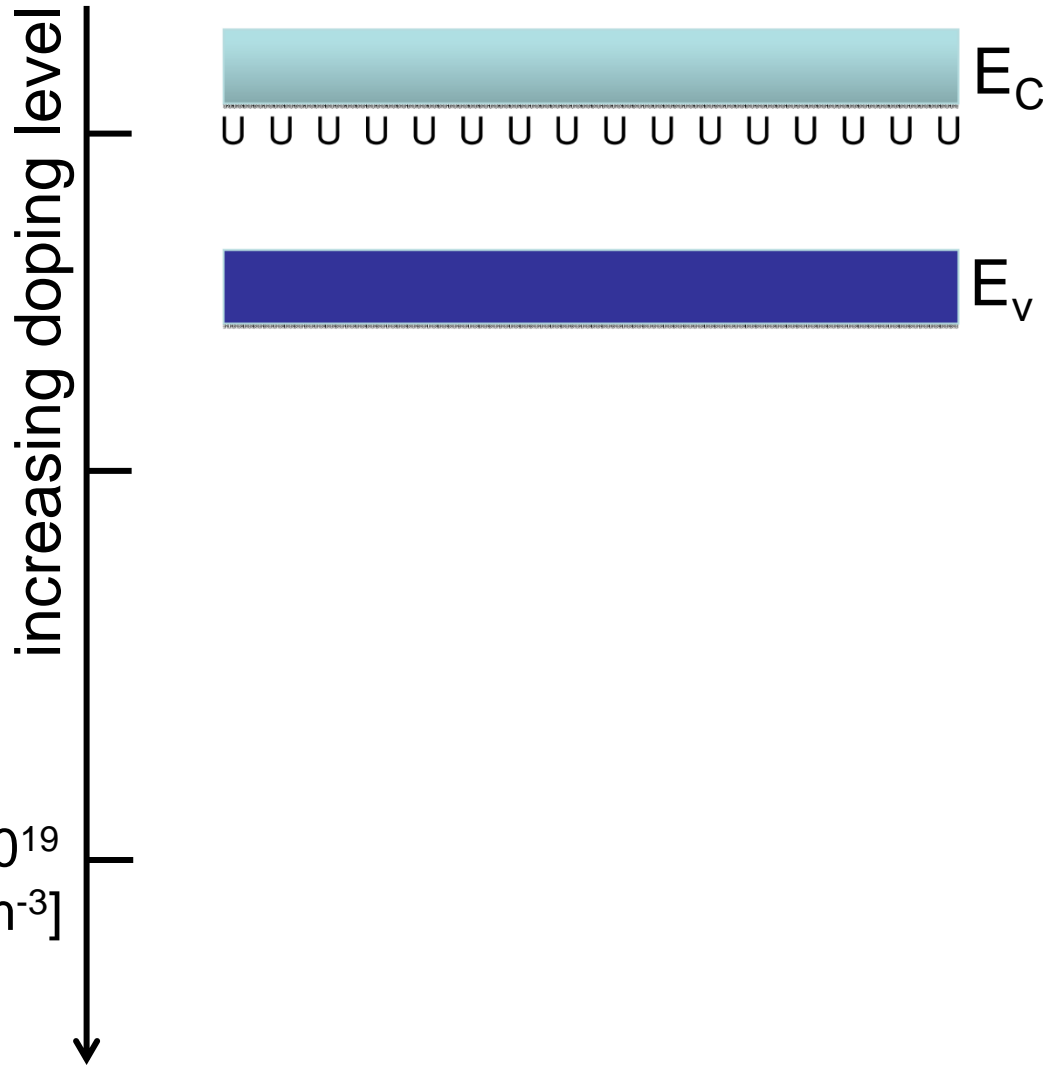
ionization energy for phosphorus: 45meV
 $kT|_{70K} = 6\text{meV}$



**Si BJT, Si JFET,
 commercial OpAmp
 do not work here!**

The impurity band model

Akturk et al., Silicon qubit workshop, 2009



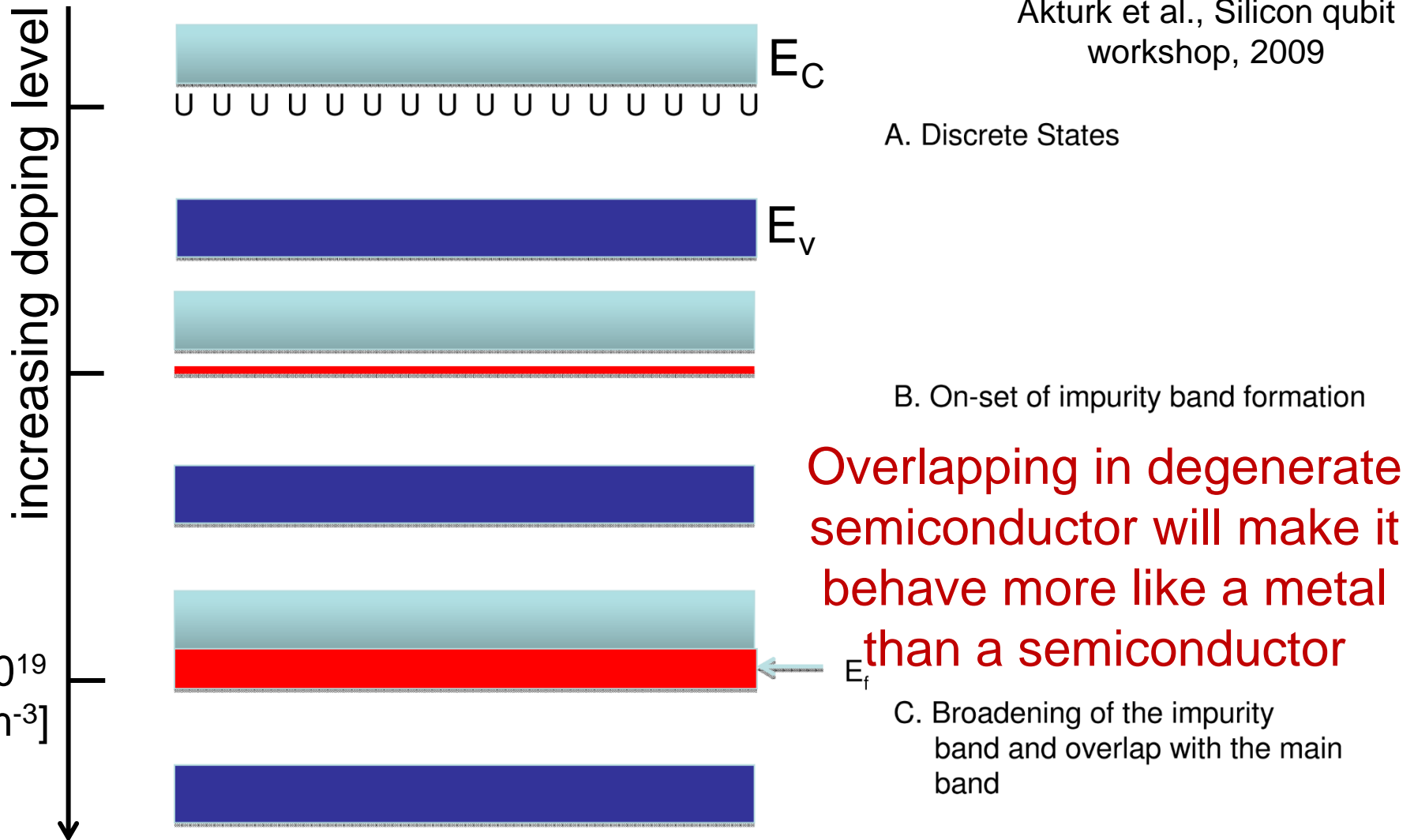
A. Discrete States

*Esther Conwell, "Impurity Band Formation In Germanium and Silicon," Phys. Rev. **103(1)**,51(1956)

E. Prati, G. Ferrari et al., Nature Nanotechnology 7, 443–447 (2012)

The impurity band model

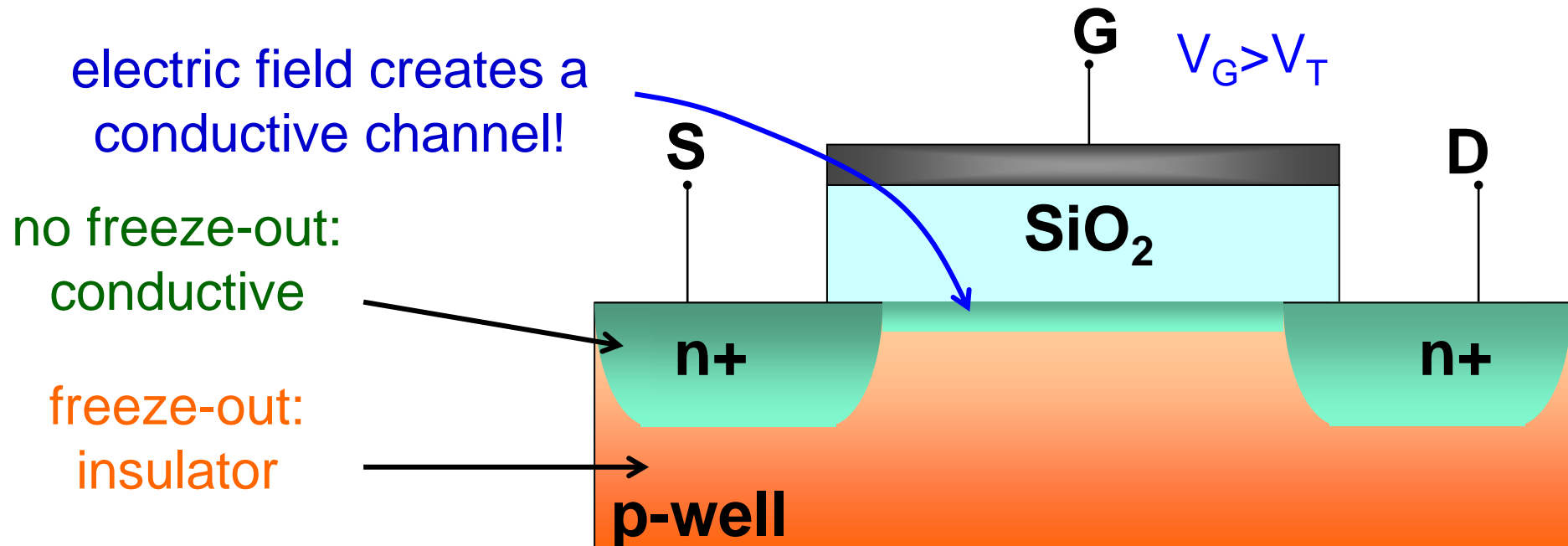
Akturk et al., Silicon qubit workshop, 2009



*Esther Conwell, "Impurity Band Formation In Germanium and Silicon," Phys. Rev. **103(1)**,51(1956)

E. Prati, G. Ferrari et al., Nature Nanotechnology 7, 443–447 (2012)

Electronics below the freeze-out temp.



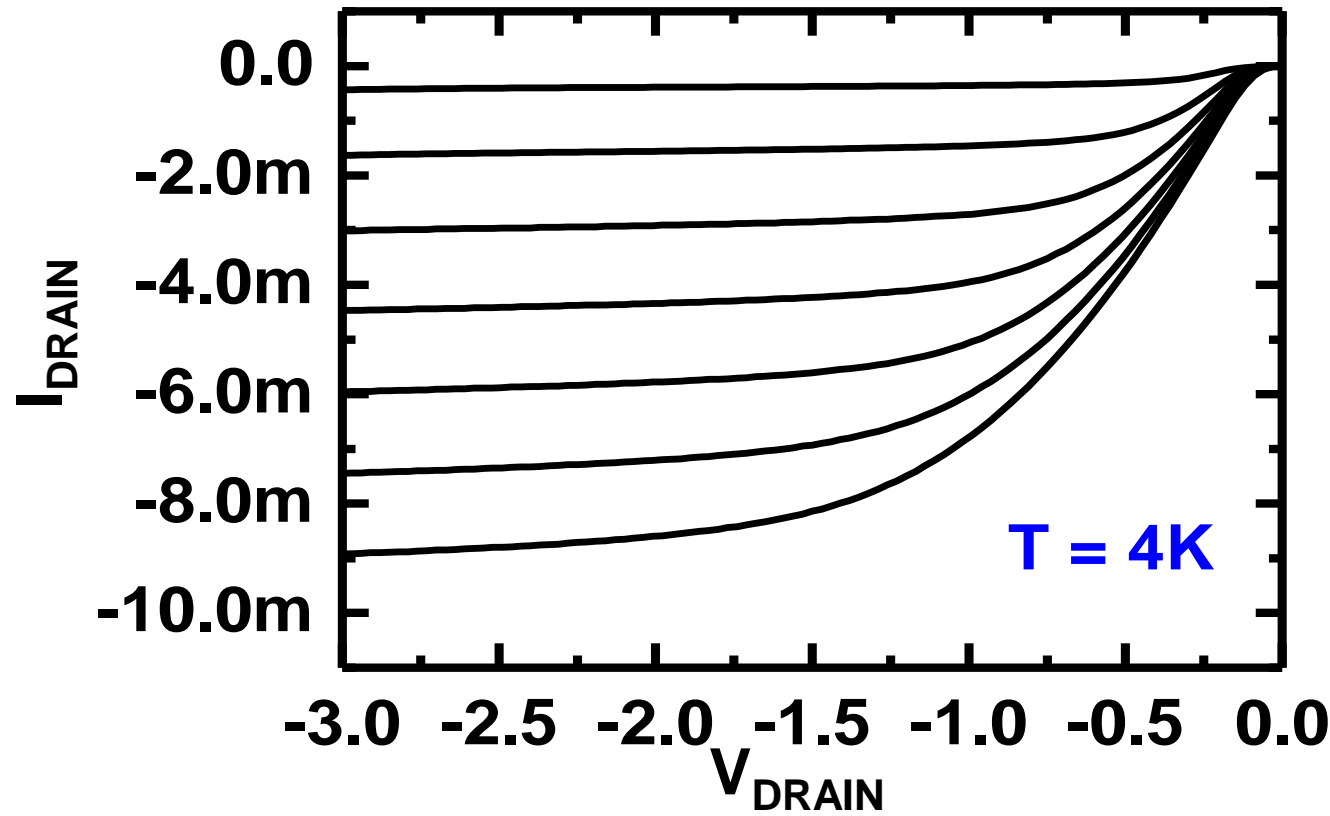
Silicon (standard) MOSFET operates below 40K!

Many GaAs devices operate at cryogenic temperature:
degenerate at 10^{16} cm^{-3}

Limitation: small (and expensive) scale integration

MOSFET operating at 4K

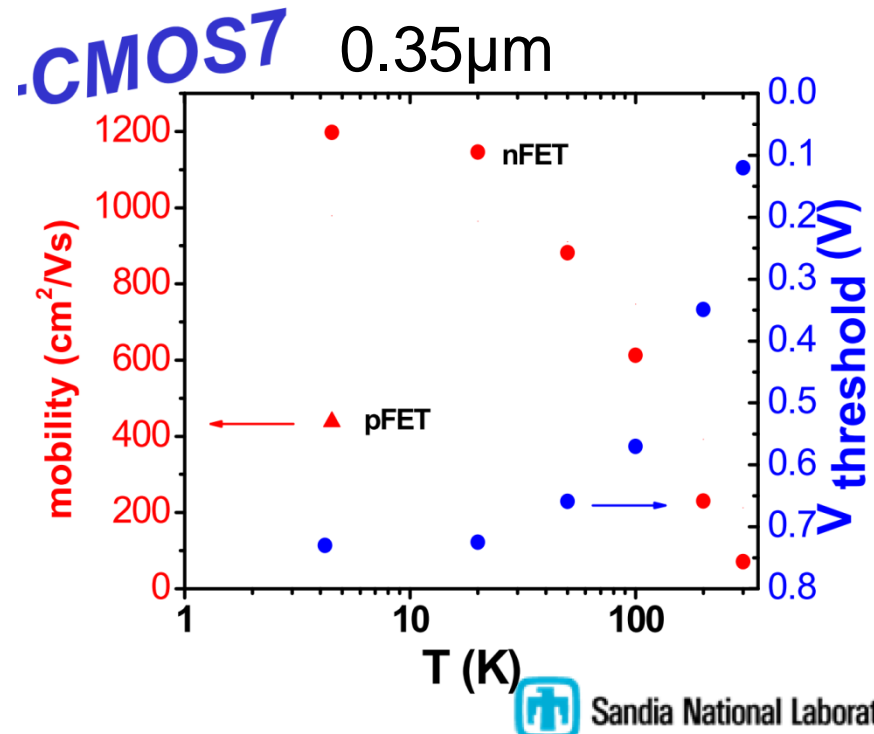
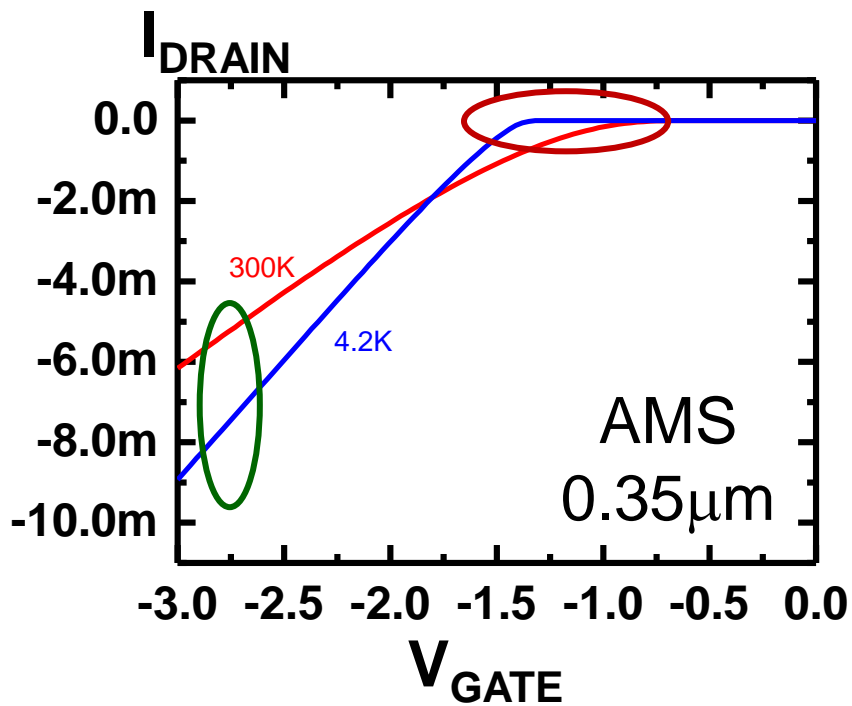
Standard analog CMOS Technology 3.3V, 0.35 μm
PMOS 50 μm / 0.7 μm



very similar to the room temperature behavior!

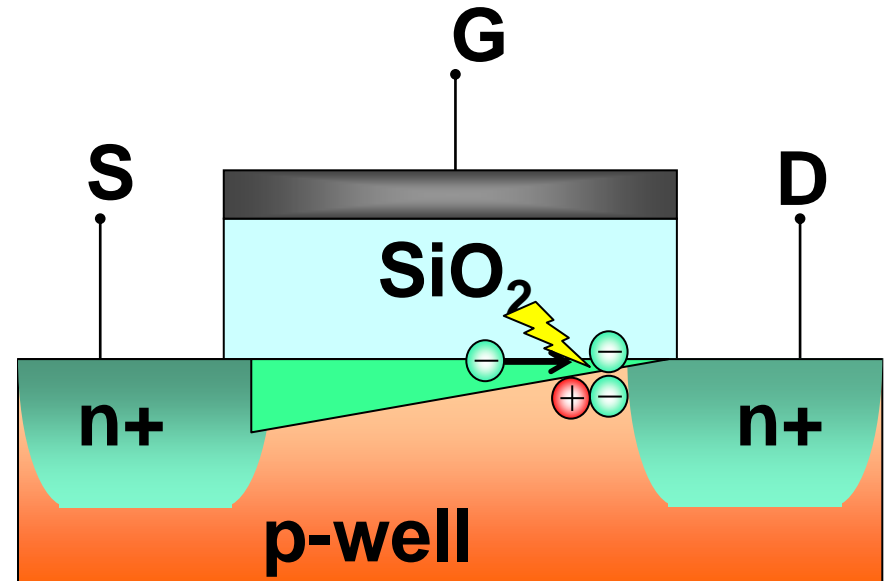
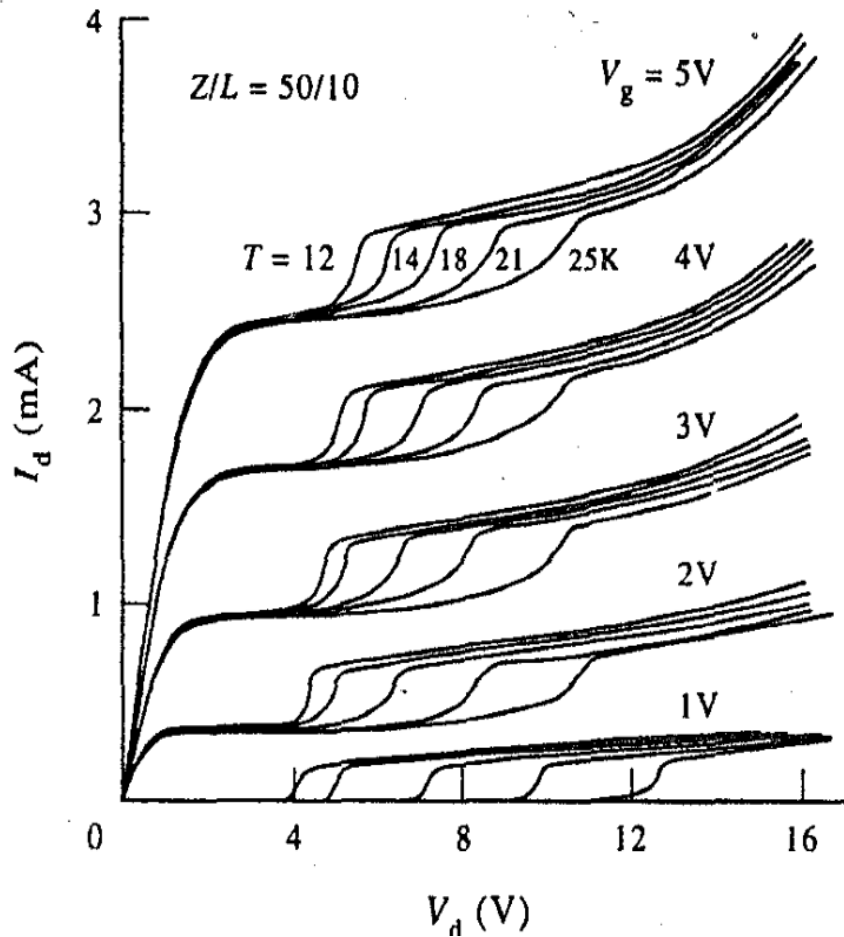
Effects of low temperature

- reduction in electron - phonon scattering
→ increase in carrier mobility
- substrate Fermi level shifts near to E_C (pMOS)
→ increase of the threshold voltage



MOSFET operating at 4K: problems

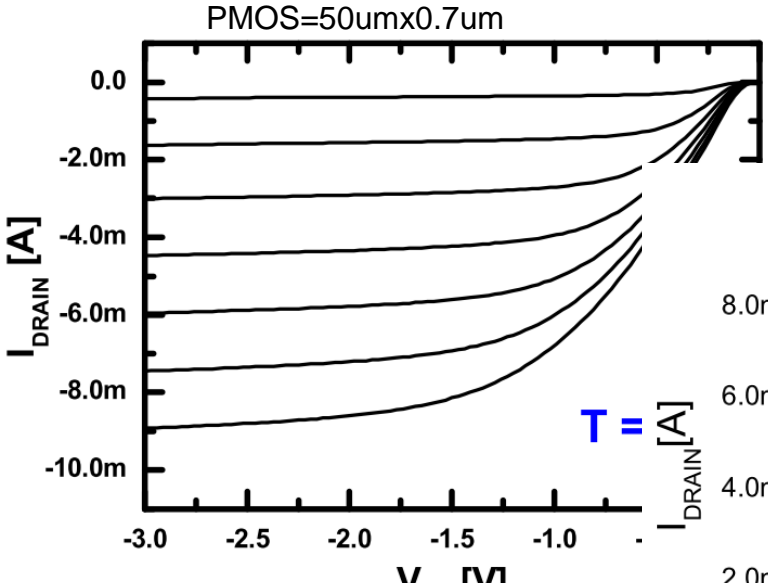
kink effect



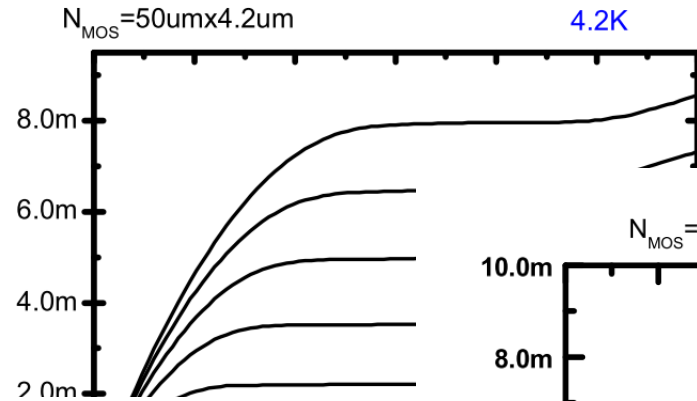
impact ionization \rightarrow accumulation of holes in the frozen bulk \rightarrow substrate potential increases $\rightarrow V_T$ decreases \rightarrow current increases

Ghibaudo, Balestra, "Low Temperature characterization of Silicon CMOS Devices", 1995

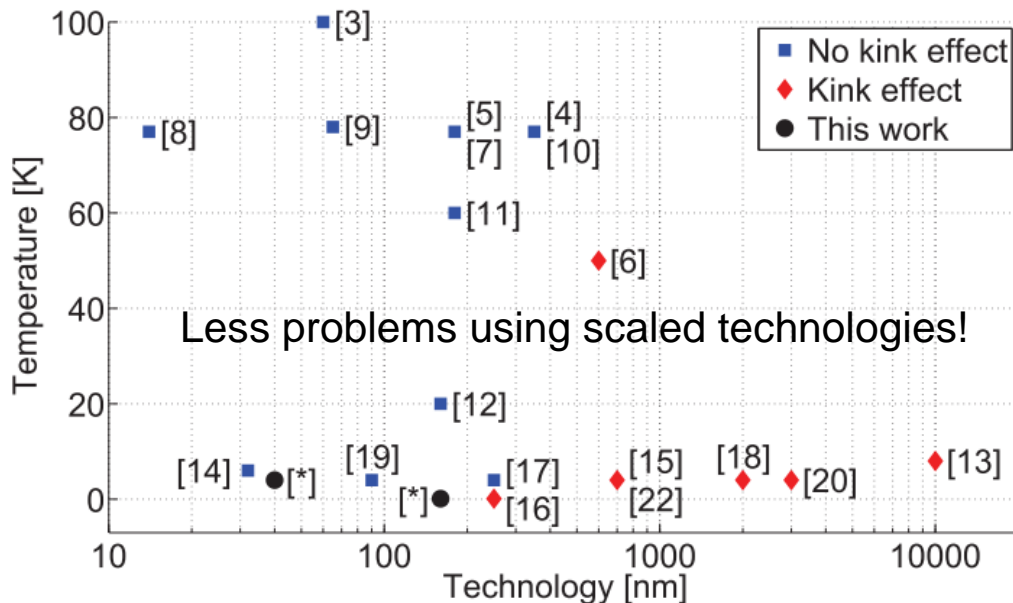
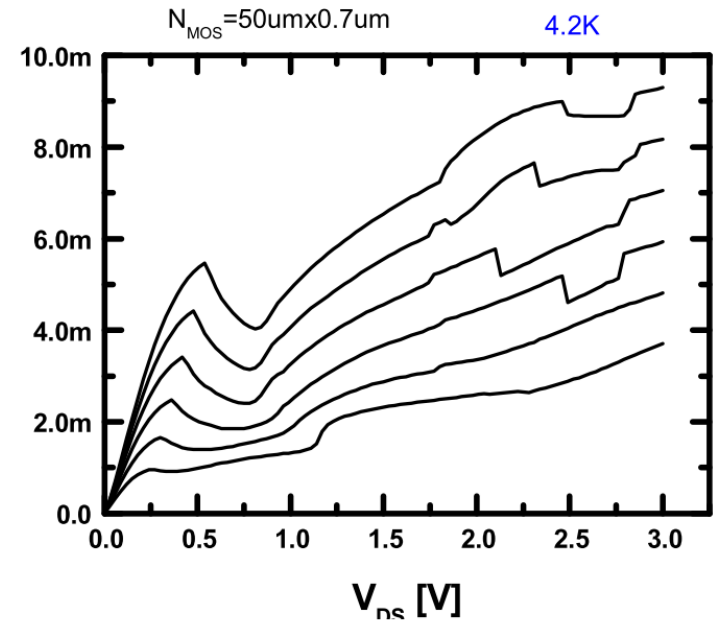
Problems are tech and size dependent



...and no models from the CMOS foundry!



AMS 0.35 μ m

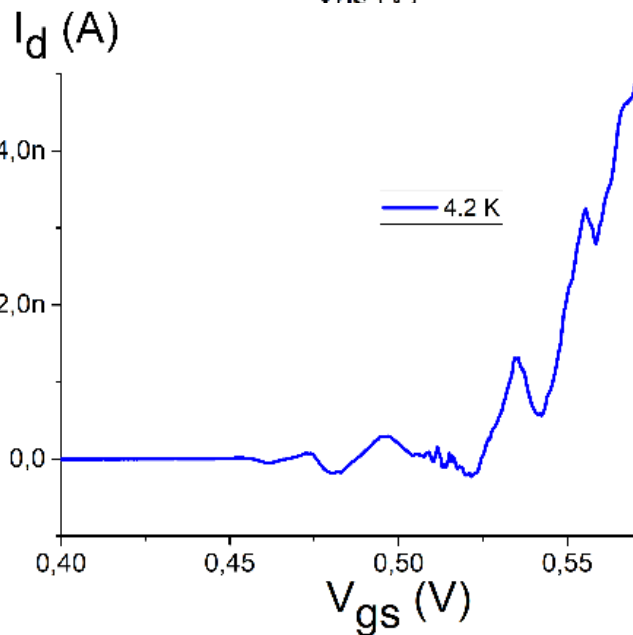
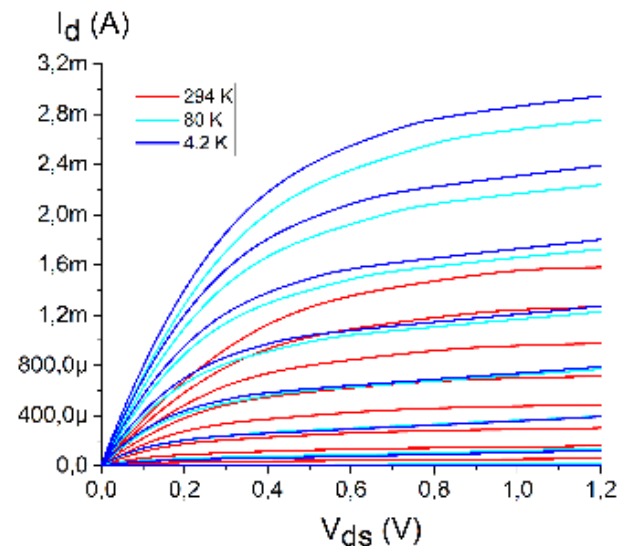
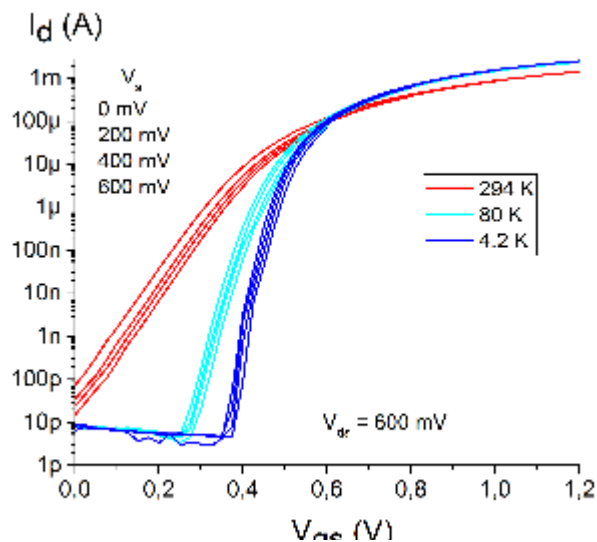


R. M. Incandela, et al., pp. 58–61, 2017 ESSDERC.

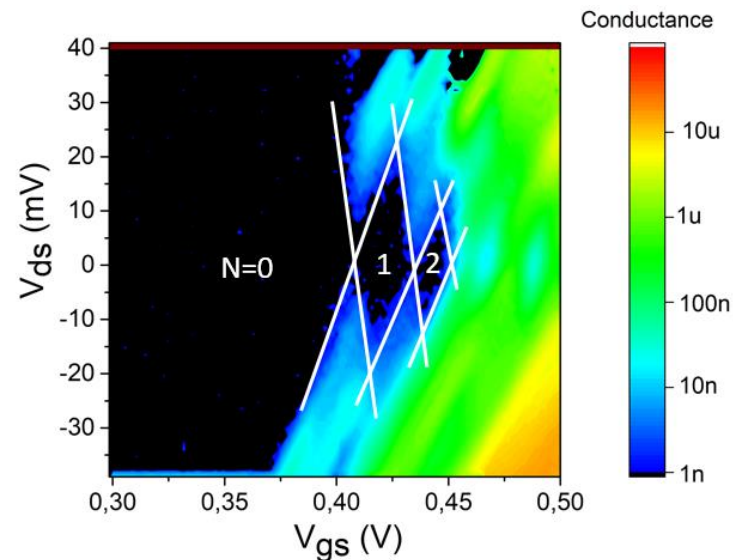
Quantum effects in small size MOSFETs!

110nm CMOS

$$\frac{W}{L} = \frac{10\mu\text{m}}{0.5\mu\text{m}}$$

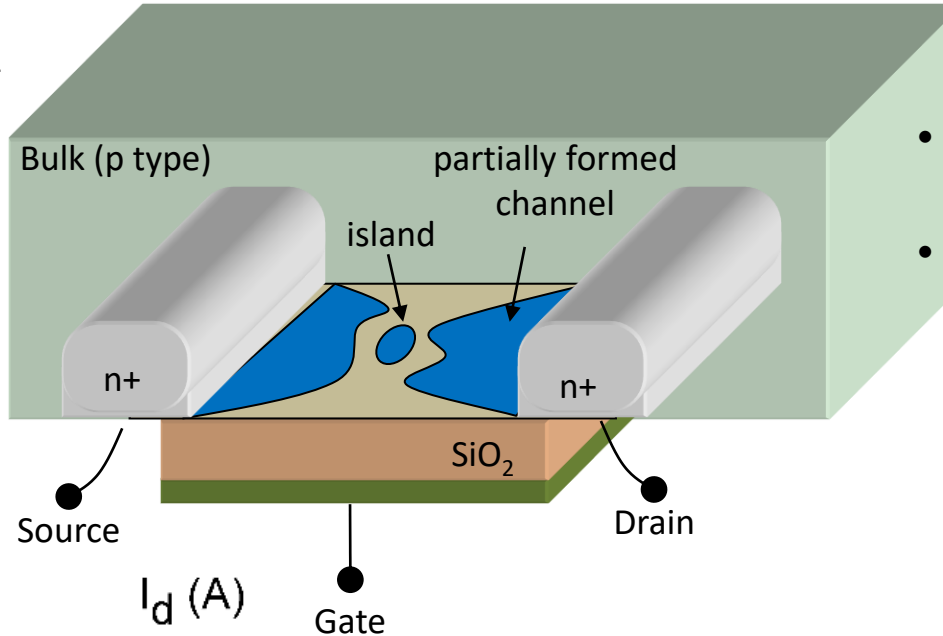


$$\frac{W}{L} = \frac{140\text{nm}}{100\text{nm}}$$

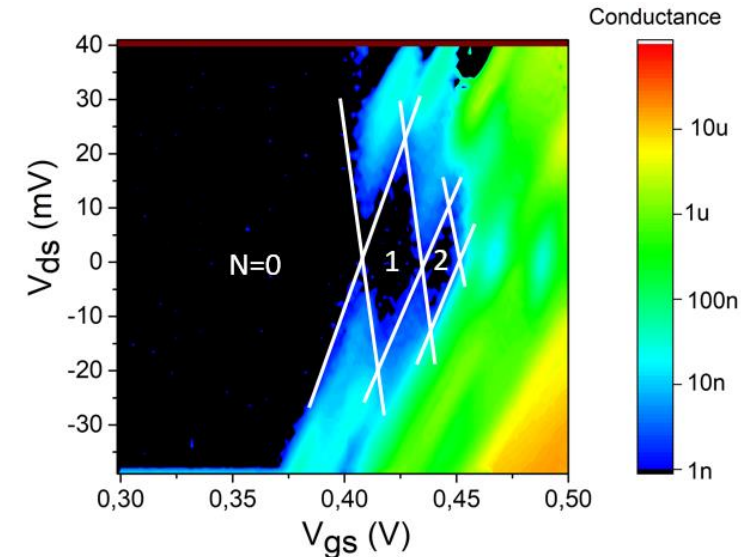
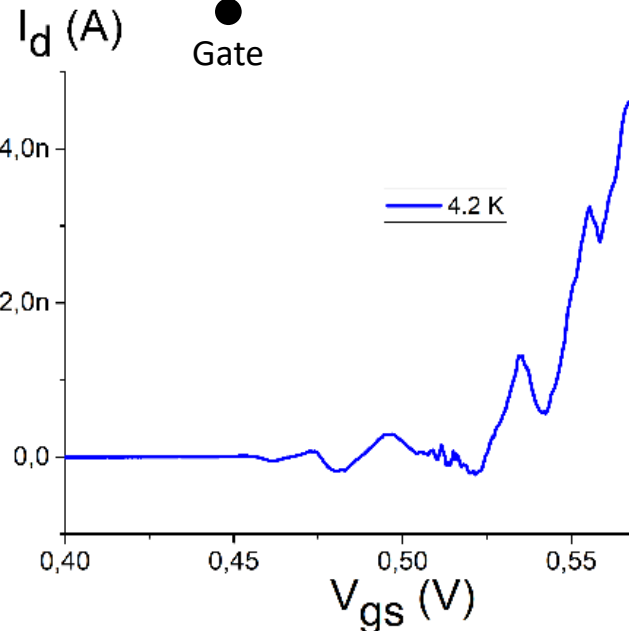


Quantum effects in small size MOSFETs!

110nm CMOS



- disorder at the Si/SiO₂ interface at $V_G \approx V_T$
- donor atoms can be randomly diffused in the channel region



$$\frac{W}{L} = \frac{140\text{nm}}{100\text{nm}}$$

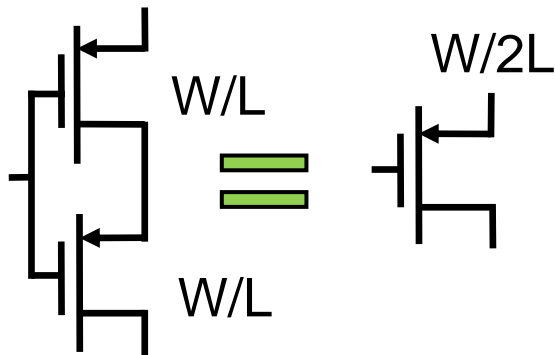
Design rule 1: characterize the technology!

MOS parameters strongly depend on the size and tech

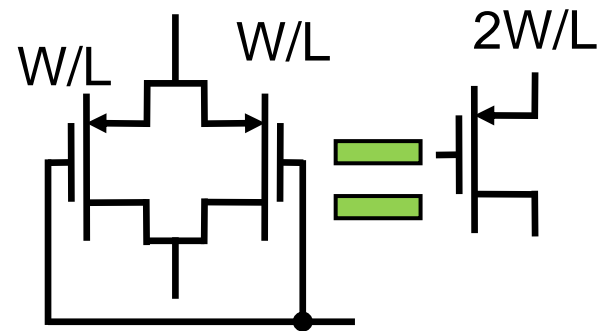


Experimental characterization of YOUR technology
is MANDATORY

For simple circuits 1 nMOS and 1 pMOS is enough
series or parallel combinations of these basic transistors

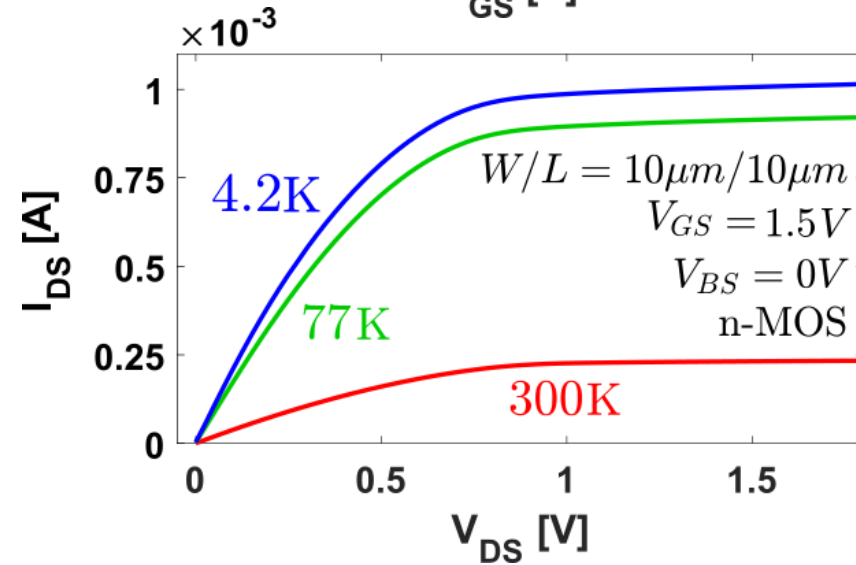
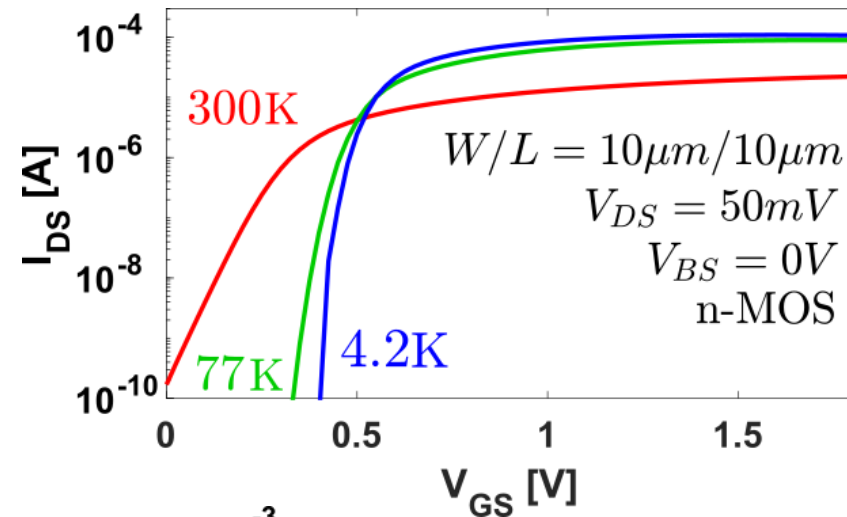


less conductive MOS



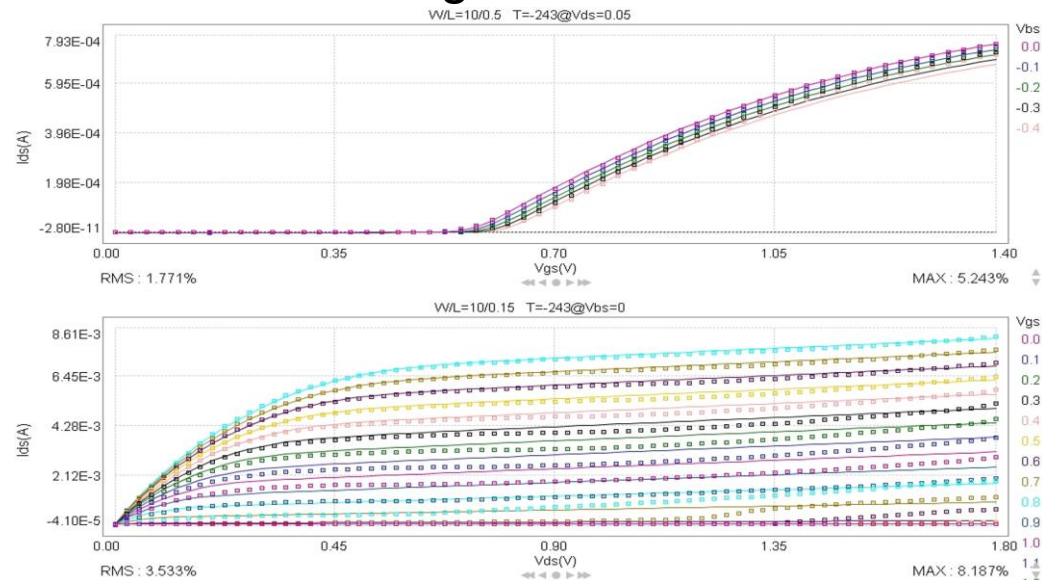
more conductive MOS

150nm CMOS technology – DC characterization



	RT	4.2K	$\Delta\%$
V_{Th}	0,4V	0,56V	+40%
μ_0	$300 \frac{cm^2}{Vs}$	$900 \frac{cm^2}{Vs}$	+200%
STS	$70 \frac{mV}{dec}$	$7 \frac{mV}{dec}$	-90%

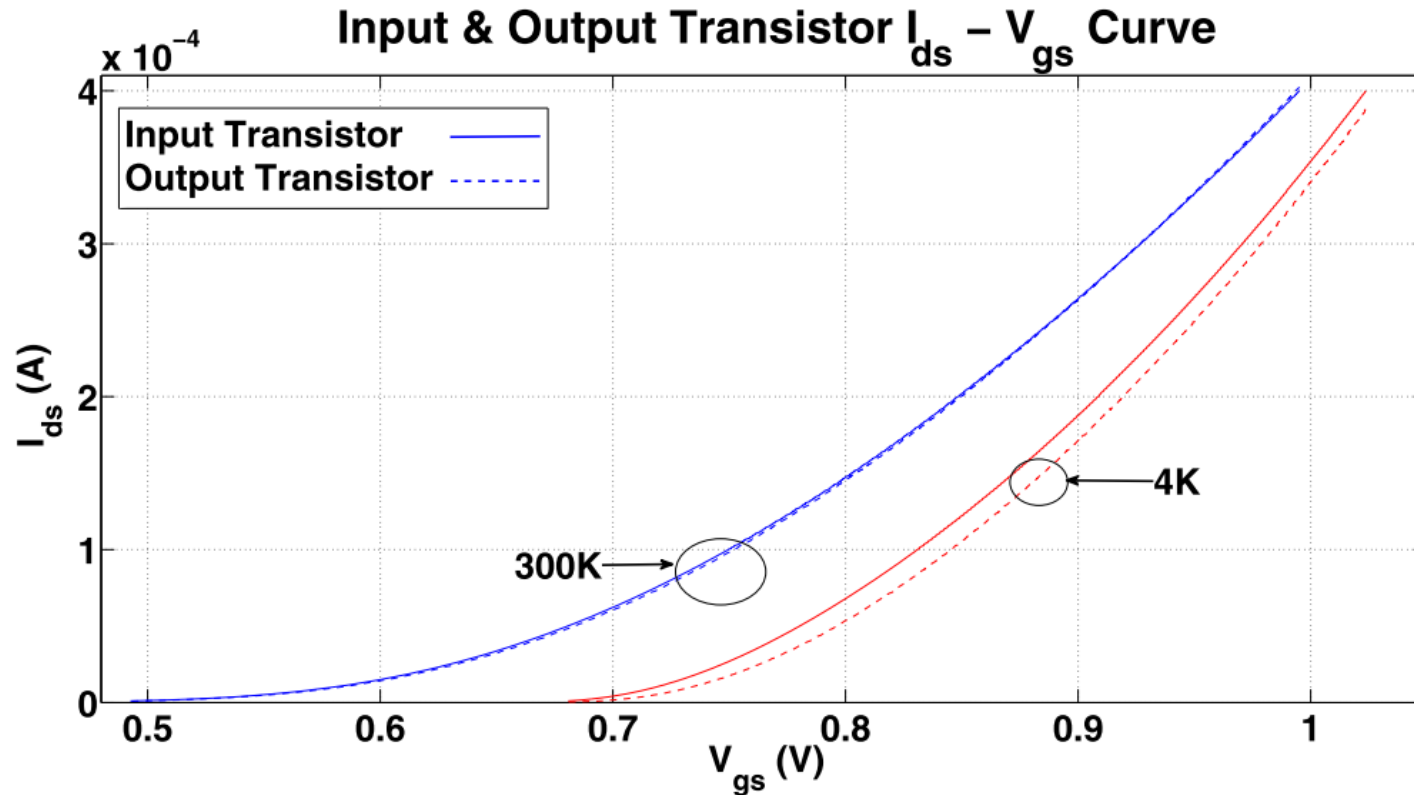
Standard BSIM models are accurate enough:



□ n-MOS $err_{MAX} \approx 15\%$ (peak 23%)

□ p-MOS $err_{MAX} \approx 18\%$ (peak 32%)

Design rule 2: pay attention to mismatch!



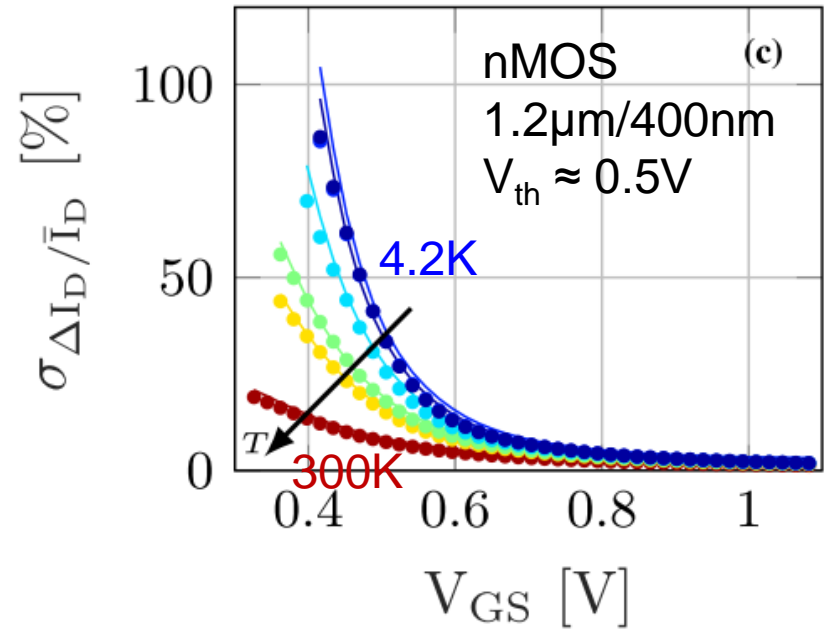
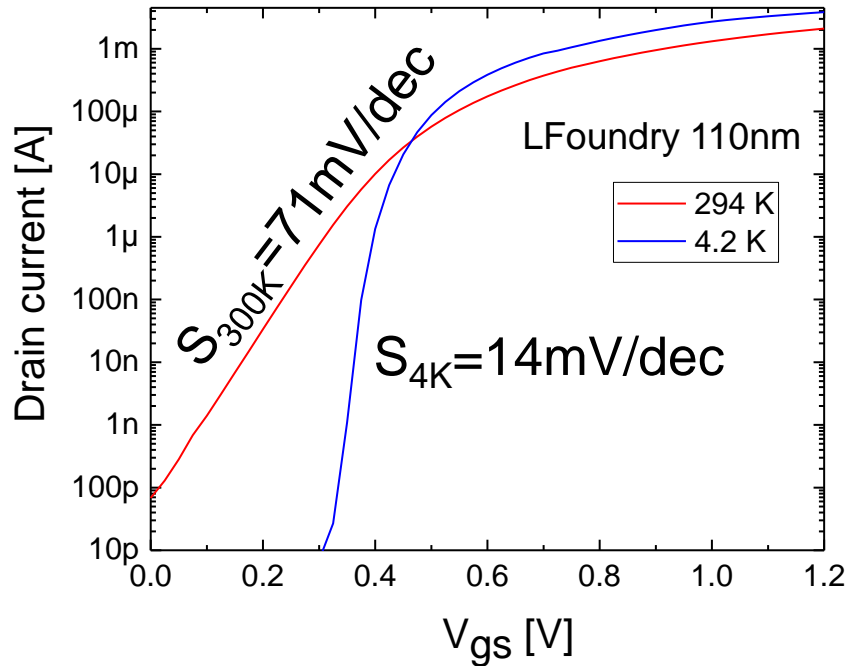
K. Das et al. EEE Symposium on Circuits and Systems, 2010

worsening of mismatch by a factor of 1.5-3 at low temperature compared to room temperature (tech dependent).



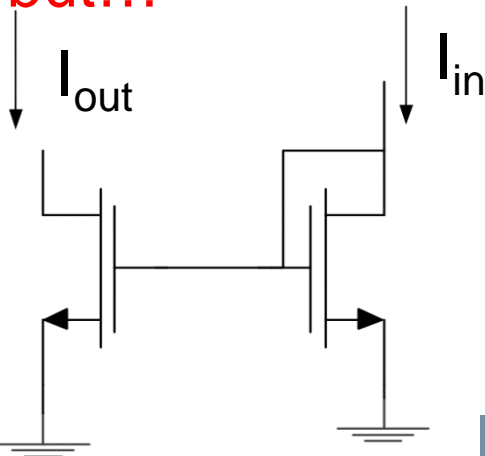
Degradation of the offset voltage, linearity of ADC, DAC, bias setting

Design rule 3: subthreshold is critical



P. A. T'Hart, et al. *IEEE J. Electron Devices Soc.*, pp. 263–273, 2020

Higher g_m and I_{on}/I_{off} , good!
but...



V_T mismatch of 5mV:

$$I_{out,300K} \approx I_{in} 10^{\frac{5mV}{S_{300K}}} = I_{in} \cdot 1.17$$

$$I_{out,4K} \approx I_{in} 10^{\frac{5mV}{S_{4K}}} = I_{in} \cdot 2.28$$

Design rule 4: dynamic range

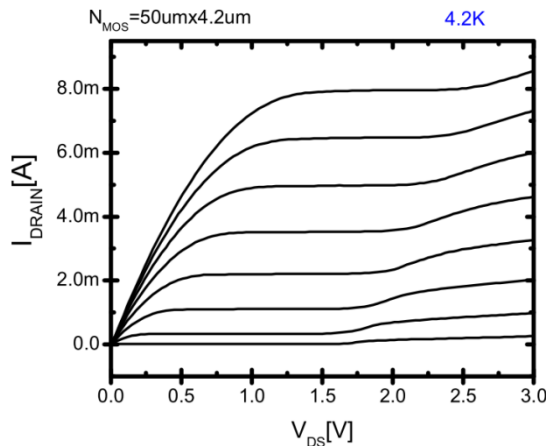
AMS 0.35 μm : parameters from 300K to 4K

- $V_{T,n}$ from 0.45V to 0.7V
- $V_{T,p}$ from -0.7V to -1.4V
- Power supply: still 3.3V
- no subthreshold

stack up few transistors!

and

kink effect



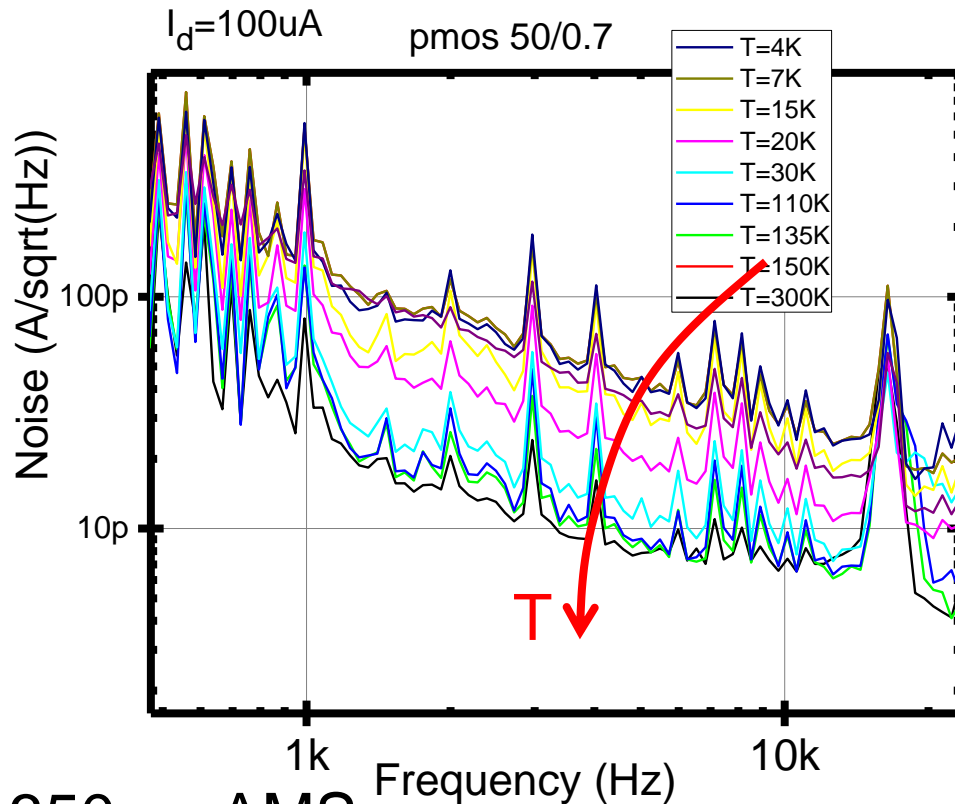
limit the V_{DS} !

Noise

Thermal noise: $\overline{e_n^2} = 4kT \frac{\gamma}{g_m}$

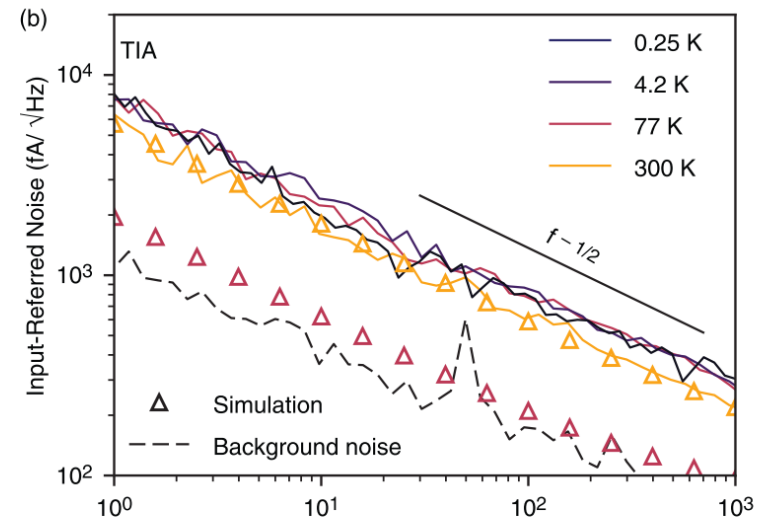
$T \searrow$, $g_m \nearrow \rightarrow$ **noise** $\searrow \searrow$
(0.1 nV/√Hz)

Flicker noise: usually does not decrease



**dominant noise up to
tens of MHz**

28nm FDSOI tech.



350nm AMS

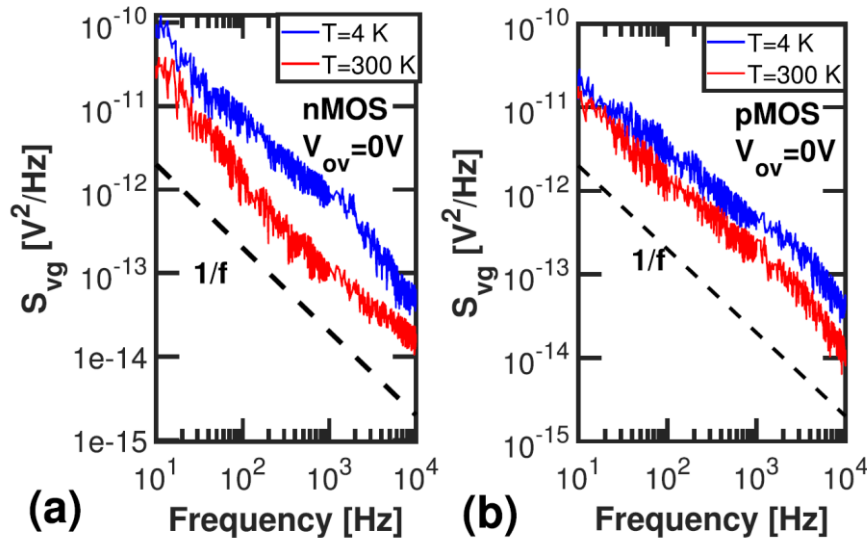
Noise

Thermal noise: $\overline{e_n^2} = 4kT \frac{\gamma}{g_m}$

$T \searrow$, $g_m \nearrow \rightarrow$ **noise** $\searrow \searrow$
(0.1 nV/√Hz)

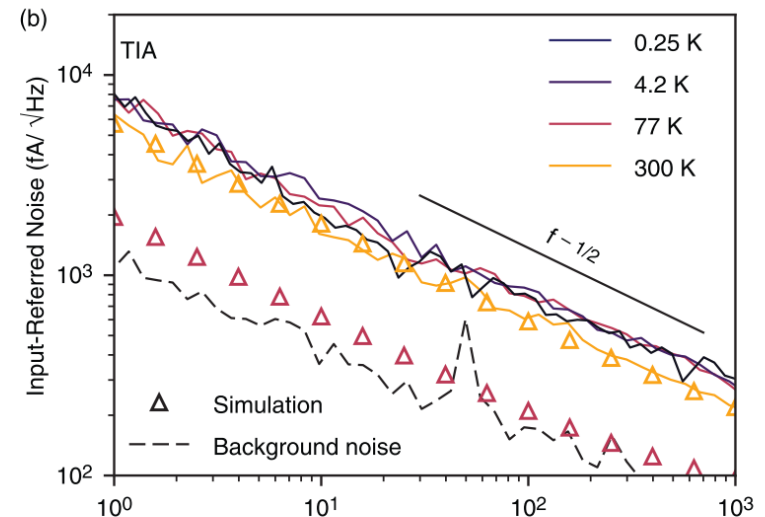
Flicker noise: usually does not decrease

28nm tech.



dominant noise up to
tens of MHz

28nm FDSOI tech.



R. Asanovski, et al., "Understanding the Excess 1/f Noise in MOSFETs at Cryogenic Temperatures," *IEEE Trans. Electron Devices*, 2023

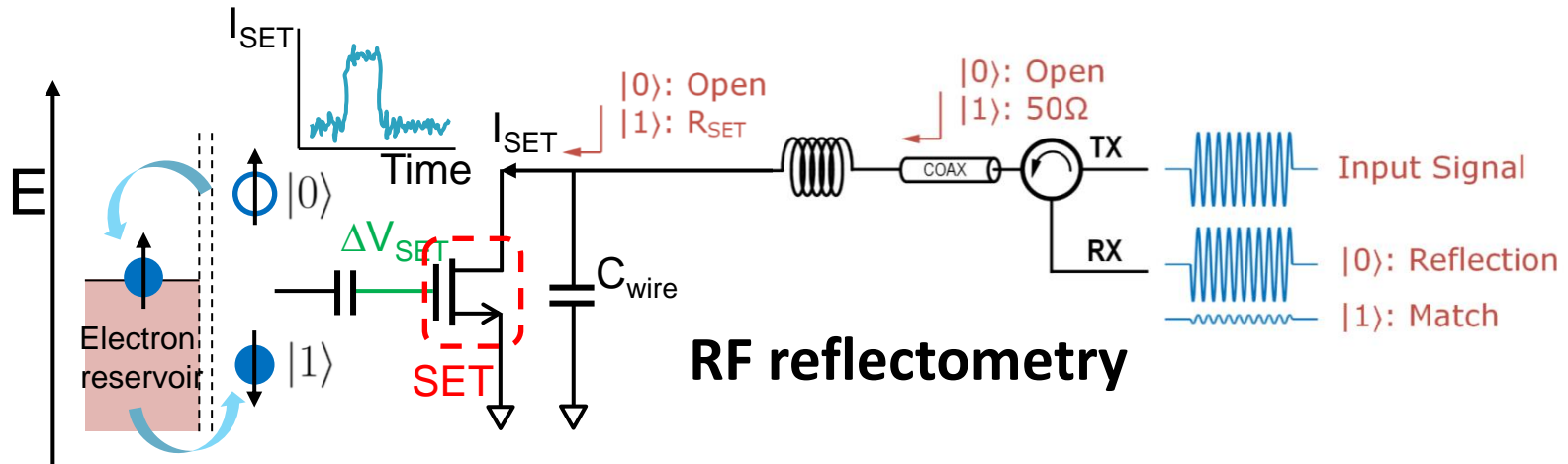
L. Le Guevel *et al.*, "Low-power transimpedance amplifier for cryogenic integration with quantum devices," *Appl. Phys. Rev.*, 2020

Outline

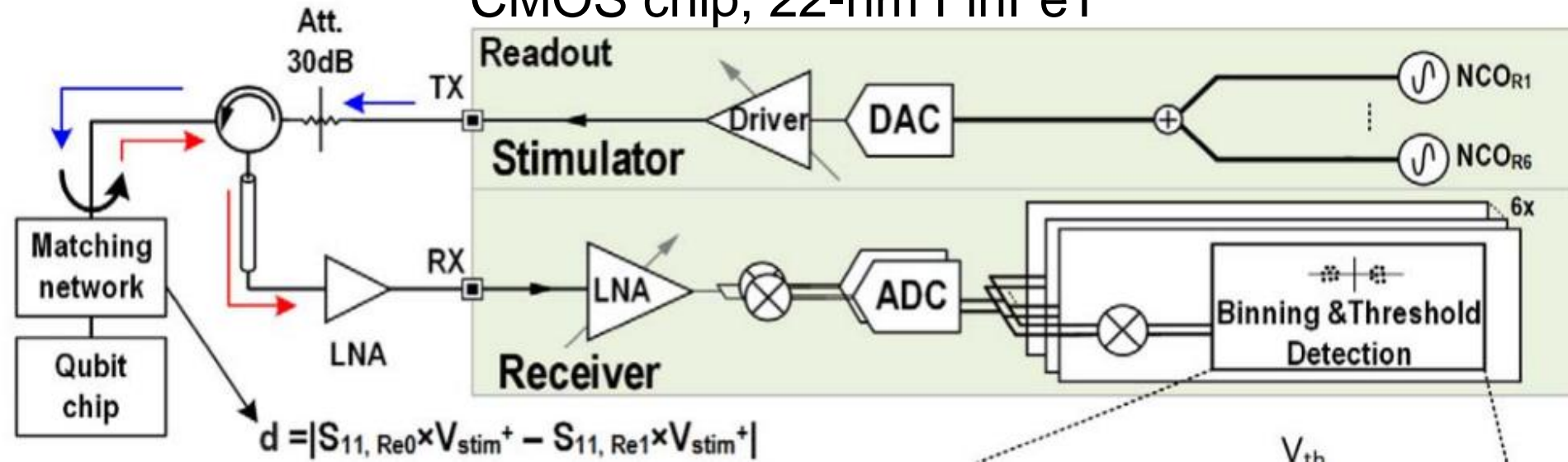
- Spin detection using room temperature instrumentation
- Cryogenic electronics
 - Challenges
 - Design rules
- **Examples**

Spin qubit readout: measurement technique

[S. Subramanian, ISSCC 2023]



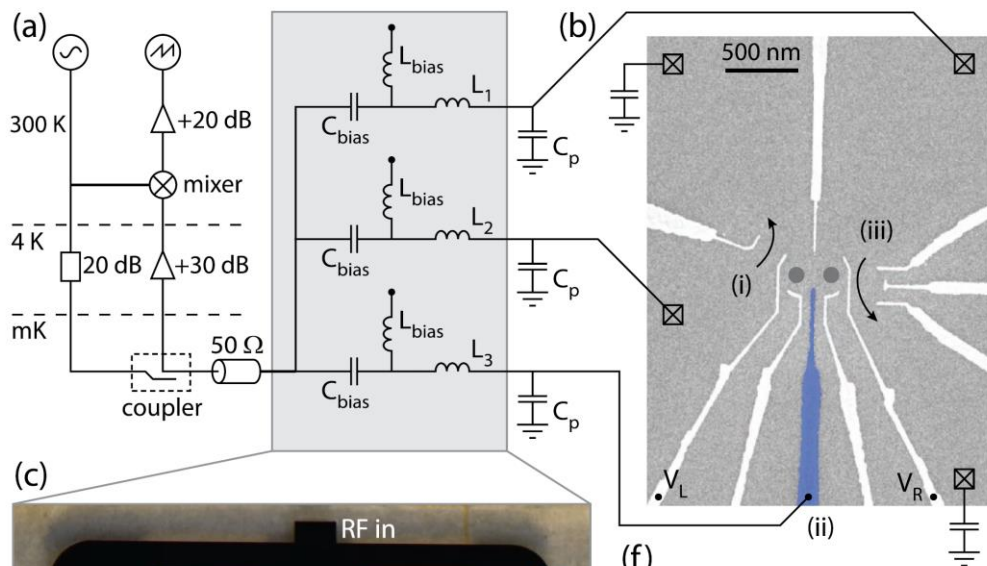
CMOS chip, 22-nm FinFeT



[Park et al, "A Fully Integrated Cryo-CMOS SoC for State Manipulation, Readout, and High-Speed Gate Pulsing of Spin Qubits", JSSC, 2021]

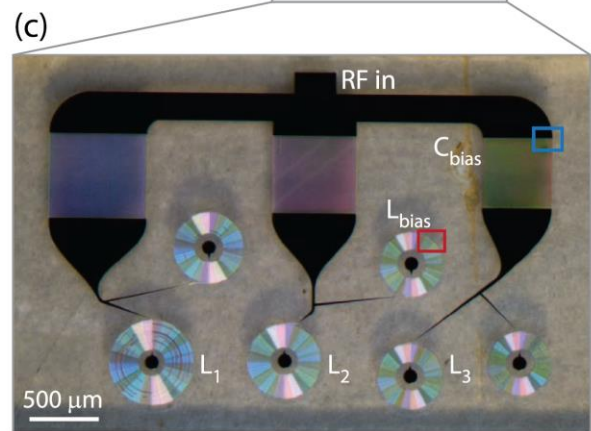
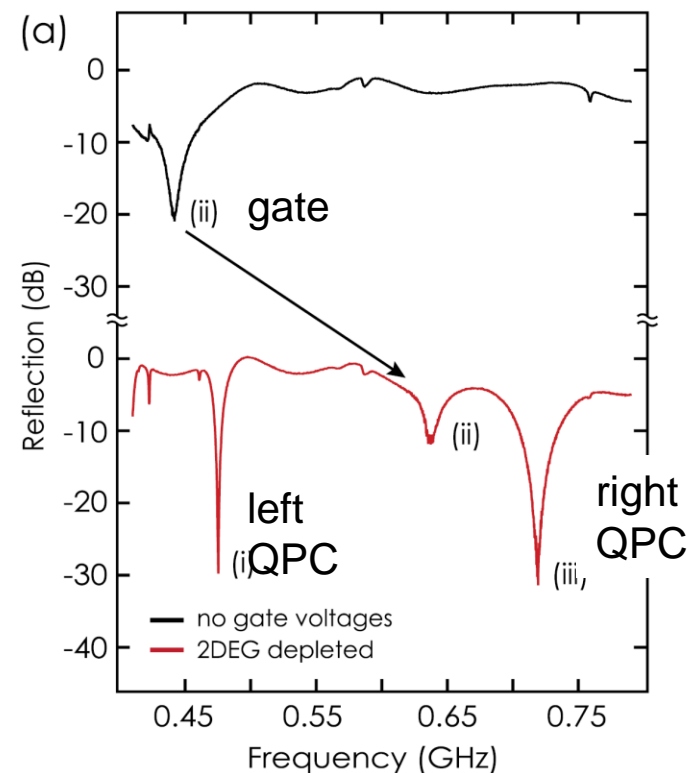
Frequency Division Multiplexing

J. M. Hornibrook et al. "Frequency multiplexing for readout of spin qubits," *Appl. Phys. Lett.*, 2014

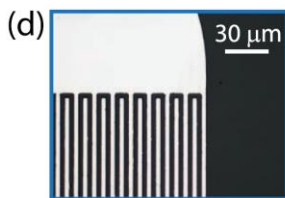


bias tees (C_{bias} , L_{bias})
2 QDs and 2 QPCs

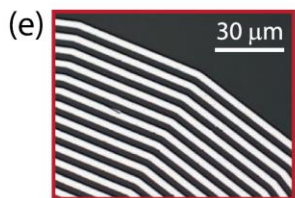
Frequency response of MUX circuit



multiplexing chip
superconducting niobium
on a sapphire substrate
(ideally, it is the same
chip of the qubits)



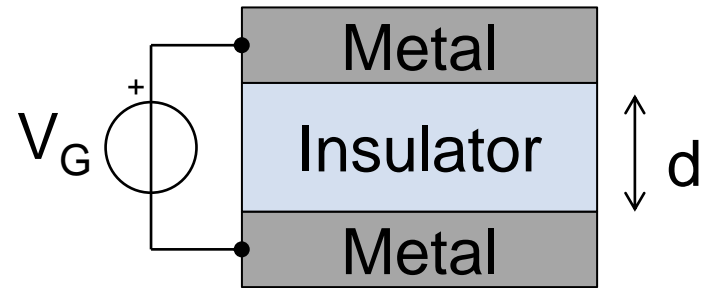
Interdigitated C



Spiral L

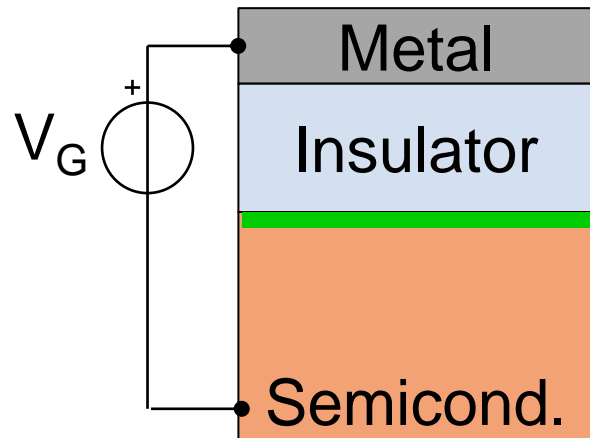
A single cable for many qubits

Quantum capacitance



$$\Delta Q = -q\Delta N_e = C_{geom}\Delta V_G \quad q=+1.6 \cdot 10^{-19} \text{ C}$$

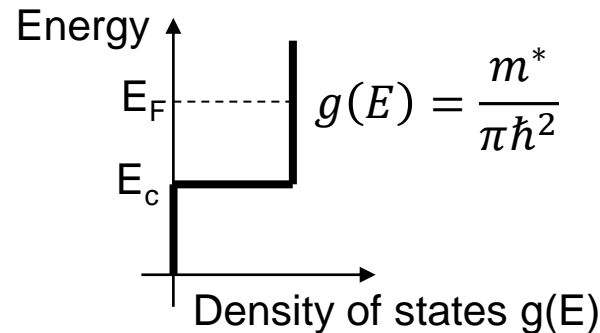
$$C_{geom} = \epsilon \frac{S}{d}$$



$$V_G > V_T$$

2D electron gas at potential V_c

$$\Delta Q = -q\Delta N_e = C_{geom}(\Delta V_G - \Delta V_c)$$



$$g(E) = \frac{m^*}{\pi \hbar^2}$$

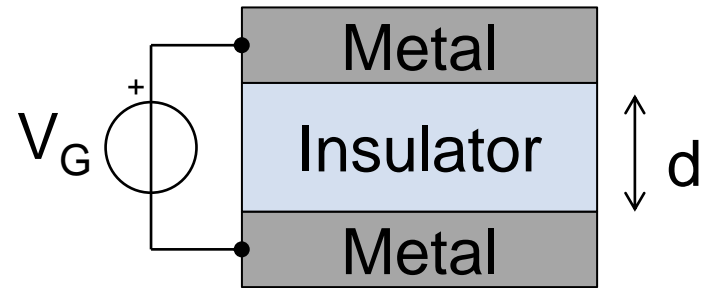
$$N_e \cong \int_{E_c}^{E_F} g(E) dE \quad (T \approx 0K)$$

$$\rightarrow \Delta N_e = -\frac{m^*}{\pi \hbar^2} q \Delta V_c$$

$$C_Q = \frac{m^*}{\pi \hbar^2} q^2$$

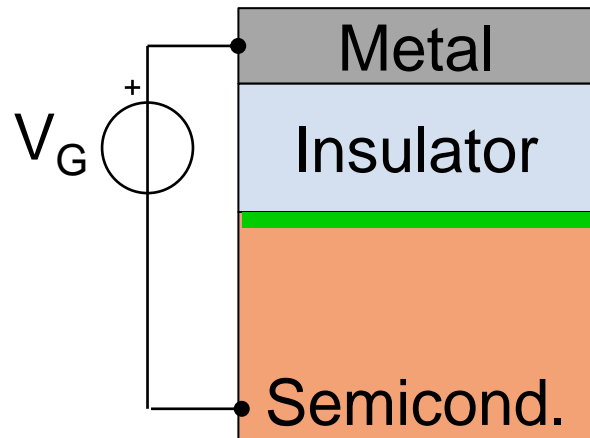
quantum capacitance

Quantum capacitance



$$\Delta Q = -q\Delta N_e = C_{geom}\Delta V_G \quad q=+1.6 \cdot 10^{-19} \text{ C}$$

$$C_{geom} = \epsilon \frac{S}{d}$$

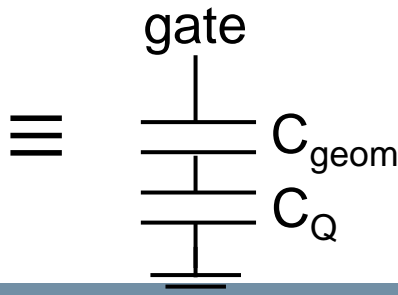


2D electron gas if $V_G > V_T$ at potential V_c

$$\Delta Q = -q\Delta N_e = C_{geom}(\Delta V_G - \Delta V_c)$$

$$-q\Delta N_e = C_{geom} \left(\Delta V_G + \frac{q\Delta N_e}{C_Q} \right)$$

$$-q\Delta N_e = \frac{C_{geom}C_Q}{C_{geom} + C_Q} \Delta V_G$$

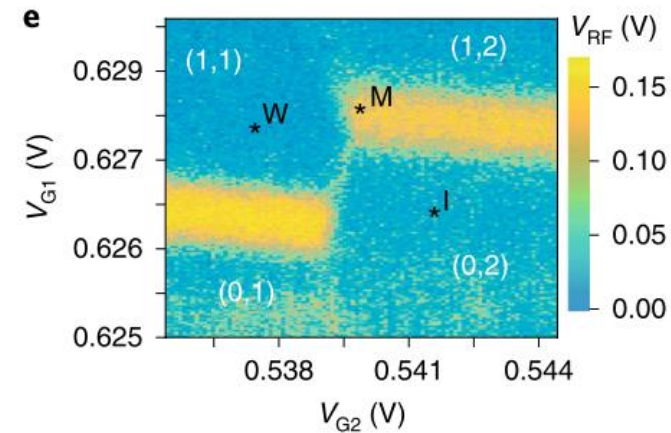
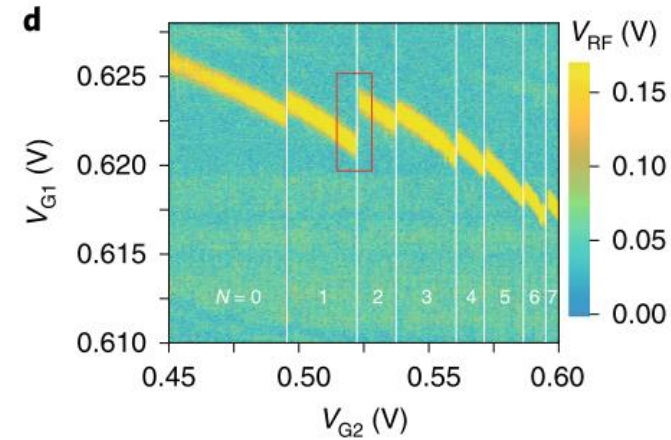
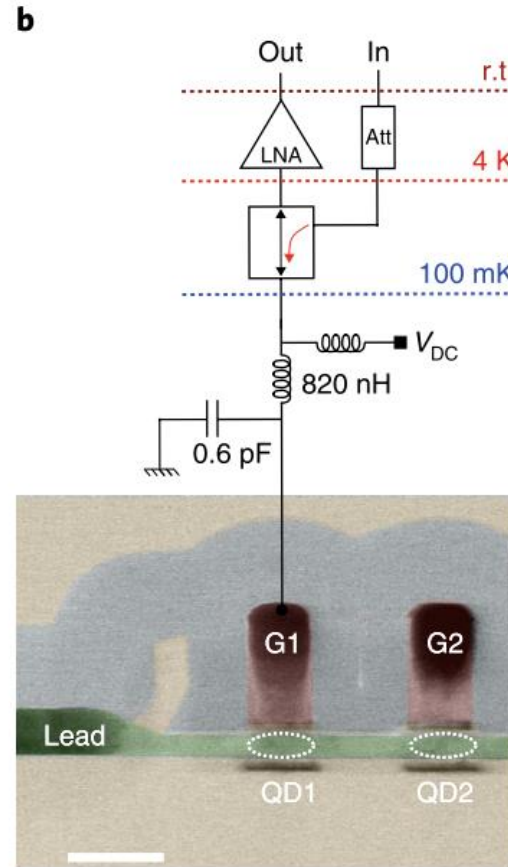
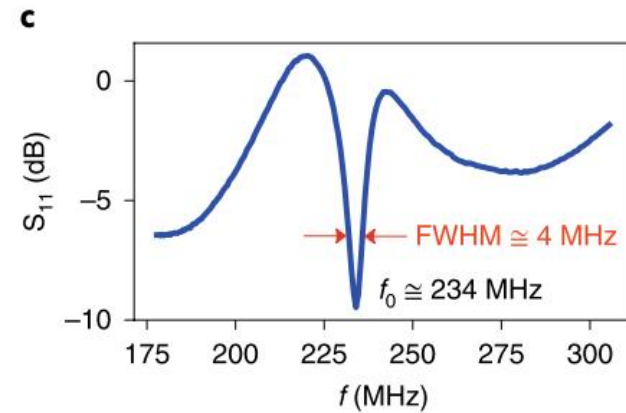
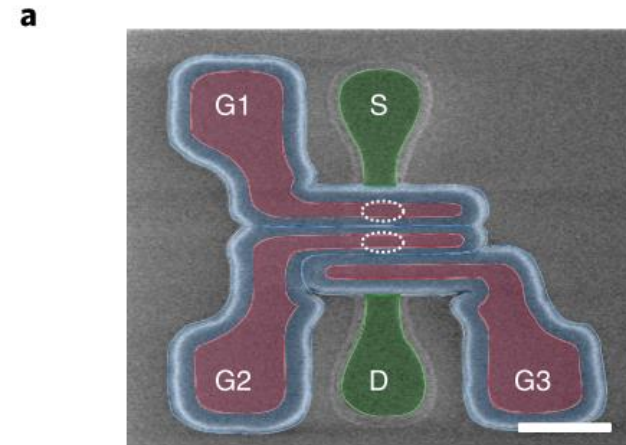


C_Q related to charge dynamics and not from geometrical parameters

$$C_Q = \frac{m^*}{\pi \hbar^2} q^2$$

quantum capacitance

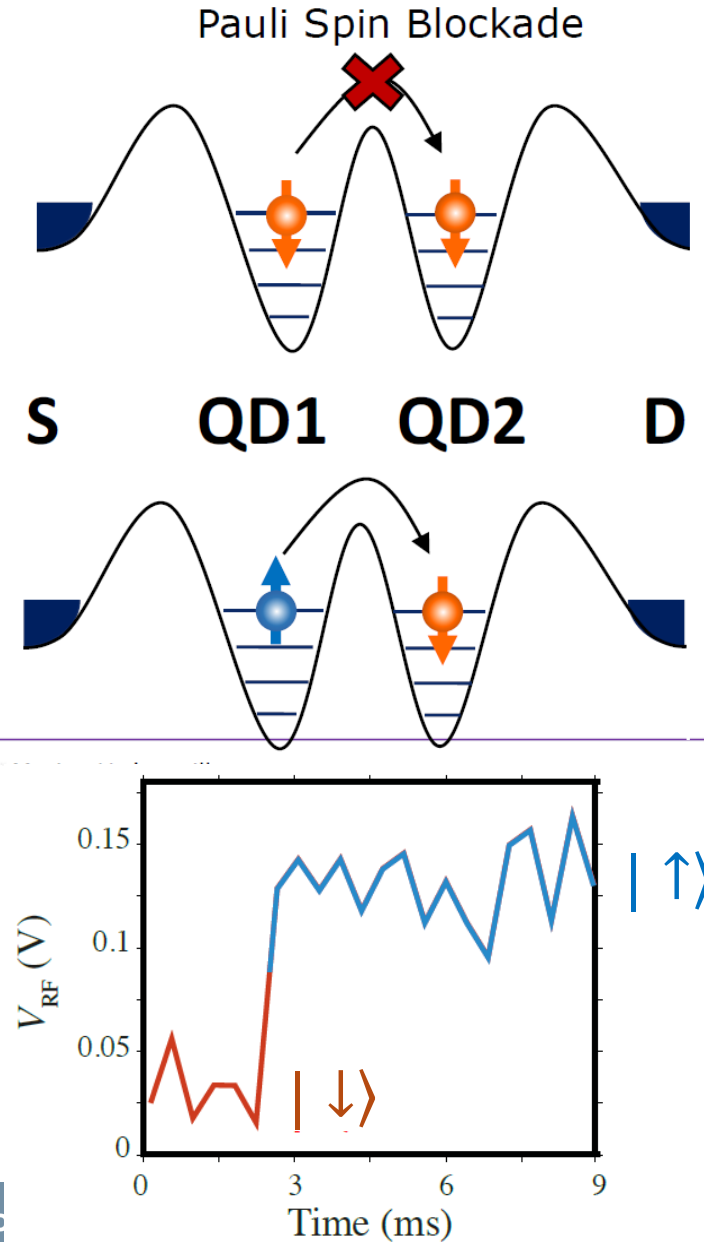
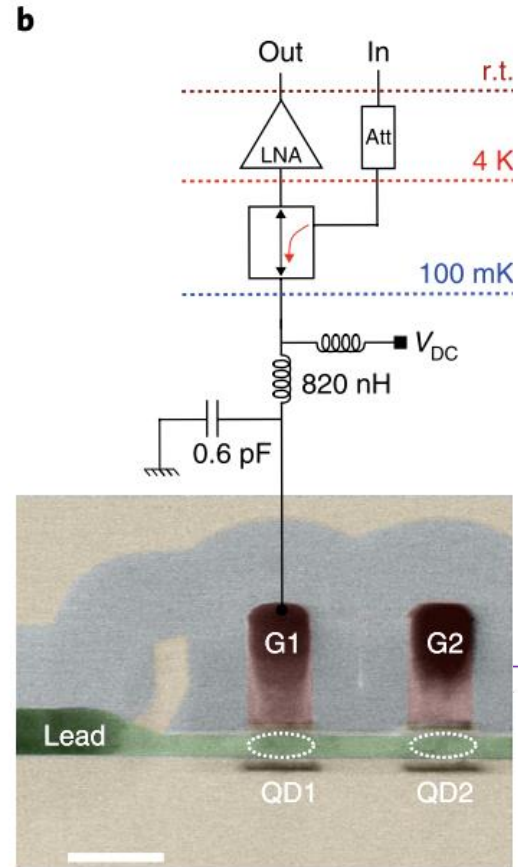
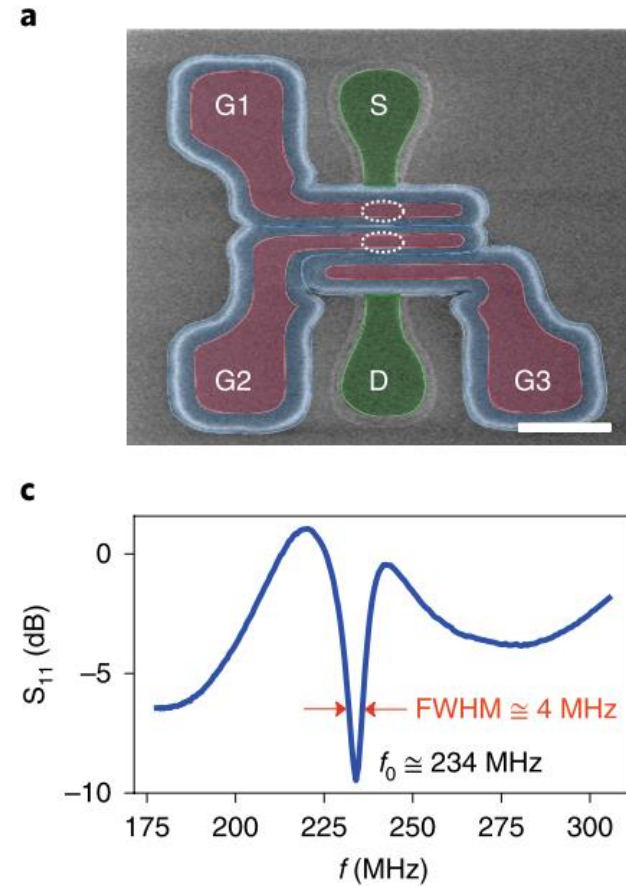
Gate-based spin readout



M. Urdampilleta, et al. "Gate-based high fidelity spin readout in a CMOS device," *Nat. Nanotechnol.*, 2019

Gate-based spin readout

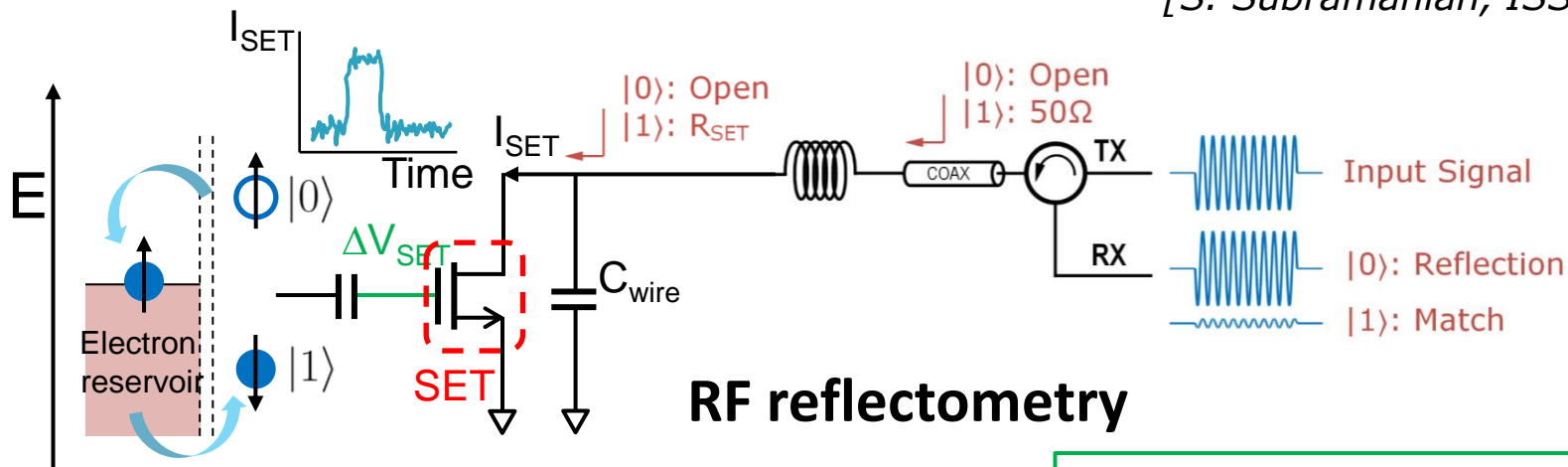
M. Urdampilleta, ESSDERC, 2020



M. Urdampilleta, et al. "Gate-based high fidelity spin readout in a CMOS device," *Nat. Nanotechnol.*, 2019

Spin qubit readout: measurement technique

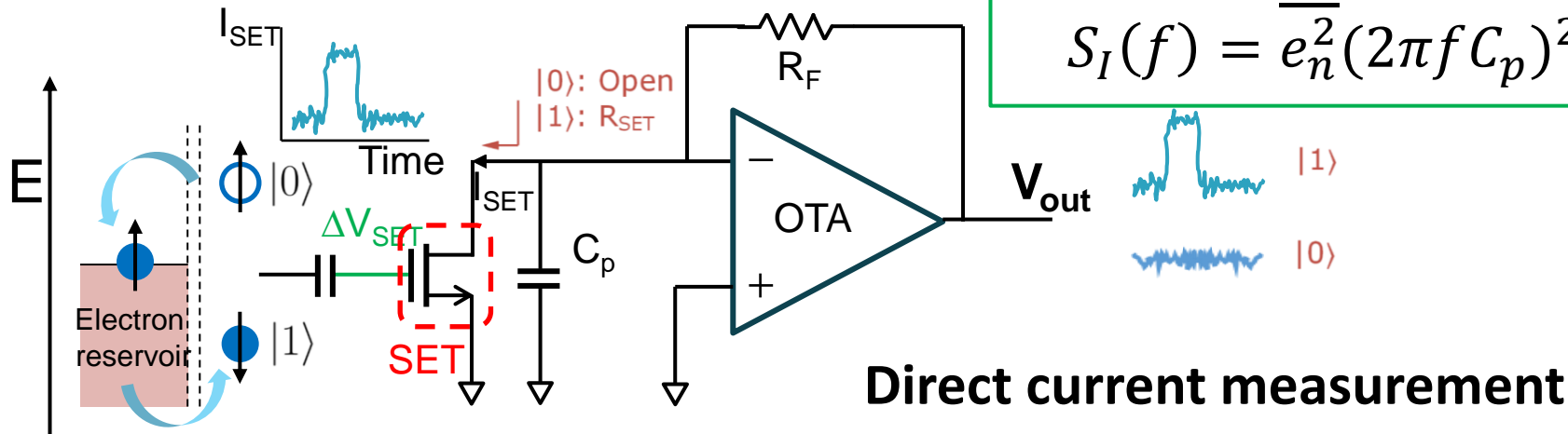
[S. Subramanian, ISSCC 2023]



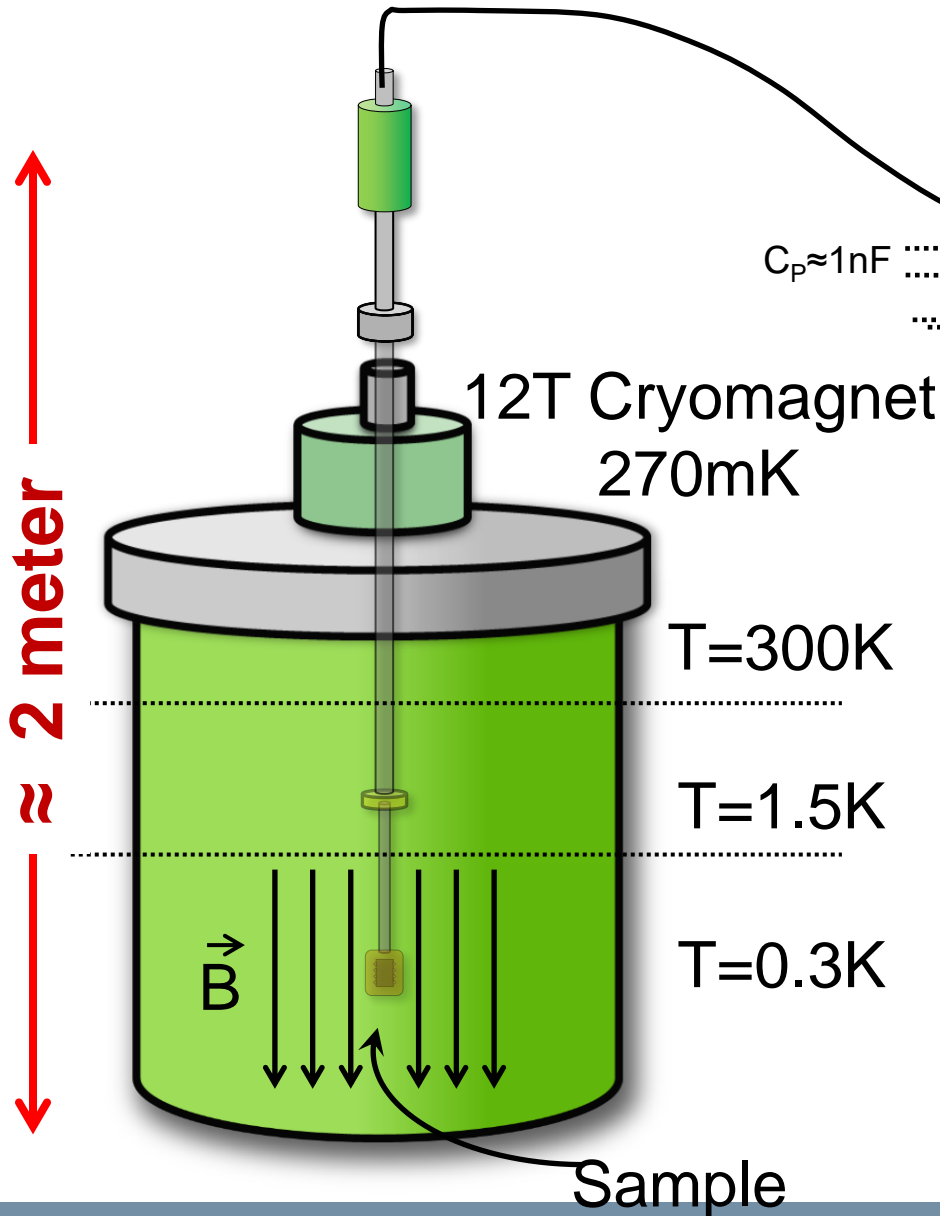
Bulky off-chip components, fast analog-to-digital converter, μ

$$BW \propto \sqrt{\frac{GBWP}{C_p}}$$

$$S_I(f) = e_n^2 (2\pi f C_p)^2$$



Cryogenic transimpedance amplifier



$$S_{i,eq} = \frac{4kT}{R_F} + \overline{e_N^2} \omega^2 C_P^2$$

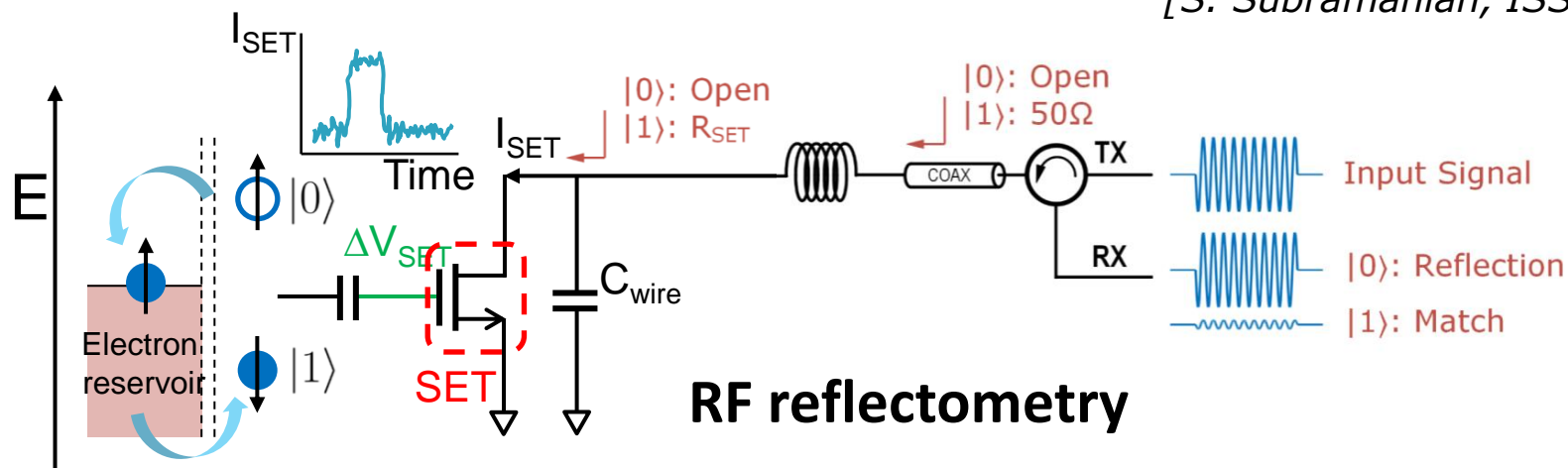
Both drastically reduced



Cryo-electronics
to improve sensitivity

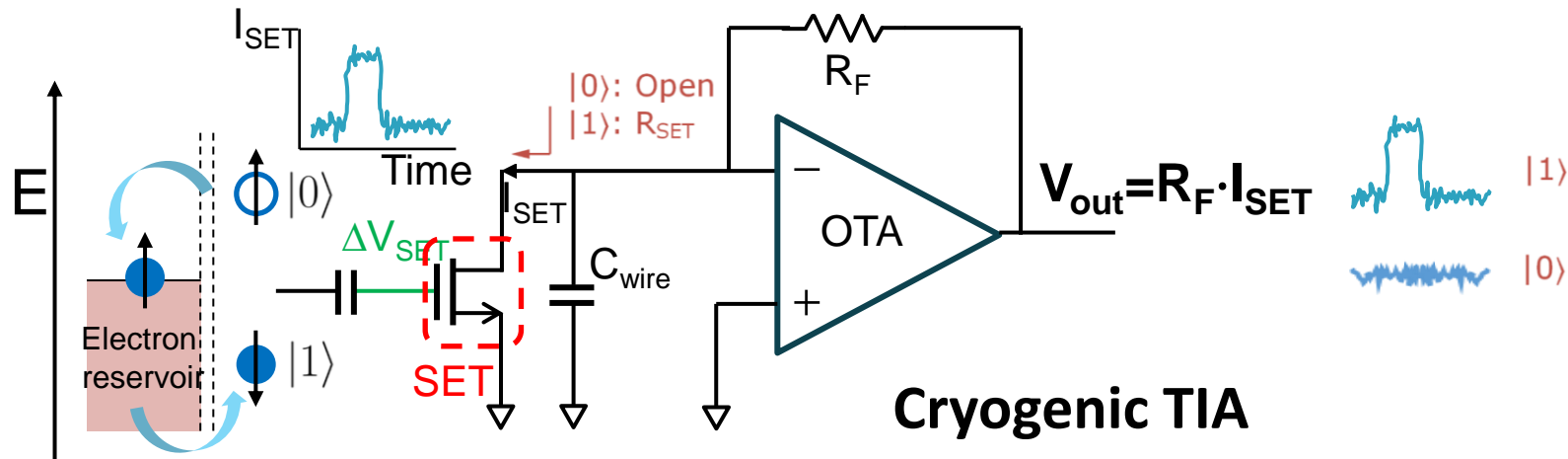
Spin qubit readout: measurement technique

[S. Subramanian, ISSCC 2023]



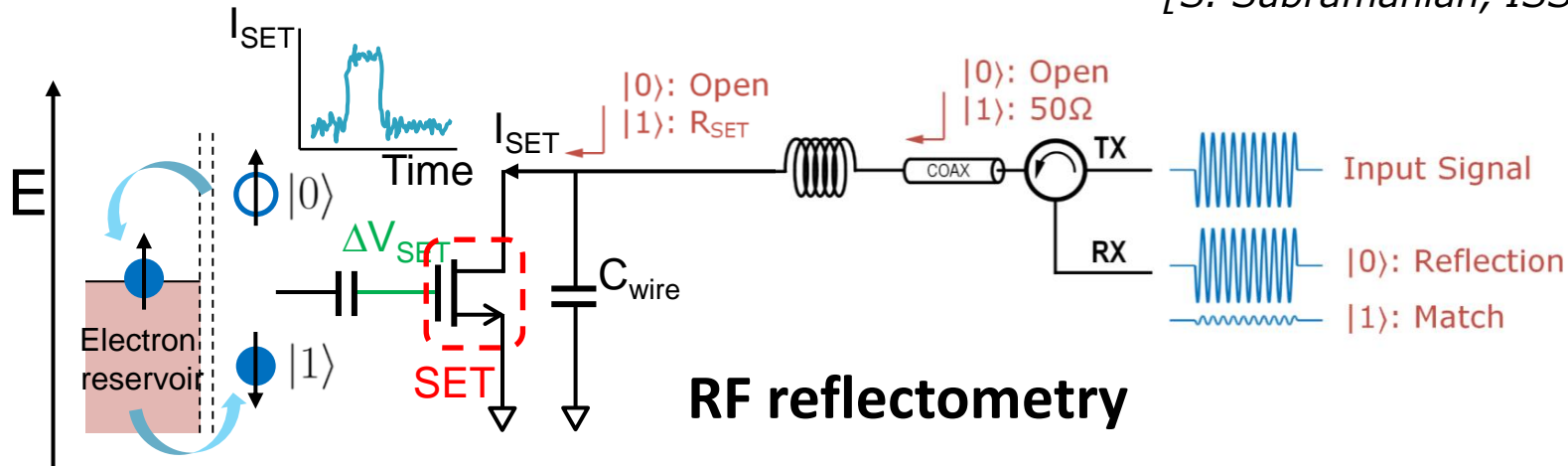
Bulky off-chip components, fast analog-to-digital converter, μ -wave signals

Fully CMOS-compatible readout operated at $T < 5K$:



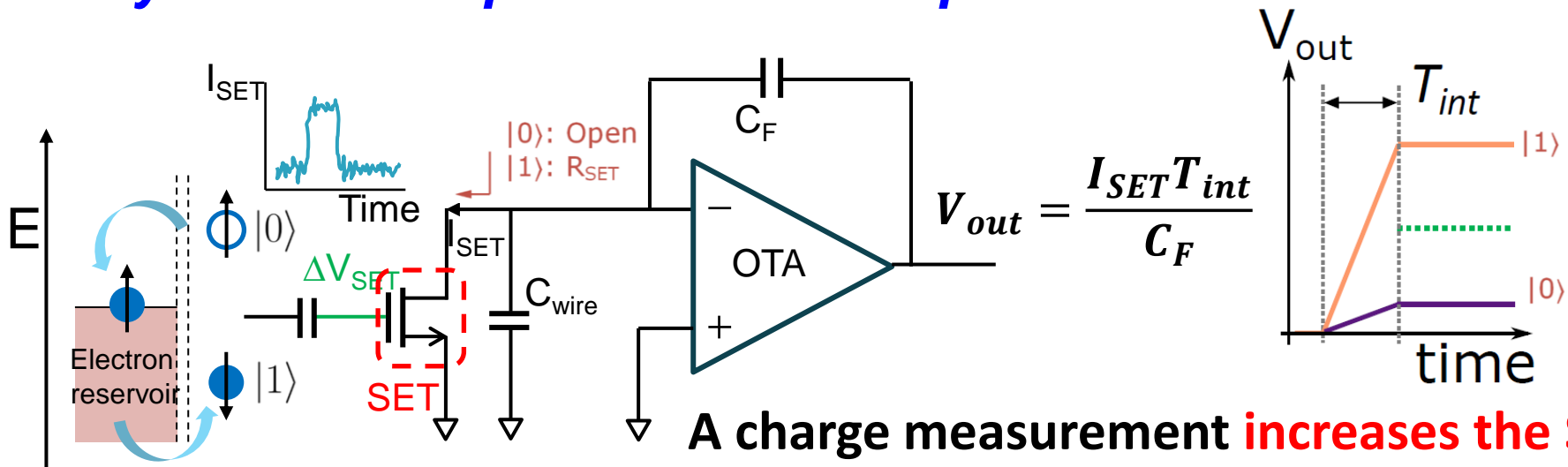
Spin qubit readout: measurement technique

[S. Subramanian, ISSCC 2023]

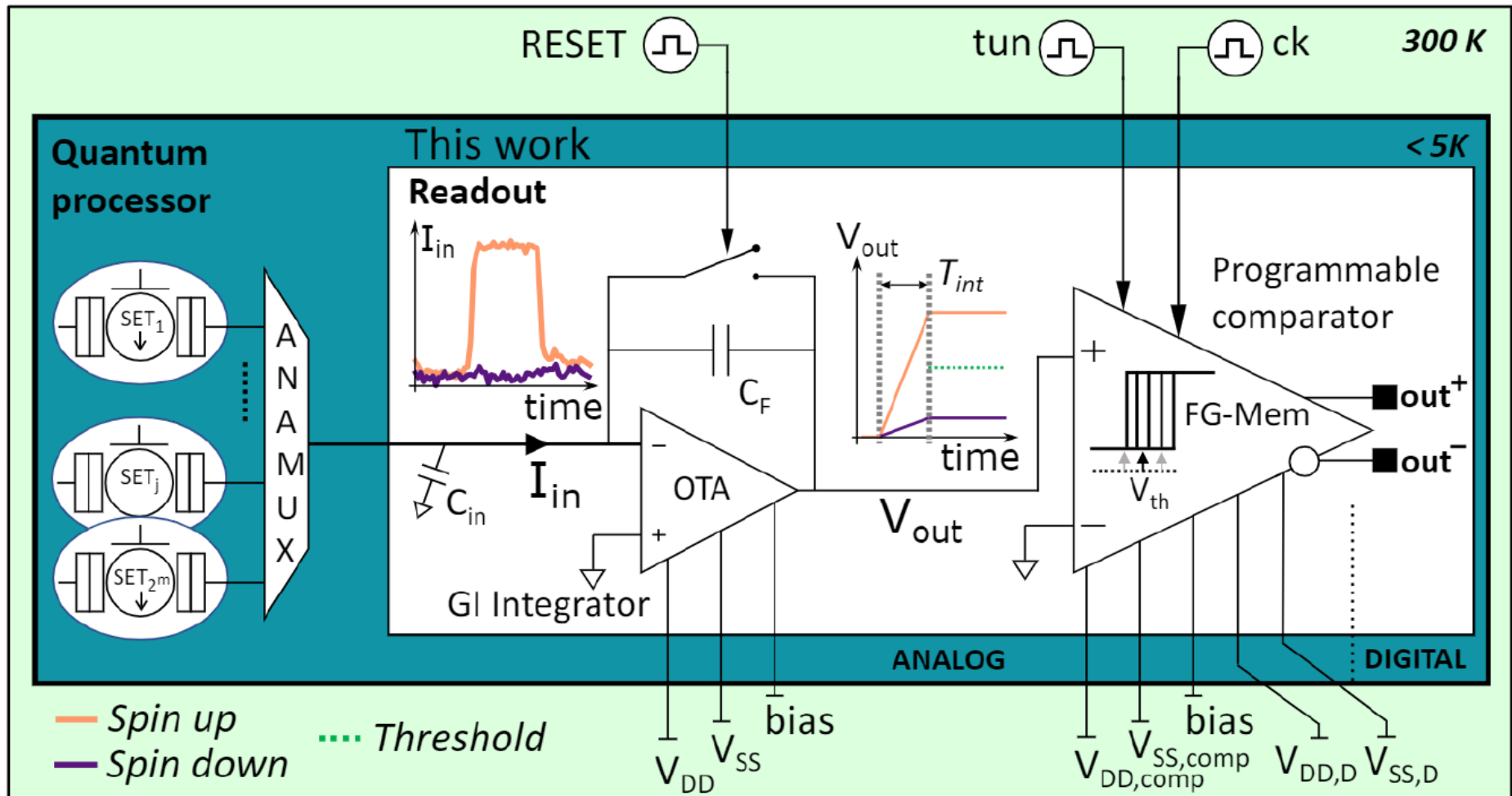


Bulky off-chip components, fast analog-to-digital converter, μ -wave signals

Fully CMOS-compatible readout operated at $T < 5K$:



Compact readout based on current measurement

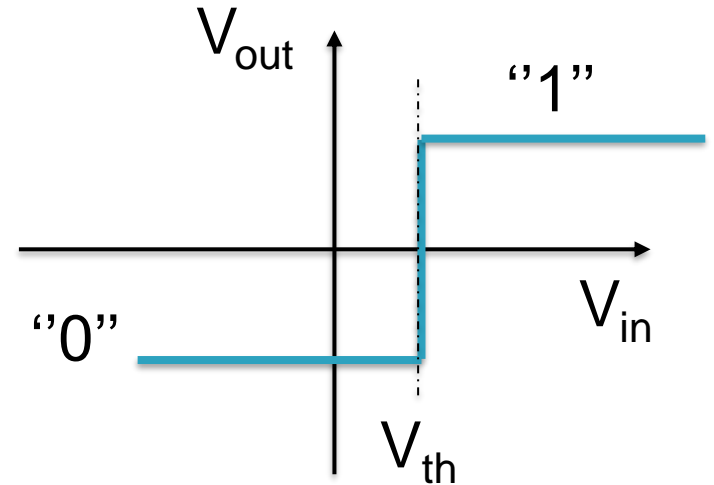
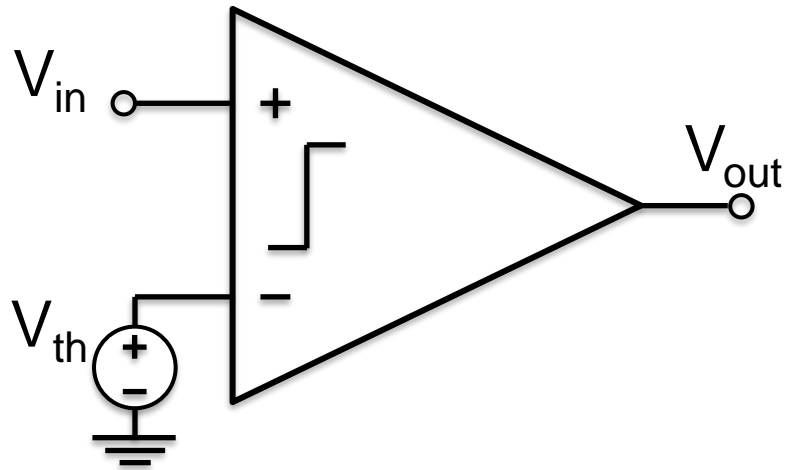


- Fully-integrated 150-nm CMOS technology
- Direct charge-to-digital conversion

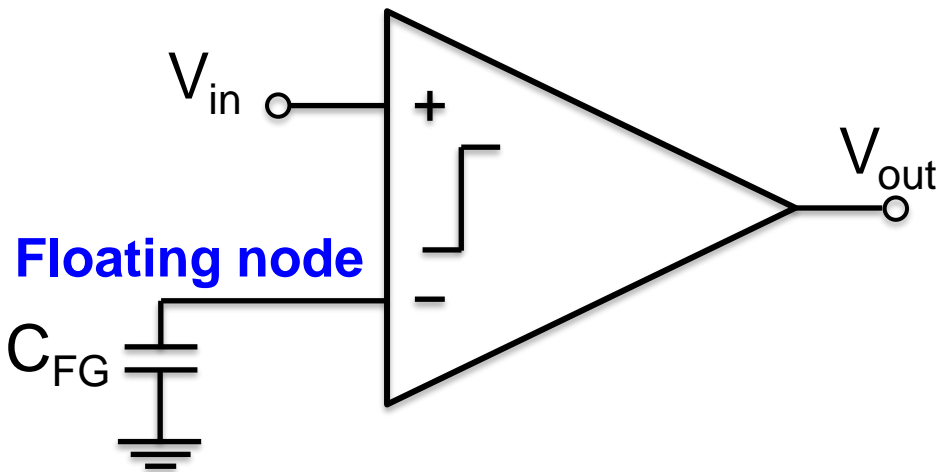
- Time division multiplexing architecture
- Low power consumption (1 mW/qubit)

[M. CASTRIOTTA et al., IEEE Solid-state Circuits Letters (2023)]

Programmable floating-gate comparator



- V_{th} few mV! Process variations are critical
- Digital-to-Analog Converter (DAC): power consumption, TDMS

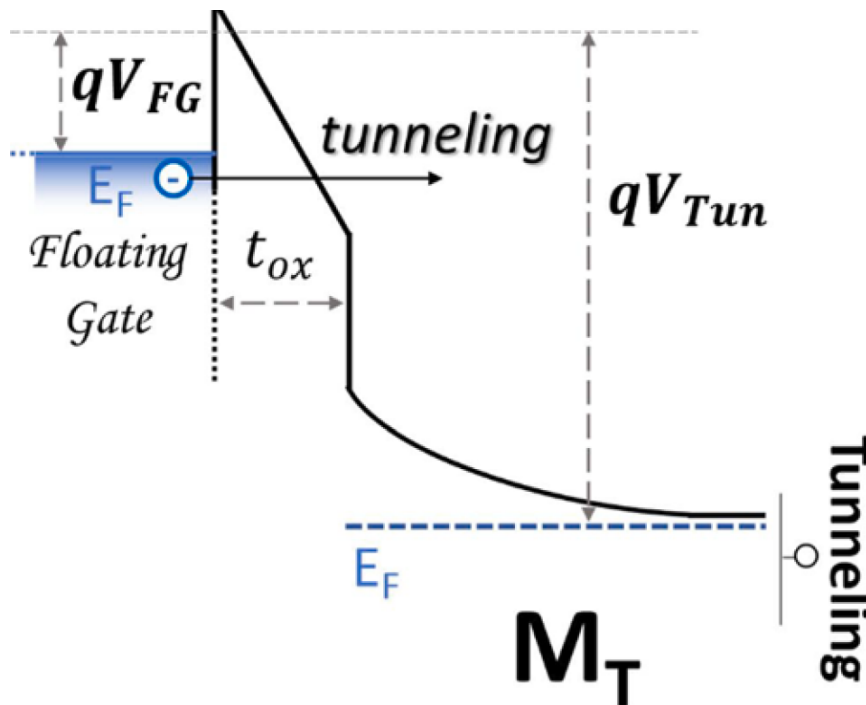
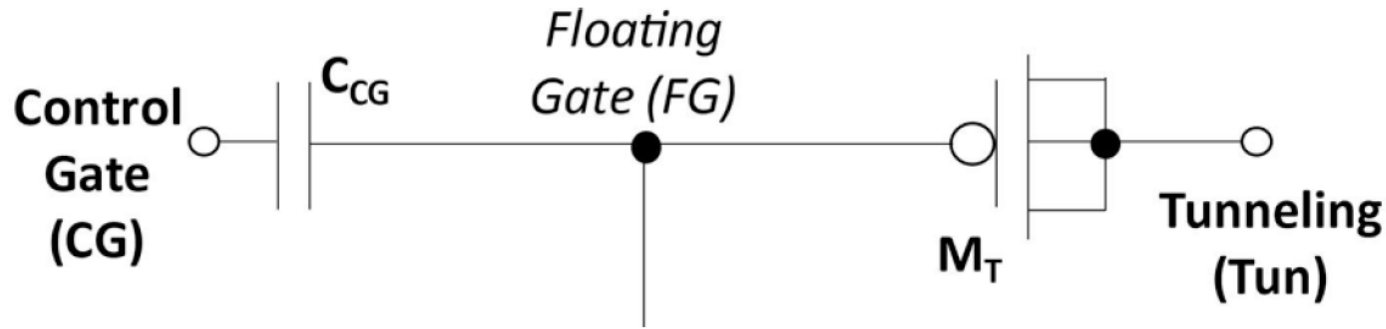


Floating node

- Floating node charged at V_{th}
- Compact and low power

- How to change the charge?
- How to compensate for the process variations?

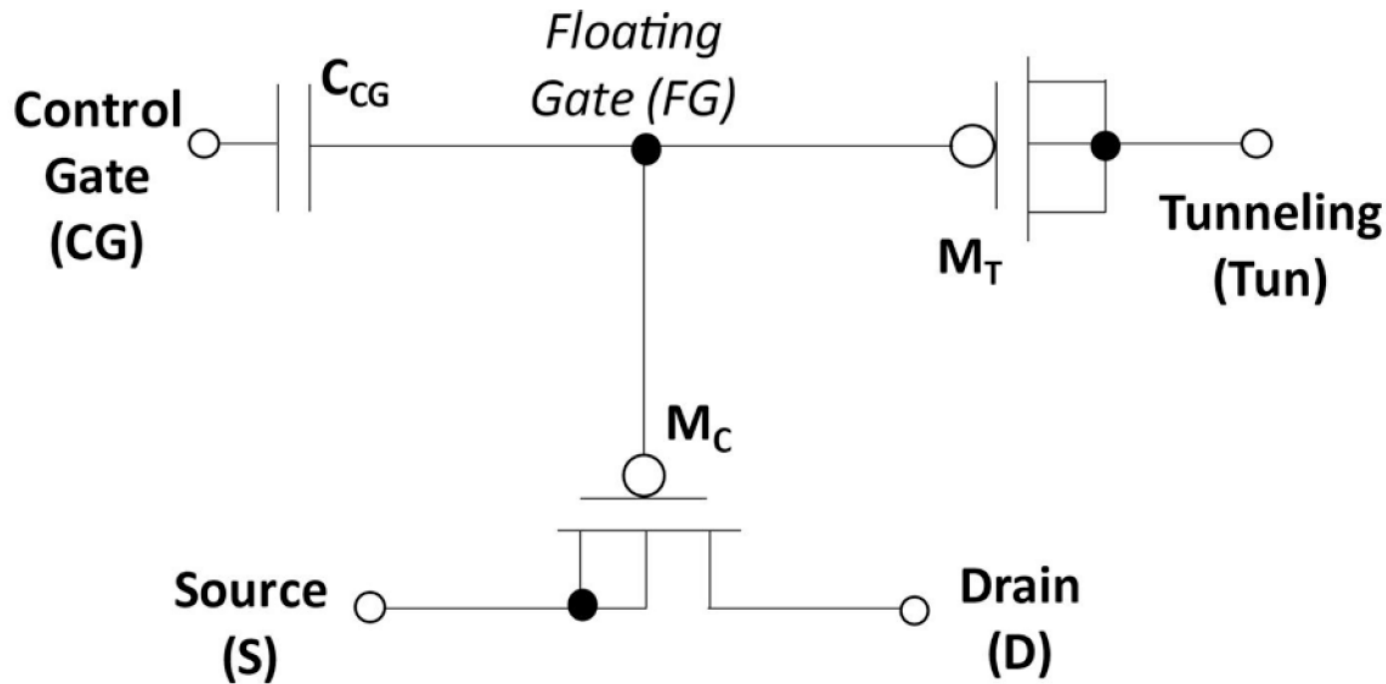
Floating gate in standard CMOS technology



- It requires high voltages to enable tunneling ($\approx 7V$ in our technology)

[M. Castriotta, Solid State Electronics 189 (2022)]

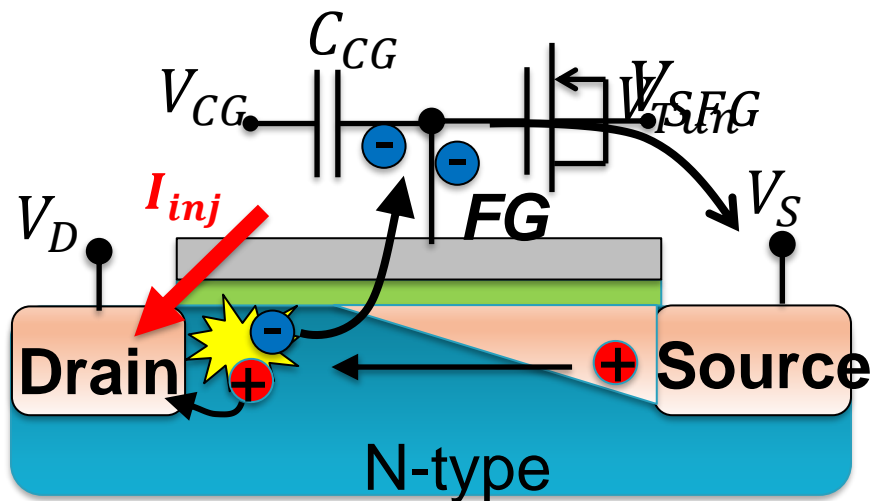
Floating gate in standard CMOS technology



- Hot electron injection using a p-type MOSFET
- The electrons are removed by tunneling (coarse global resetting of the floating gates)

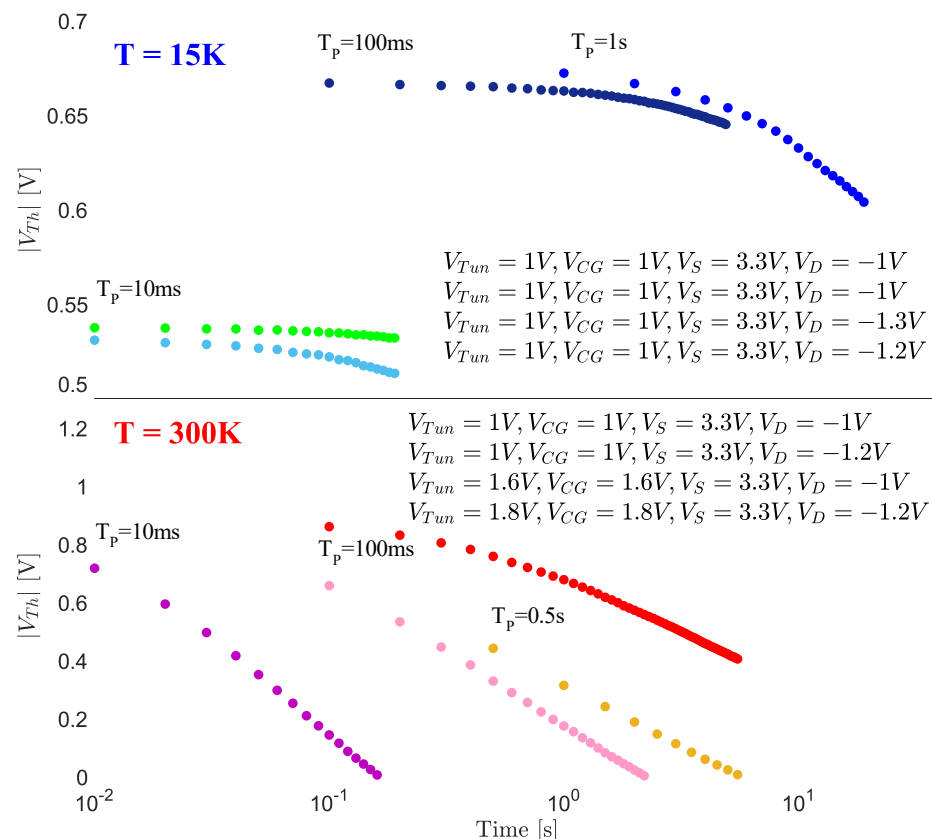
[M. Castriotta, *Solid State Electronics* 189 (2022)]

Hot electron injection in p-type FG transistor



holes collide with sufficient energy ($\approx 3/2 E_{\text{gap}}$) to liberate additional electron-hole pairs

- $V_{\text{SFG}} > |V_{\text{T}}|$ (ON)
- $V_{\text{SD}} \gg 0\text{V}$ (high electric field)
- $V_{\text{SD}} \gg V_{\text{SFG}}$ ($V_{\text{FG}} > V_{\text{D}}$)

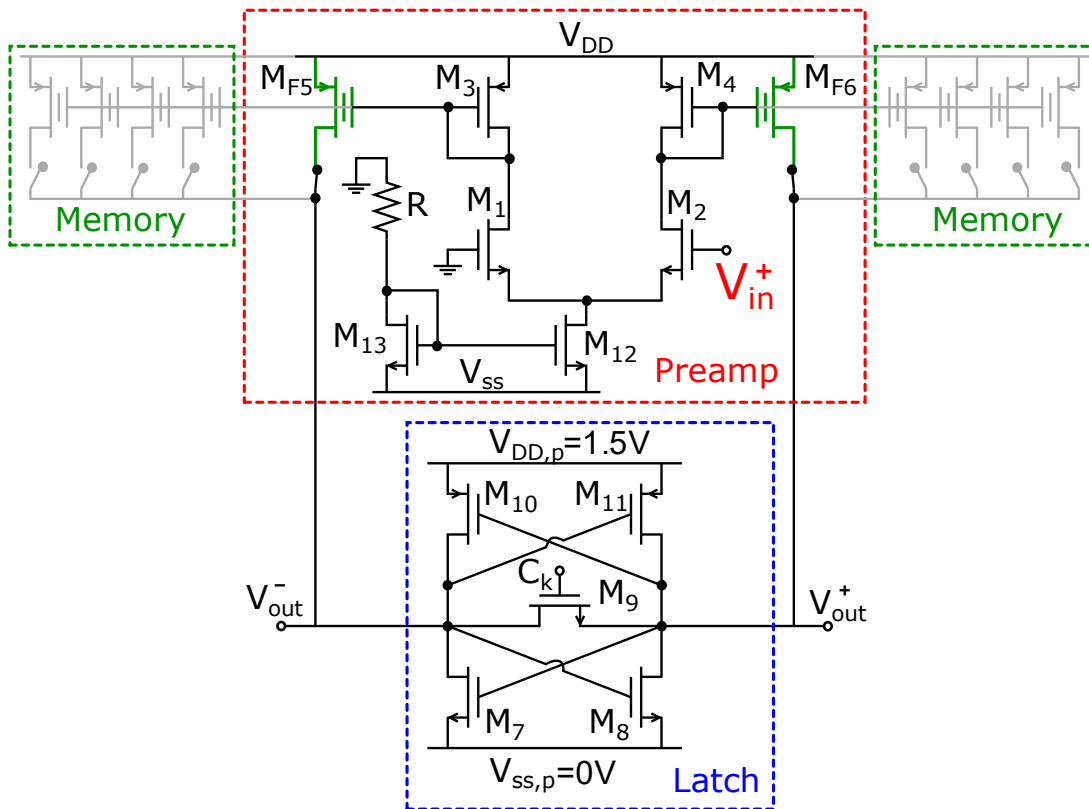


$$I_{\text{inj}} = C(V_{\text{SD}} - \gamma V_{\text{ov}})^3 I_{\text{d}} e^{-\frac{B}{V_{\text{SD}} - \gamma V_{\text{ov}}}}$$

[M. Castriotta, Solid State Electronics 189 (2022)]

Programmable comparator based on FGs

Standard 150-nm CMOS Technology

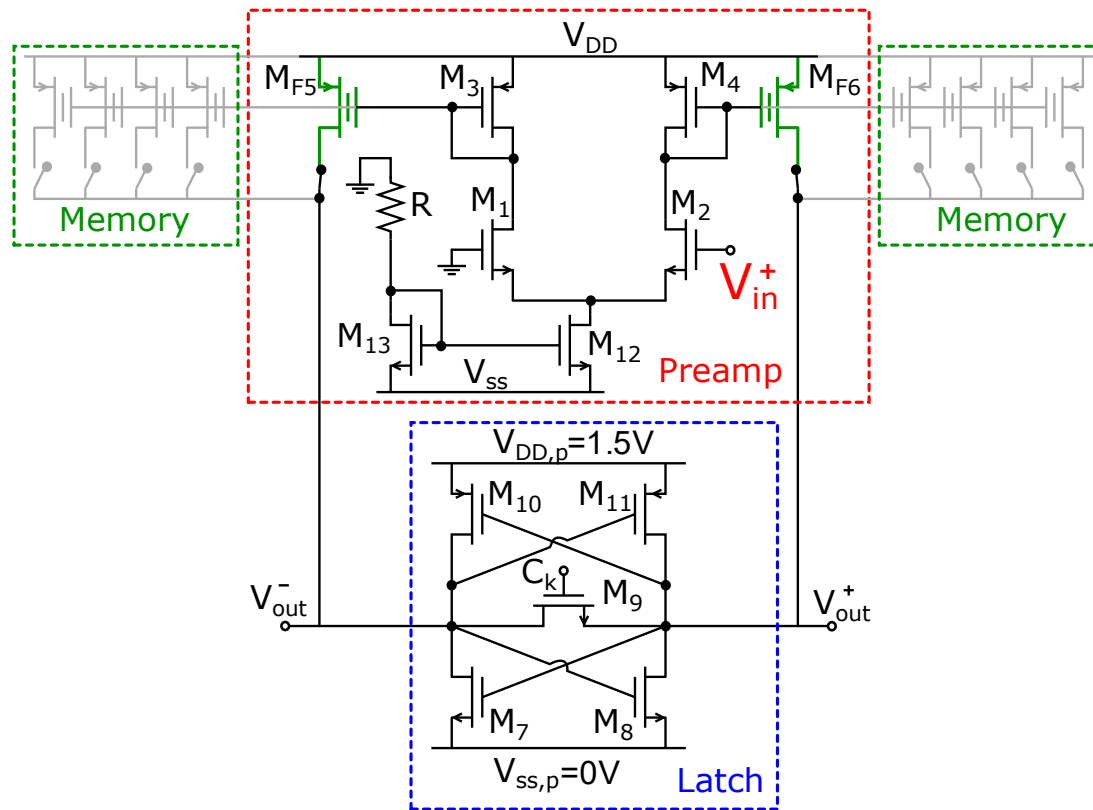


For standard latched comparator:

- $M_{F5} = M_{F6} = M_3 = M_4$
- if $V_{in} > 0V$ and C_k goes low:
 - $I_{F6} > I_{F5}$
 - $V_{out+} \nearrow, V_{out-} \searrow$

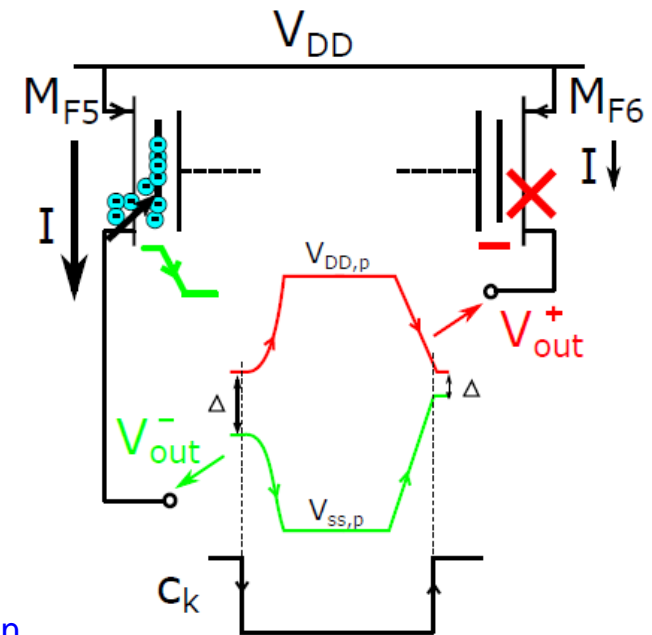
Programmable comparator based on FGs

Standard 150-nm CMOS Technology



□ Programming phase:

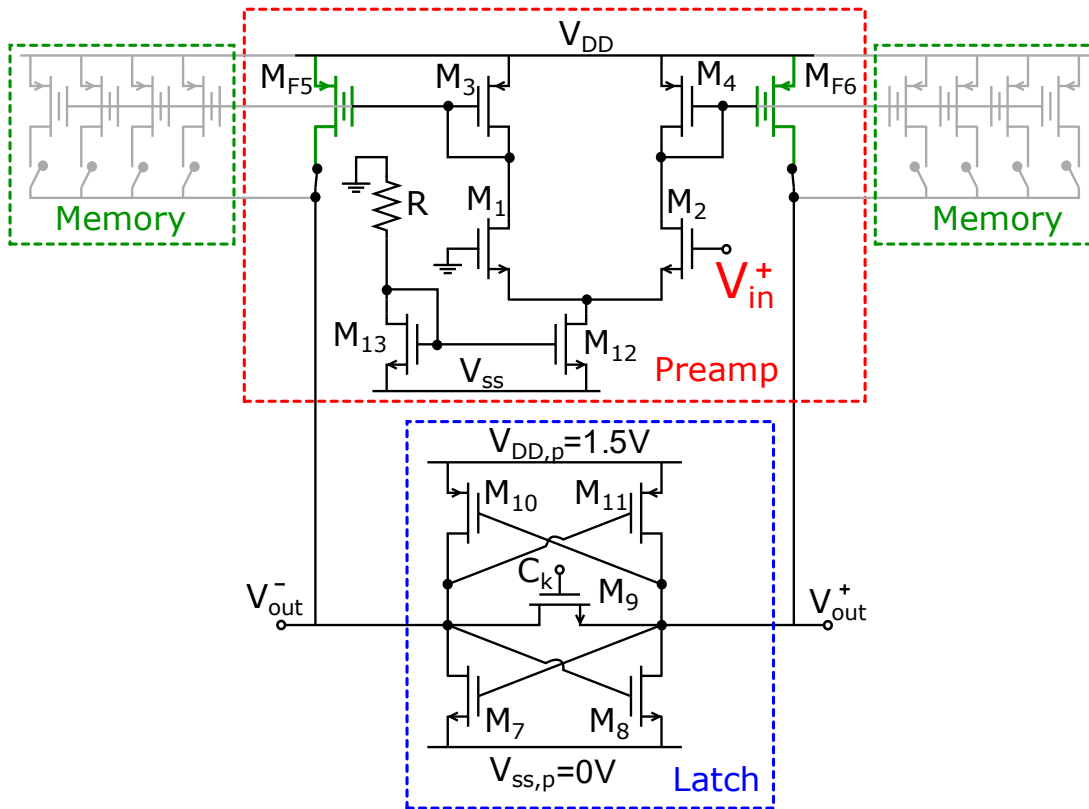
- $V_{DD,p}$, $V_{SS,p}$ and C_k shift down by 2.3V
- Differential charge injection
- $|V_{th}|$ of M_{F5} decreases and its current increases
- The comparator threshold is increased after each clock cycle



After tens of clock cycles, the threshold voltage of M_{F5} is such that $I_{F5} \approx I_{F6}$
 \rightarrow the threshold voltage of the comparator is $\approx V_{in}$

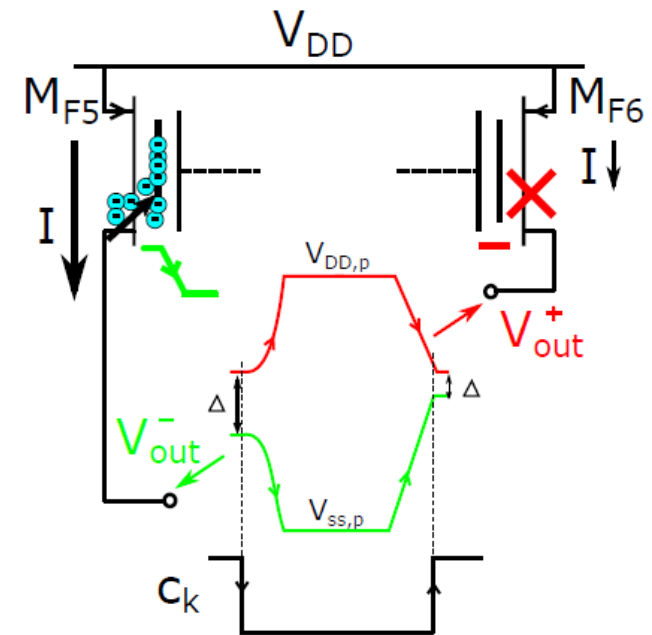
Programmable comparator based on FGs

Standard 150-nm CMOS Technology



□ Programming phase:

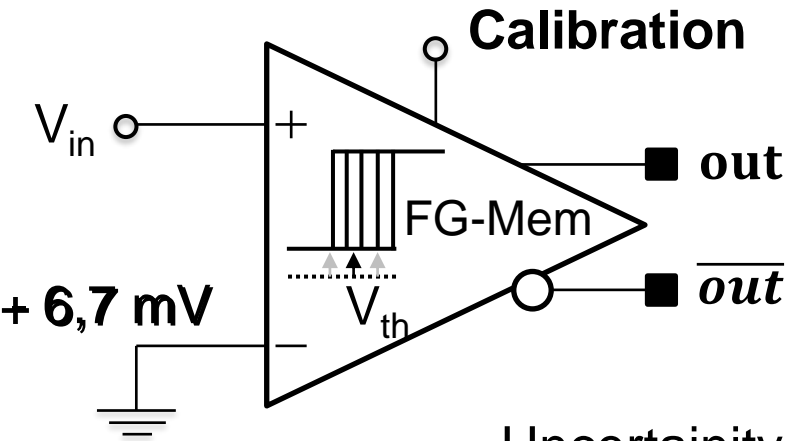
- $V_{DD,p}$, $V_{SS,p}$ and C_k shift down by 2.3V
- Differential charge injection
- $|V_{th}|$ of M_{F5} decreases and its current increases
- The comparator threshold is increased after each clock cycle



□ Evaluation phase:

Standard latched comparator with threshold stored in a pair of FG-transistor M_{F5} and M_{F6}

Characterization of the FG comparator at 4,2 K

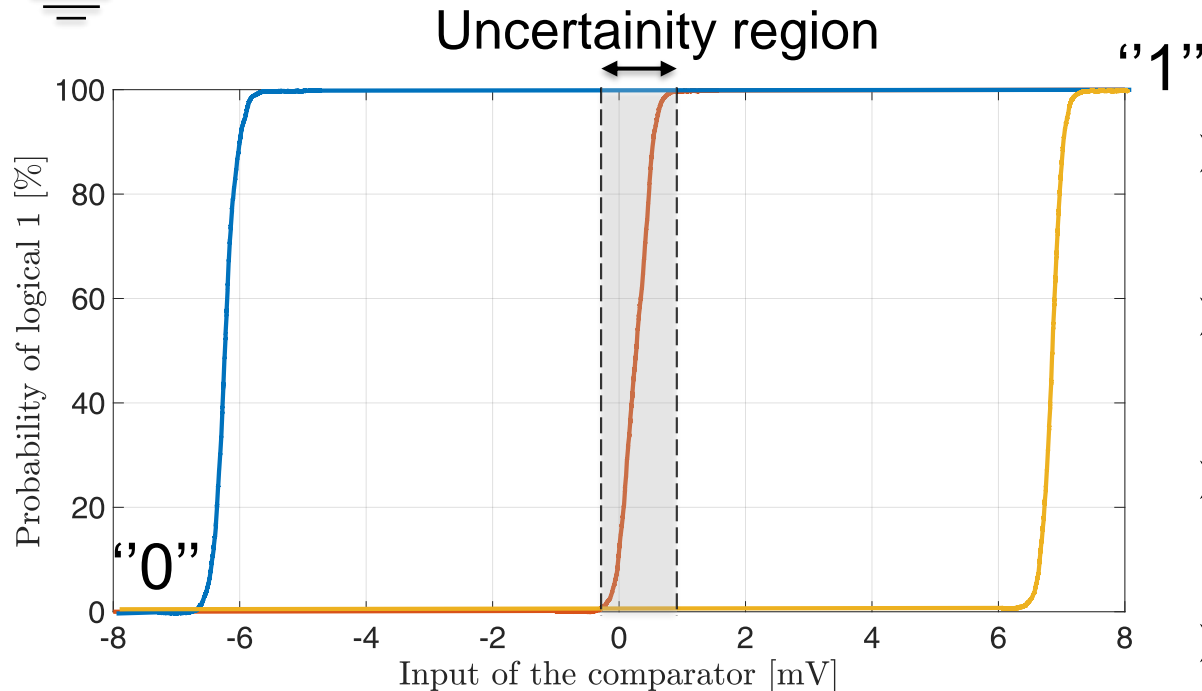


Programming accuracy: **300 μ V**

6 Sigma: **840 μ V**

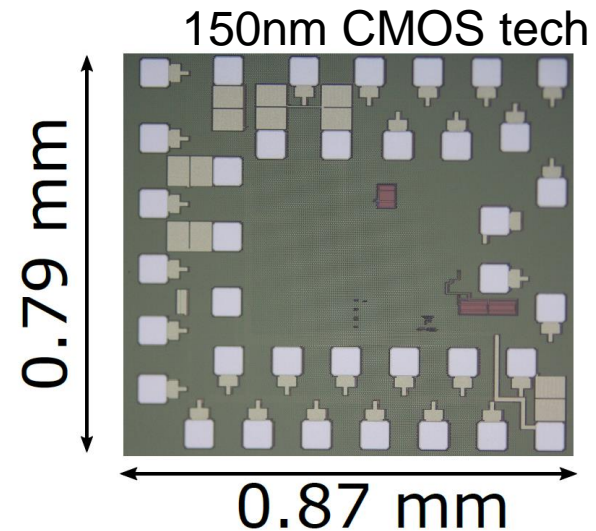
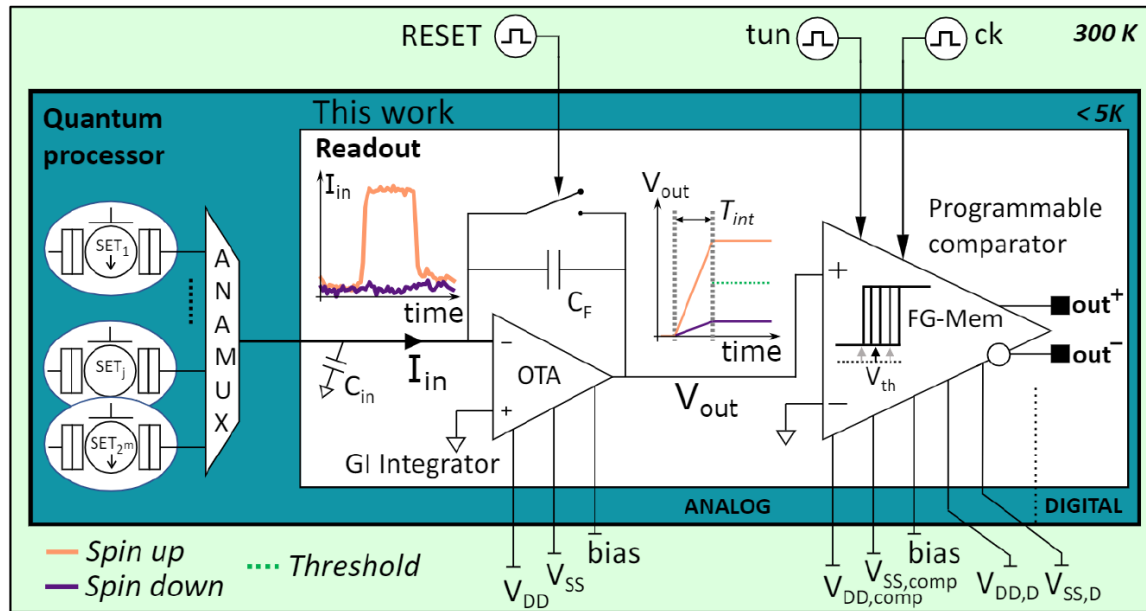
Calibration time: **175 ms**

Fall/rise time: **2 ns**

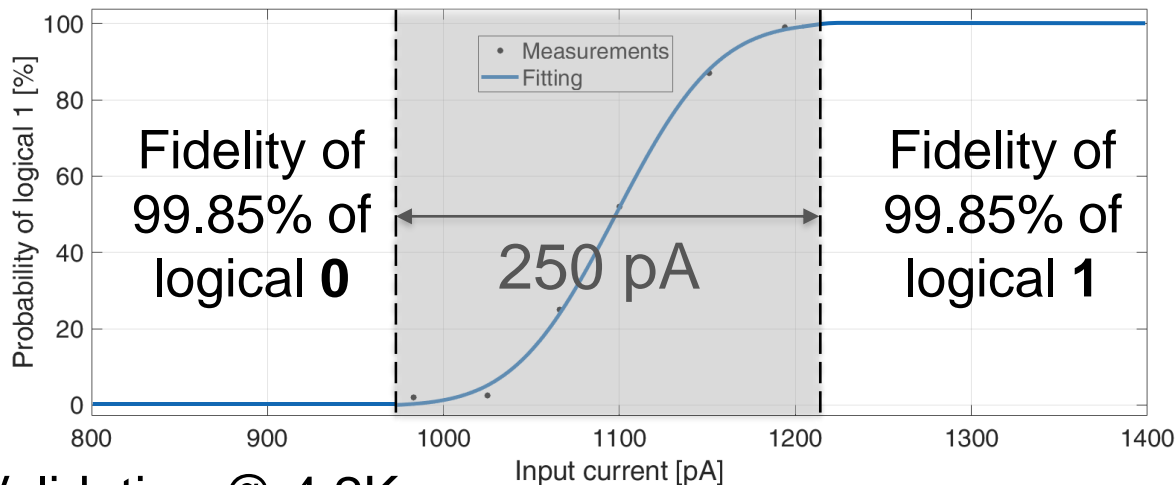


- Self-programmable threshold voltage
- Internal permanent FG memory
- "Zero" power dissipated by the memory
- Easy implementation of a TDM architecture

Characterization of the readout at 4.2 K



No off-chip components!



Threshold current: 1.1 nA

6 Sigma: 250 pA

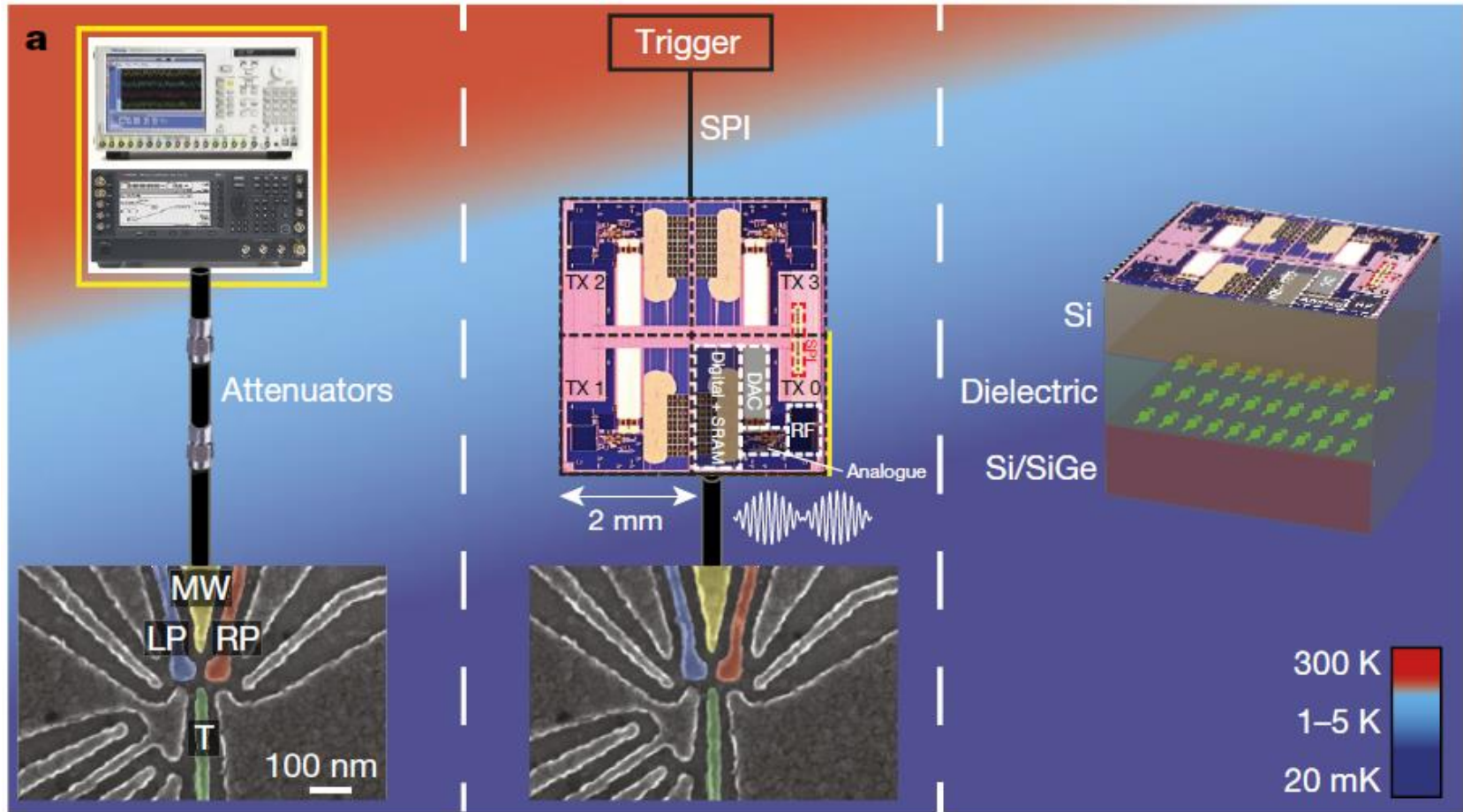
Readout time: 500 ns

Power consumption: 1.2 mW

Validation @ 4.2K

[M. CASTRIOTTA et al., IEEE Solid-state circuits letters (2023)]

Cryogenic quantum controllers



Today

Tomorrow

Future

X. Xue *et al.*, "CMOS-based cryogenic control of silicon quantum circuits," *Nature*, pp. 205–210, 2021

Cryogenic quantum controllers

Home > Quantum Computing

Intel Launches Horse Ridge Chip for Quantum Computing Systems

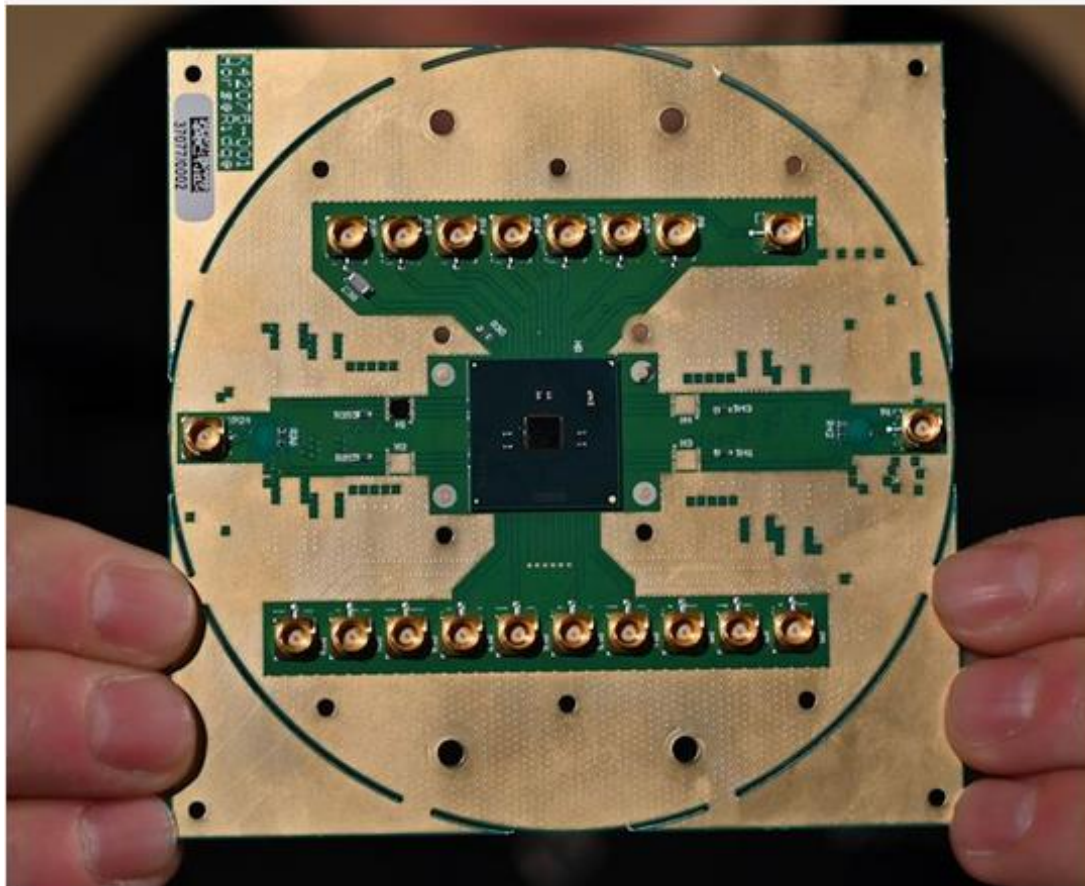
by [Anton Shilov](#) on December 10, 2019 2:15 PM EST

Posted in [Quantum Computing](#) [Intel](#) [Servers](#) [Horse Ridge](#)

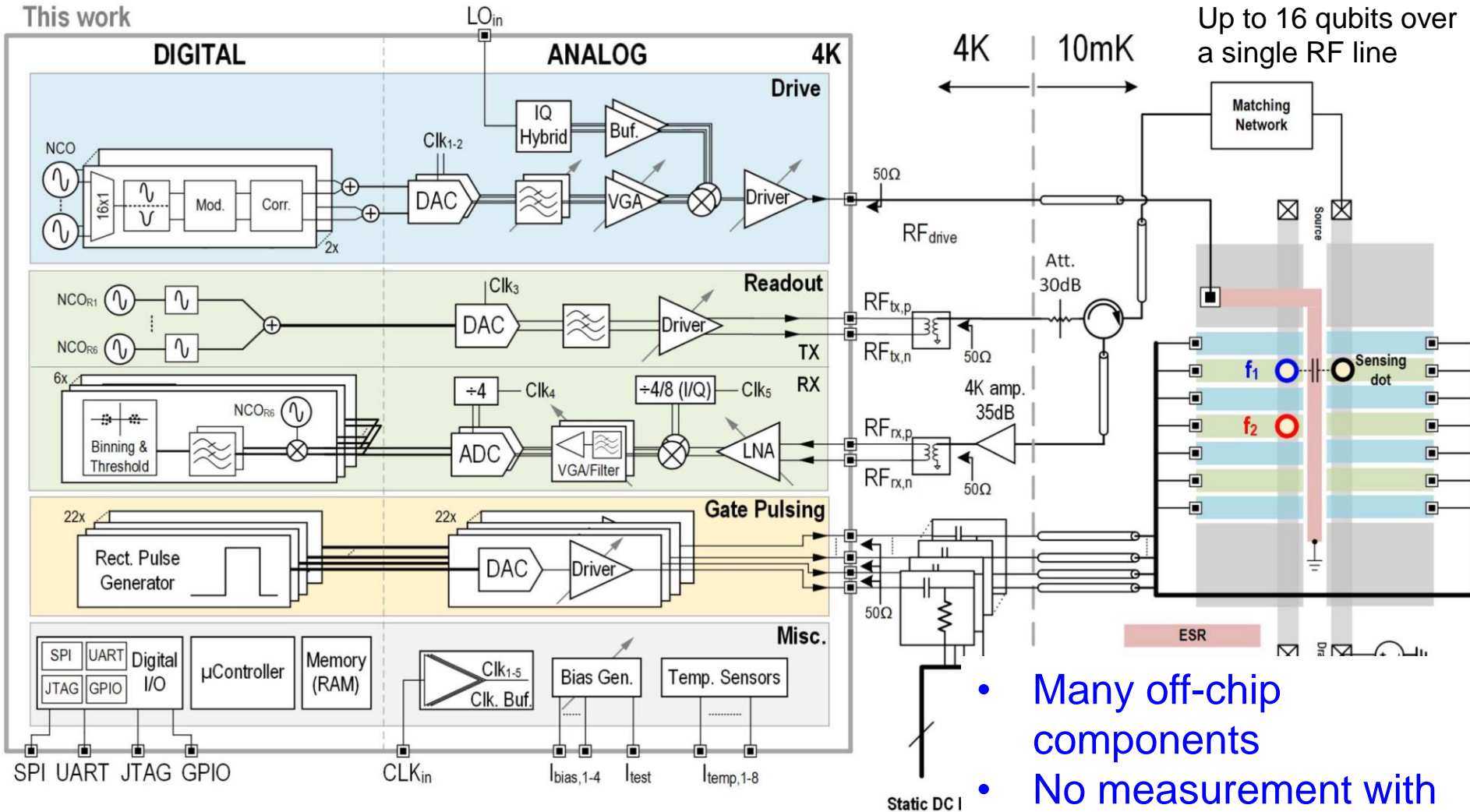
10

Comments

[+ Add A Comment](#)



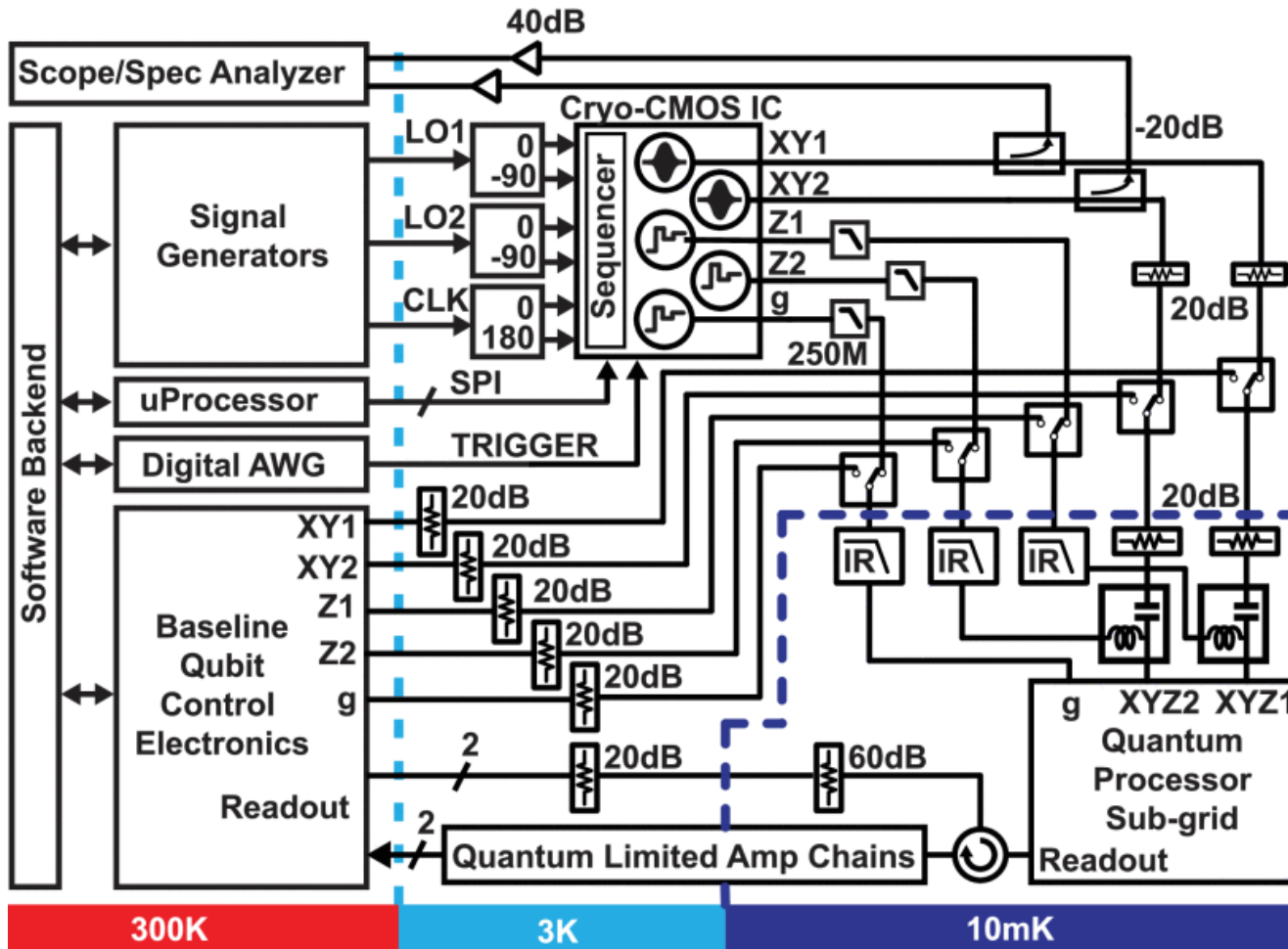
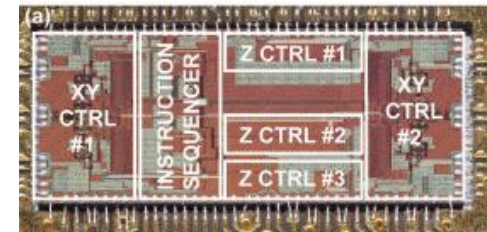
Cryogenic quantum controller (spin q.) - Intel



J. Park, et al. ,“A Fully Integrated Cryo-CMOS SoC for State Manipulation and Pulsing of Spin Qubits,” *IEEE J. Solid-State Circuits*, vol. 56, no. 11, pp. 3289–3306, 2021

Cryogenic quantum controller - Google

- superconducting qubits
- control of 2 qubits (measured!)
- 4mW/qubit
- RT readout
- 28 nm CMOS
- 1.8mm x 3.9mm



J. Yoo *et al.*, "Design and Characterization of a <4-mW/Qubit 28-nm Cryo-CMOS Integrated Circuit for Full Control of a Superconducting Quantum Processor Unit Cell," in *IEEE Journal of Solid-State Circuits*, vol. 58, no. 11, pp. 3044-3059, Nov. 2023,

Thank you for you attention!

